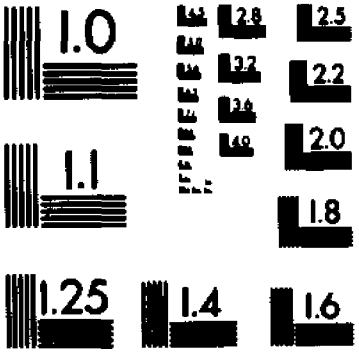

MICROCOPY RESOLUTION TEST CHART
NATIONAL BUREAU OF STANDARDS
STANDARD REFERENCE MATERIAL 1010a
(ANSI and ISO TEST CHART No. 2)

Jon, Domingo Inocencio

MEASUREMENTS OF LOW AND ULTRALOW INTERFACIAL TENSION BY MEANS OF THE BLADE, SPINNING DROP, PENDANT DROP AND LASER LIGHT SCATTERING METHODS

City University of New York

PH.D. 1986

PLEASE NOTE:

In all cases this material has been filmed in the best possible way from the available copy. Problems encountered with this document have been identified here with a check mark ✓.

1. Glossy photographs or pages _____
2. Colored illustrations, paper or print _____
3. Photographs with dark background _____
4. Illustrations are poor copy _____
5. Pages with black marks, not original copy _____
6. Print shows through as there is text on both sides of page _____
7. Indistinct, broken or small print on several pages ✓
8. Print exceeds margin requirements _____
9. Tightly bound copy with print lost in spine _____
10. Computer printout pages with indistinct print _____
11. Page(s) _____ lacking when material received, and not available from school or author.
12. Page(s) _____ seem to be missing in numbering only as text follows.
13. Two pages numbered _____. Text follows.
14. Curling and wrinkled pages _____
15. Dissertation contains pages with print at a slant, filmed as received ✓
16. Other _____

_____

_____

University
Microfilms
International

MEASUREMENTS OF LOW AND ULTRALOW INTERFACIAL TENSION BY MEANS OF THE BLADE, SPINNING DROP, PENDANT DROP AND LASER LIGHT SCATTERING METHODS

by

DOMINGO INOCENCIO JON

A dissertation submitted to the Graduate Faculty in
Chemistry in partial fulfillment of the requirements
for the degree of Doctor of Philosophy,
The City University of New York.

1986

This manuscript has been read and accepted for the Graduate Faculty in Chemistry in satisfaction of the dissertation requirement for the degree of Doctor of Philosophy.

02/04/1986
date

Chairman of Examining Committee

2/6/86
date

Executive Officer

Supervisory Committee

The City University of New York

Abstract

MEASUREMENTS OF LOW AND ULTRALOW INTERFACIAL TENSION BY MEANS OF THE BLADE, SPINNING DROP, PENDANT DROP AND LASER LIGHT SCATTERING METHODS

by

Domingo Inocencio Jon

Mentor: Professor Henri L. Rosano

Measurements of low and ultralow interfacial tension, γ_i, ranging from 0.3 to 3 mN/M, on water/toluene interfaces containing various amount of 1-propanol and from 10^{-1} to 10^{-3} mN/M on toluene/ SDS/ 1-butanol/ Saline NaCl interfaces containing various concentration of NaCl has been undertaken with laser light scattering, spinning drop, pendant drop and Wilhelmy blade methods. The instrument contribution to the spectrum obtained from the laser light scattering method was found to be represented by a Lorentzian-squared function. The interfacial viscosity is then calculated from the spectral linewidth using this instrumental function and compared to the bulk viscosity. Measurements of phase volume and interfacial tension on water/toluene/1-propanol systems indicate that a requirement for formation of O/W dispersion is low γ_i, but for overall stability, γ_i, although small, must be positive. From extrapolation of the measured γ_i values on water/toluene/1-propanol systems, it has been found that a residual positive value of 0.2 mN/M is still observed at cosolubilization.

Acknowledgements

In all human endeavor no man stands alone in his search for excellence. I owe a great deal of thanks to friends and professors for their constant encouragement and moral support. Special thanks should go to Professor Henri L. Rosano, my mentor. He is one educator who always takes the best interest of his students to heart. His constant concern, encouragement, and extreme patience during moments of tribulations has made an indelible impression on me. During these years of graduate studies, I have had the fortune of knowing him better. He has become more than an advisor to me.

A great deal of thanks should also go to Professor Herman Z. Cummins. Without his expert guidance and the time he devoted to me, away from his busy schedule, the present would not be possible.

I am also very grateful to Professors David Locke and John Arents, for they took time out to guide and to help me along the way. And finally to John L. Cavallo who made this stage of my life more enjoyable than otherwise.

To my mother
Olga Kan de Jon
who always loved me

Table of Contents

List of Figures

CHAPTER 2

CHAPTER 3

CHAPTER 4

CHAPTER 5

List of Tables

CHAPTER 3

CHAPTER 4

CHAPTER 5

CHAPTER 6

APPENDIX B

CHAPTER 1

INTRODUCTION

It is experimentally difficult to measure low (below 1 mN/M), and ultralow interfacial tension, γ_i. Presently, the spinning drop method is used widely in determining low and ultralow γ_i values. In the last few years, a laser light scattering method has been developed that could determine both γ_i and the interfacial viscosity. This technique has the advantage that it does not perturbe the interfacial thermal equilibrium and may be used to measure low and ultralow γ_i.

It has been known, since V. Smoluchowski (1) remarked in 1908, that the surface of a liquid is constantly distorted by thermal motions and, therefore, should present certain roughness. This roughness has a height of about 10 Å and it can be expressed, at a given instant, as a sum of Fourier components. Each of the components, ζ_q, can act like a sinusoidal diffraction grating which scatters light incident at the interface, the zero order (regular reflection) and the first order diffraction being the only important ones due to the size of the asperities. From the Bragg condition, the angle of measurement of the scattered light is related linearly to the wavevector of the fluctuations. These surface fluctuations can be studied by either Homodyne or Heterodyne Optical Intensity Fluctuation Spectroscopy which measures the photocurrent produced in a photomultiplier by the scattered light and analyzes it statistically in either the frequency or time domain. In the analysis, one has to relate the temporal statistics of the scattered light to the statistics of the surface. One then has to relate the statistics of the electric field to the detected photocurrent.

The statistics of the surface Fourier components, corresponding to a single

wavevector, have been computed for both a clean surface and for a surface containing monolayer (2,3). From the study of these surface waves it is possible to obtain information about the interfacial tension and the viscosity of the system at the interface. Presently, there is a considerable amount of published work, both theoretical and experimental, concerning the propagation and evolution of these waves (4-8). However, until recently, most of the reported studies were on air/liquid interfaces ($\gamma_i > 15$ mN/M) and on microemulsion systems, where γ_i is ultralow ($10^{-4} < \gamma_i < 10^{-2}$ mN/M) and the capillary waves are overdamped (9-12). Recently, Löfgren and Newman (13) reported a study on liquid/liquid interfaces where the interfacial tension was high and the capillary waves were slightly damped. These researchers found a good agreement of the interfacial tension and the viscosity between the light scattering method and other more conventional forms of measurement (Wilhelmy blade, spinning drop, du Nouy ring methods for the interfacial tension and Ostwald viscometer for the bulk viscosity).

Here, Laser Light Scattering measurements, in the frequency domain, have been performed with two systems

1) toluene/ water / 1-propanol

2) toluene/ sodium dodecyl sulfate/ 1-butanol/ NaCl solution

Values of interfacial tension ranging from a few mN/M to 10^{-3} mN/M were obtained from these systems and were correlated with measurements taken with the blade method, spinning drop method and pendant drop method.

The dual purpose of this study was to show further the applicability of the light scattering technique to liquid/liquid interfaces at low and ultralow interfacial tension and moderate viscosity and to determine γ_i values of a toluene/water interface just before cosolubilization upon the addition of 1-pro-

panol, where the oil/water interface disappears.

Due to the finite resolution of the experimental apparatus, the measured power spectrum is an overlap of several power spectra corresponding to different wavevectors with an intensity distribution that depends on the instrumental parameters. An equation has been found which adequately represents this intensity distribution, or instrumental broadening, of the measured spectrum. This equation for the power spectrum was used to calculate the interfacial tension and the viscosity of the solution from the experimental spectrum. The calculated viscosity was compared with that of the bulk viscosity, and the interfacial tension was compared with the values obtained with other techniques. It is hoped that this study will further advance the application of the light scattering technique to liquid/liquid interfaces at low and ultra-low interfacial tension and moderate viscosity.

CHAPTER 2

CONVENTIONAL METHODS OF MEASURING LOW AND ULTRALOW INTERFACIAL TENSION

2.1 INTRODUCTION

It is known that short range van der Waals forces of attraction exist between molecules and that they are responsible for the existence of a liquid state. The phenomenon of surface and interfacial tension can be explained in terms of these forces. Molecules located within the bulk of a liquid are, on the average, subjected to equal forces of attraction in all directions, whereas those located at an interface experience an unbalance cohesive force resulting in a net inward pull. As many molecules as possible will leave the liquid surface for the interior of the liquid; the surface will therefore tend to contract spontaneously. The interfacial tension, γ_i, of a liquid is thus defined as the force tangential to the surface on a line of 1 cm length on the boundary of the interface, and has the units of mN/M (or dynes/cm). An equivalent way of looking at the phenomenon is in terms of the surface free energy of the liquid. The surface free energy (and thus the surface tension) could be ascribed to a very narrow region, of infinitesimal thickness, in the immediate neighborhood of the physical surface of separation between any two phases. It has long been recognized, however, that there exists no sharp separation between phases. As the interface is approached from within the bulk of the phase, in a direction normal to the plane of separation, there is a gradual change in properties from one phase to the other (14,15). It should not, then, be correct to assume that the excess free energy resides in the plane of the interface. In fact, the "excess" free energy for elements inside the bulk of any particular phase, due to the interaction between

these phases, is zero. As the interface is approached, in a direction normal to it, there will be a gradual change in excess free energy, until the maximum is reached in the outermost layer, where there exists a rapid alteration of the field of force.

The above picture implies a static state of affairs. However this apparent quiescent liquid interface is in a state of great turbulence on the molecular scale as a result of two way traffic between the bulk of the liquid and the interface.

In this research, the interfacial tension of liquid/liquid interfaces was measured with the laser light scattering method and the values are correlated with conventional methods of measuring interfacial tension, such as the blade method, spinning drop method, pendant drop method. The present chapter explains the theory and the experimental proceadure followed in determining the interfacial tension with the blade, spinning drop and pendant drop methods.

2.2 THE BLADE METHOD

2.2.1 THEORY

In the determination of the interfacial tension (or surface tension) a wettable blade is brought to the surface until it just touches the surface (figure 2.1). A force is then exerted on the blade, and measured. The interfacial tension is obtained from the following equation.

$$\gamma_i \cos\theta = \frac{F}{P} \qquad [2.1]$$

where

γ_i = Interfacial or surface tension in mN/M.

F = Force exerted on the blade by the liquid.

P = perimeter of the blade in cm.

θ = angle of contact between the blade and interface

When the material of the blade is completely wettable by the solution, the angle of contact, θ , becomes 0 and the measured value becomes the tension of a flat interface. Thus a blade is selected for its wettability by the liquid (aqueous or oil).

2.2.2 EXPERIMENTAL

The apparatus consisted essentially of

1) Rosano Surface Tensiometer, model LG (Arenberg-Sage)

2) 5 cm sandblasted platinum blade

3) 5 cm sandblasted teflon blade

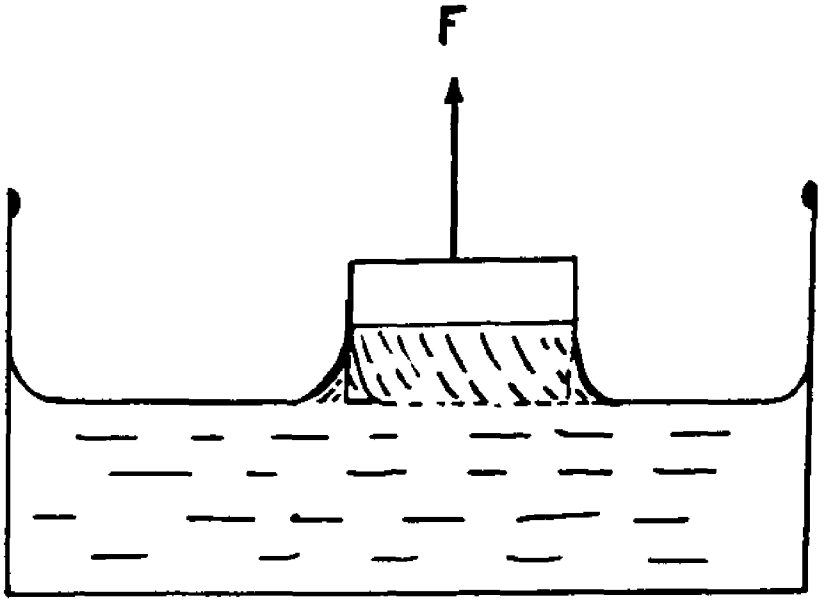

Figure 2.1 Profile of the Wilhelmy blade.

Surface tension measurements were taken with a platinum blade, whereas interfacial tension measurements were taken with a teflon blade. The perimeter of the platinum blade was determined by measuring the force exerted on the blade by an air-water interface using A 250 ml crystallizing dish cleaned with fresh sulfochromic acid mixture (Sodium dichromate/H_2SO_4 concentrated) as the container. A platinum blade, cleaned by flaming in a non-carbon producing flame, was brought down to the level of the liquid until it contacted its surface. The force exerted on the blade was recorded with a Rosano Surface Tensiometer, and the temperature of the solution was recorded with a glass thermometer. Taking the values for the surface tension of water as those given in *The CRC Handbook*, where it is tabulated as a function of temperature, the perimeter of the blade was calculated using equation 2.1.

The perimeter of the teflon blade was determined with the following relation

$$P\,(teflon) = \frac{F\,(teflon) \times P\,(platinum)}{F\,(platinum)} \qquad [2.2]$$

where :

$P(platinum)$= perimeter of the platinum blade

$P(teflon)$= perimeter of the teflon blade

$F(teflon)$= force exerted on the teflon blade by the liquid

$F(platinum)$= force exerted on the platinum blade by the liquid

The platinum blade was brought to an air-benzene interface, and the force exerted on the blade was measured. On the same solution, a teflon blade was also brought to the interface and the force exerted on the teflon blade was determined. The perimeter was then calculated from equation 2.2.

The interfacial tension of the systems studied were measured with the

teflon blade immersed in the water phase and brought slowly toward the interface until it contacted that interface. Due to the wettability of the blade by the oil, a force, exerted in the direction of the oil phase, was measured with a tensiometer, and the interfacial tension was calculated from equation 2.1.

2.3 THE SPINNING DROP METHOD

2.3.1 THEORY

When a drop of liquid is introduced in another liquid of higher density contained in a cylindrical tube and the whole mass allowed to rotate, as shown in figure 2.2, the drop will move to the center forming a drop astride the axis of revolution. With increasing frequency of rotation the drop will elongate from a sphere to a prolate ellipsoid to an elongated cylinder. The centripetal force, due to the rotation, opposes the interfacial tension-drive toward minimum interfacial area. The interfacial tension is determined from the balance of these forces. The general analysis is treated in appendix A. Here it is considered the case of a very elongated, cylindrical drop.

Consider a section of the elongated drop of volume V (figure 2.3), where the centrifugal force on the volume element is $\omega^2 r \Delta\rho$, and where ω is the speed of revolution in radians and $\Delta\rho$ is the difference in density. The potential energy at a distance r from the axis of revolution is

$$\frac{\omega^2 r^2 \Delta\rho}{2} \qquad [2.3]$$

and the total potential energy from a cylinder of length l is

$$l \int_0^{r_o} \left| \frac{\omega^2 r^2 \Delta\rho}{2} \right| 2\pi r dr = \frac{\pi \omega^2 \Delta\rho \, r_o^4 l}{4} \qquad [2.4]$$

The interfacial energy is $2\pi r_o l \gamma_i$. The total energy is thus

$$E = \frac{\pi \omega^2 \Delta\rho \, r_o^4 l}{4} + 2\pi r_o l \omega = \frac{\omega^2 \Delta\rho \, r_o^2 V}{4} + \frac{2V\gamma}{r_o} \qquad [2.5]$$

since $V = \pi r_o^2 l$. Setting $dE/dr_o = 0$, we obtain the equation

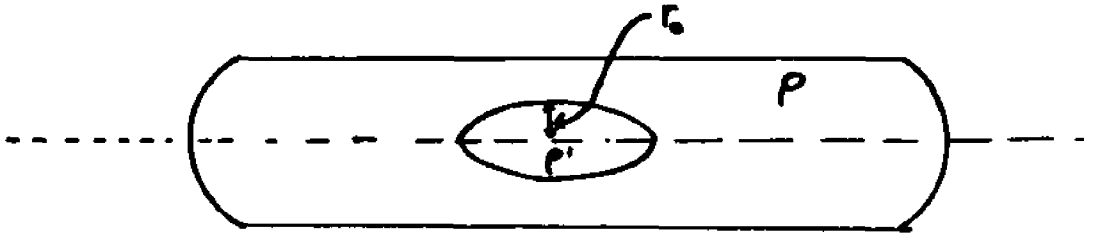

Figure 2.2 Profile of a spinning drop

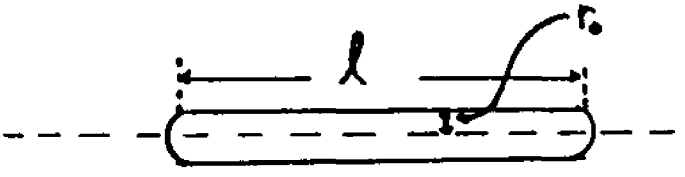

Figure 2.3 Spinning drop elongated to a cylindrical shape.

$$0 = \frac{\frac{\omega^2 \Delta\rho V(2r_o)}{4} - 2V\gamma}{r_o^2} \qquad [2.6]$$

$$\frac{2V\gamma}{r_o^2} = \frac{\omega^2 \Delta\rho V(2r_o)}{4} \qquad [2.7]$$

$$\gamma_i = \frac{\omega^2 \Delta\rho\, r_o^3}{4} \qquad [2.8]$$

Equation [2.8] is referred to as the limiting case equation; it is applicable only when the drop is elongated and cylindrical in shape.

This limiting case is also referred as Vonnegut's equation (16), who first suggested this method of measuring interfacial tension. According to Silberberg (17) Vonnegut's equation is applicable when the axis ratio, r/ *l*, of the drop is greater than 3.5, although the choice of this critical value is arbitrary and depends on the accuracy being sought. Values around 0.001 dynes/ cm can be measured readily and accurately with this method. This limiting case equation was selected to measure the interfacial tension with the spinning drop technique. The size of the drop was selected such that the ratio of r/ *l* is greater than 3.5.

2.3.2 EXPERIMENTAL

The apparatus consisted of

1) 2 mm bore × 95 mm long tubes
2) A Gaertner filar eyepiece micrometer microscope.
3) A spinning drop interfacial tensiometer model 500 from the University of Texas, Austin.

In measuring the interfacial tension, a horizontal tube was soaked overnight in fresh sulfuric acid / potassium dichromate solution. The tube was filled with liquid from the lower phase, and a small drop of the upper phase was then introduced into the tube with a small syringe. The tube was made to spin with a sufficient centrifugal force to elongate the small drop to a cylindrical shape until the drops were on the order of 1/2 to 1 cm in length depending on its width. The diameter of the drop was read by bringing the hairline of the microscope to the bottom edge of the drop and then moving it uniformly upward to the upper edge of the drop. The radius of the drop was read at half hour intervals until three consecutive readings agreed to within ± 0.001 cm. The measured radius of the drop was corrected by the refractive index. The interfacial tension was calculated from equation 2.8. The experimental setup is shown in figure 2.4

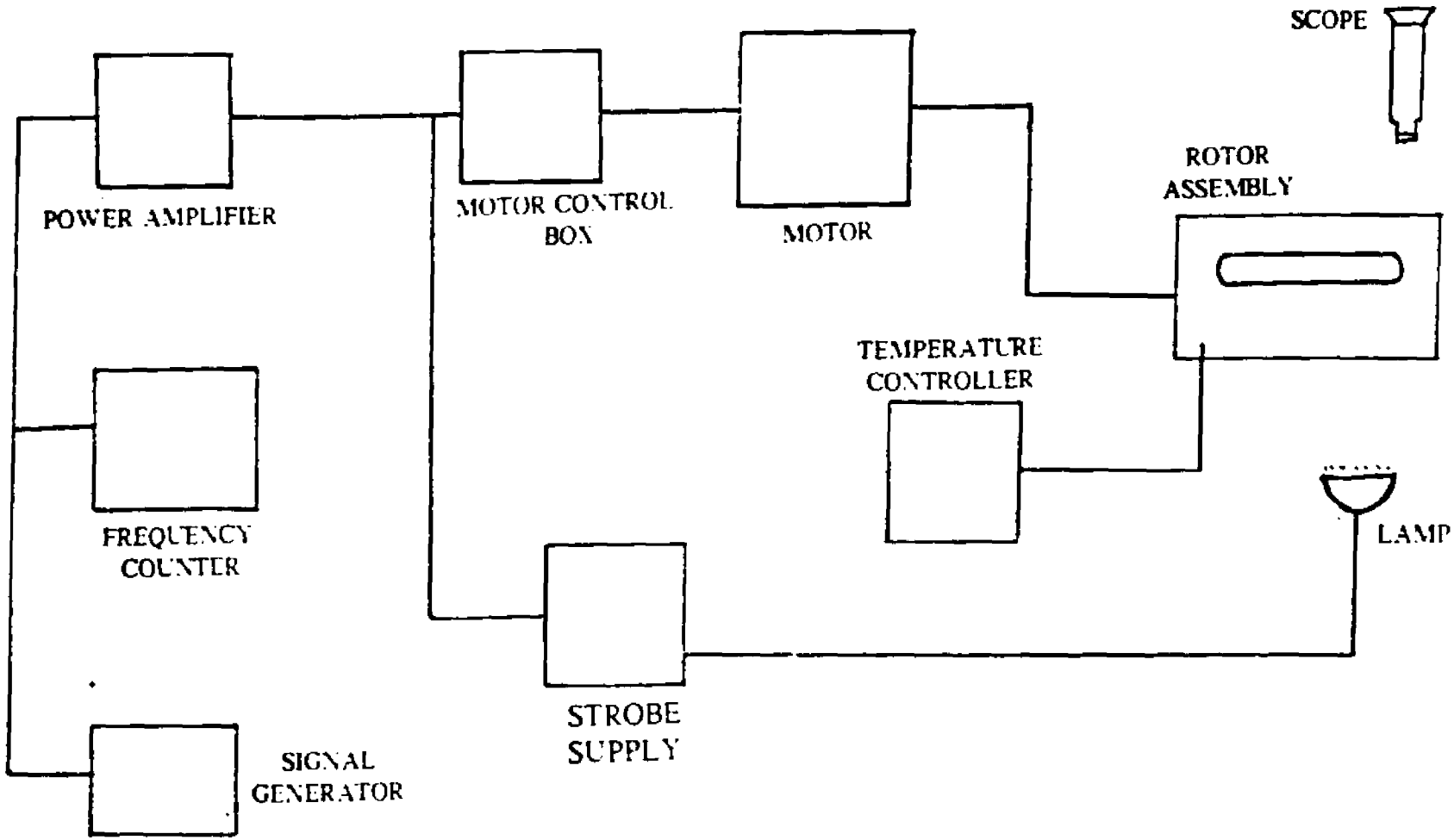

Figure 2.1 Equipment setup of the spinning drop method.

2.4 THE PENDANT DROP METHOD

2.4.1 THEORY

Imagine a droplet hanging from the extremity of a vertical cylinder horizontally cut (figure 2.5). Let define R_1 and R_2 as the two principal orthogonal radii of curvature at any point P on the surface of a droplet. When going across the surface from the outside to the inside, the Laplace pressure at any point of the drop equals

$$\Delta P_L = \gamma_i \left(\frac{1}{R_1} + \frac{1}{R_2} \right) \qquad [2.9]$$

From the shape of such pendant drop, the surface (or interfacial) tension could be determine. The general analysis of the pendant drop method is treated in appendix B. Here a brief version is given. Taking the pendant drop as a figure of revolution, both radii of curvature must be equal at the apex (point 0). Defining b as the radius of curvature at the apex, The Laplace pressure equals $2\gamma_i/b$. Therefore,

$$\Delta P = \gamma_i \left(\frac{1}{R_1} + \frac{1}{R_2} \right) = \Delta\rho g z + \frac{2\gamma_i}{b} \qquad [2.10]$$

Where $\Delta\rho g$ is the hydrostatic pressure term. Equation (2.10) may be rearranged so as to involve only dimensionless parameters

$$\frac{\frac{1}{R_1}}{b} + \frac{\sin\phi}{X} = \beta Z + 2 \qquad [2.11]$$

where:

$$R_2 = \frac{x}{\sin\phi}.$$

$X = x/b$

$Z = z/b$

and the dimensionless parameter β is given by

$$\beta = \frac{\Delta\rho g b^2}{\gamma_i} \qquad [2.12]$$

From analytical geometry the curvature of a line may be expressed as

$$\frac{\frac{1}{R_1}}{b} = \frac{Z''}{\left|1 + (Z')^2\right|^{\frac{3}{2}}} \qquad [2.13]$$

where Z' and Z'' denote the first and second derivative with respect of X. Substituting into equation 2.11 yields a second order differential equation.

$$\frac{Z''}{\left|1 + (Z')^2\right|^{\frac{3}{2}}} + \frac{\sin\phi}{X} = \beta Z + 2 \qquad [2.14]$$

This equation may be reduced to two first order differential equations with the following two initial conditions.

$X = 0 \qquad Z = 0$

$X = 0 \qquad Z' = dX/dZ = 0$

This equation was solved using the fourth order Runge-Kutta method (18).

The parameter β, negative in the case of a pendant drop, is not measured directly, but as a shape determining variable it is related to others whose determination may be easier. In the pendant drop case, Andreas *et. al* (19) suggested the relation S=ds/de as the best measurable, shape determining quantity. As indicated in figure 2.5, de is the equatorial diameter and ds is the diameter measured at a distance de up from the bottom of the drop. Andreas *et. al* also defined

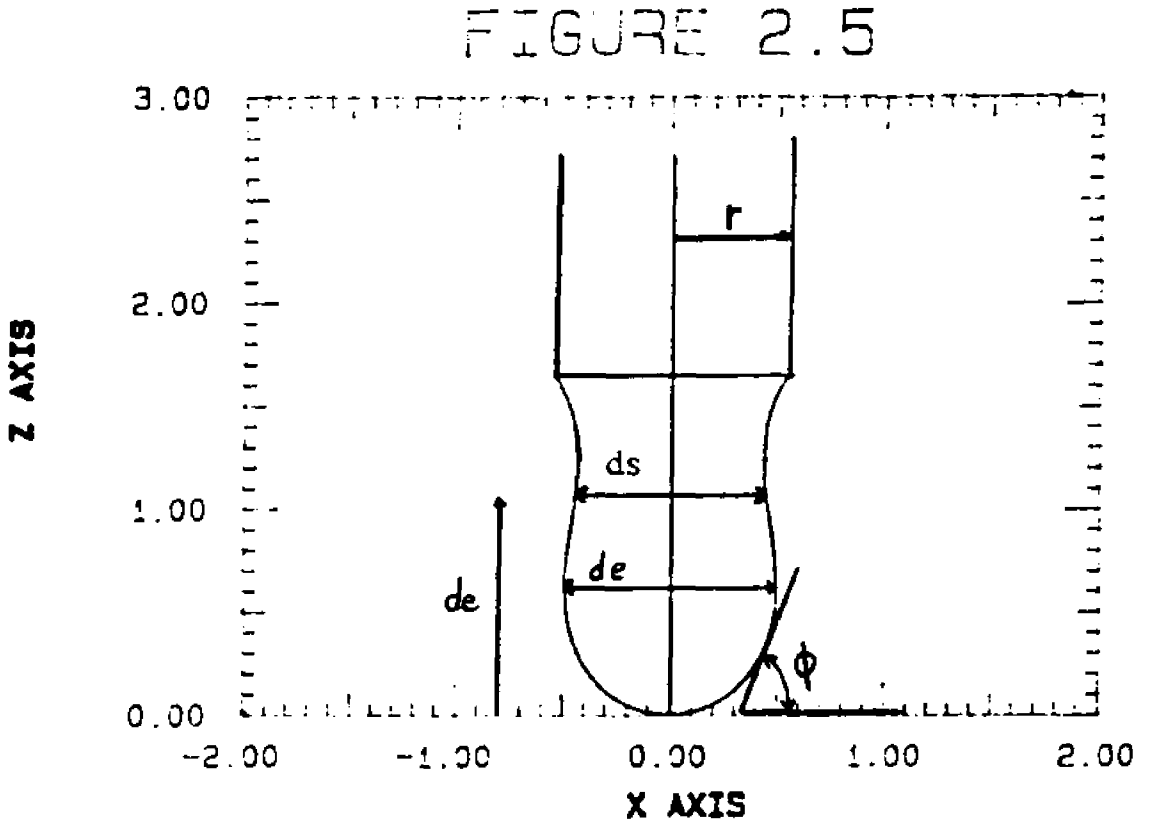

Figure 2.5 Profile of a pendant drop

a new quantity H as

$$H = -\beta\left(\frac{de}{b}\right)^2 \qquad [2.15]$$

Thus from equation 2.12

$$\gamma_l = \frac{-\Delta\rho g b^2}{\beta} = \frac{\Delta\rho g de^2}{H} \qquad [2.16]$$

The relationship between the shape dependent quantity H and the experimentally measurable quantity S was determined originally using pendant drops of water; the error was as much as 1%. Presently, a set of accurate values of 1/H versus S obtained with a numerical integration procedure using the Bashford and Adams tables (20) exists and was based on the fundamental equation 2.11.

2.4.2 EXPERIMENTAL

The apparatus consisted of

1) Rame-Hart NRL C.A. Goniometer model #A-100 stand;
2) a light source;
3) a variety of different sized glass tips;
4) a Polaroid land camera.

The drops were formed vertically from a glass tip with the aid of a micrometer. The systems studied were placed in a rectangular glass cuvette and allowed to reach physical equilibrium before the drop was formed. The systems were totally enclosed to prevent liquid evaporation.

The droplet was photographed at a shutter speed of 1/125 sec. and the optical magnification of 10 to 15 was used to photograph the pendant drop in the systems studied.

The micrometer, with the syringe and glass tip, was mounted on a separate stand with the capability of being moved in all directions smoothly so as to maintain physical equilibrium with minimum vibrations and ease of experimentation. The experimental setup is shown in figure 2.6

In our determination of low interfacial tension, a program has been written (appendix D) that, for a given value of de, ds, $\Delta\rho$, and optical magnification, will calculate the shape of the pendant drop from the above derived equation 2.14. The procedure used to determine the interfacial tension is as follows.

1.- The drop is formed and photographed.

2.- de, ds, and $\Delta\rho$ and the optical magnification are measured as precisely as possible.

3.- γ_i is calculated from equation 2.16, using these data and a polynomial function of 1/H vs S that has been incorporated in the computer program (appendix B).

4.- β was obtained as a function of S using a numerical expression similar to that of Huh and Reed (21) (appendix B). Once β has been calculated from the experimentally determined S, b can then be determined from equation 2.12.

5.- The computer calculates the shape of the drop and the results of the numerical solution are then plotted.

6.- Two possible cases have to be considered:

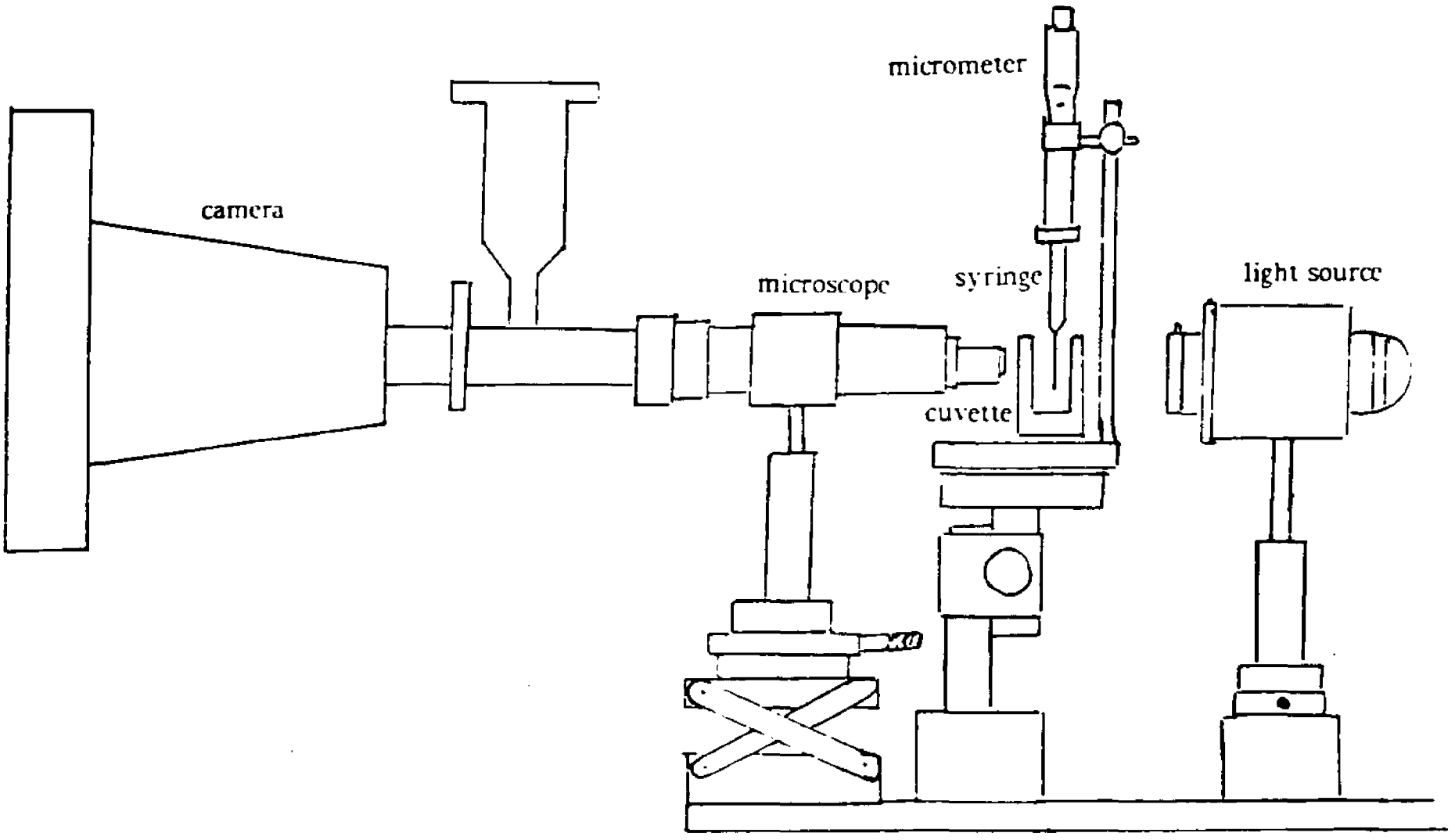

Figure 2.6 Equipment setup of a pendant drop method.

6.1- The plotted curve fits the photograph of the droplet. Therefore, the calculated value in step 3 of γ_i is acceptable.

6.2- The plotted curve does not fit the photograph exactly. Therefore, de, ds and $\Delta\rho$ or the optical magnification were not measured accurately and the measurements are then repeated until the curve fits the photograph (case 6.1).

2.4.3 THE GLASS TIP

When measuring the surface or interfacial tension of a particular system by the pendant drop method, it is necessary for higher accuracy that S be near unity (the drop should be cylindrical as opposed to spherical). It is therefore convenient to be able to estimate the diameter of the tip of the syringe to be used to produce an S as close to unity as possible.

For a particular system with $\Delta\rho$ and g known along with a range of γ_i, one can estimate the diameter of the tip (DT), yielding a nearly cylindrical drop. Referring to figure 2.5, the following may be deduced,

$$DT = de = 2r \qquad [2.17]$$

$$S = 1 \qquad [2.18]$$

$$\frac{1}{H} = 0.30586 \qquad [2.19]$$

Substitution of the above equation into equation 2.10 yields

$$\gamma_i = \frac{\Delta\rho g (de)^2}{H} = \Delta\rho g (2r)^2(0.30586) \qquad [2.20]$$

rearranging

$$r^2 = \frac{2\gamma_i}{\Delta\rho g(8)(0.30586)} = \frac{\alpha^2}{2.447} \qquad [2.21]$$

where α is the square root of the capillary constant. Therefore,

$$r = \alpha(0.64) \qquad [2.22]$$

Experience has also shown that when

$$r \leq \alpha(0.64) \qquad [2.23]$$

the drop formed is nearly cylindrical. Note that in the case of a solution wettable to the tip, r includes the outer glass perimeter of the tip.

For the system of CCl_4 and air at 25°C

Density of CCl_4	1.585 g/cm^3
Density of air	0.001 g/cm^3
The difference in density	1.584 g/cm^3
Surface tension γ	26.0 dynes/cm

Therefore

$$r = \sqrt{\frac{2\gamma_i}{\Delta\rho g(2.447)}} = \sqrt{\frac{2(26)}{1.584(980.4)2.447}} = 0.12 \text{ cm.}$$

and the diameter of the tip should be 0.24 cm or less.

Glass tips were made by taking various capillary tubes and heating them while rotating them. Once the tube began to melt it was pulled to various sizes ranging from 0.1 to 20 mm. The tips were then cut perpendicularly and measured. If the tip is not nearly perpendicular, the forces acting along the circular perimeter of the tip are not equally distributed due to the excess liquid volume. This produces the drop to fall (as has been observed), making it difficult to

obtain static equilibrium and also difficult to photograph. If the drop achieves static equilibrium and the tip is not nearly perpendicular the resulting drop sometimes is not axisymmetric.

It should be carefully noted that 1) the glassware has to be cleaned with a fresh sulfochromic acid solution; and 2) at low interfacial tension the droplet has a tendency to detach itself, so vibrations should be avoided.

CHAPTER 3

LIGHT SCATTERING METHOD OF MEASURING LOW AND ULTRALOW INTERFACIAL TENSION

3.1 INTRODUCTION

The mechanism of light scattering may be described as follows: liquid interfaces are constantly distorted by thermal motion in the form of waves. These waves have a small amplitude compared to their wavelength (about 10 Å high), and are subjected to capillary and gravitational restoring forces and their motion is damped by viscosity. The spatial and temporal evolution of this capillary waves can be described, on a macroscopic scale, by hydrodynamic laws.

At a given instant, the vertical displacement of the surface fluctuations can be expressed as a sum of Fourier components with each component, ζ_q, behaving as a sinusoidal diffraction grating. Thus, light incident at the interface is scattered by a moving grating and experiences frequency changes due to the Doppler effect. Because of the small amplitude, the zeroth order (regular reflection) and the first order scattering are the only important ones. Thus selecting a single scattering angle is equivalent to selecting one wavevector from the continuous distribution of surface waves. In the far field, a single angle of measurement corresponds to each wavevector on the grating.

The scattering process is considered as an inelastic collision between the incident photon and a surface phonon (a quantum of the capillary wave) which is either annihilated or created. A surface vibration mode, or surface phonon, with a given wavevector q scatters light by the process

Incident photon ± surface phonon ⟶ scattered photon

The scattered light is, therefore, concentrated in a well defined direction related to **q** through momentum conservation on the surface plane during the scattering process (figure 3.1)

$$\mathbf{q} = \mathbf{k}' - \mathbf{k} \qquad [3.1]$$

where:

$\mathbf{k}'$ = the projection of the wave vector of the scattered beam on the surface plane

$\mathbf{k}$ = the projection of the wave vector of the reflected beam on the surface plane.

To create a surface vibration mode of wavevector **q**, it is necessary to work against gravitational and capillary forces. In cases where the gravitational force is negligible, the capillary force energy is proportional to the increase in surface area, *i.e.* to q^2 times the square of the amplitude $|\zeta|^2$. From the equipartition theorem for the surface mode, $\langle|\zeta_q|^2\rangle = k_B T/(\gamma_i q^2 + \Delta\rho g)$ (22). Consequently the scattered intensity is inversely proportional to both q^2, and to the surface tension γ_i.

Since capillary waves are damped by viscosity, their amplitude decrease with time either exponentially, at hight viscosity, or as a damped oscillator, at low viscosity. At high viscosity, the spectrum of the scattered light is a Lorentzian centered at ω_o, whereas at low vicosity, the spectrum consists of two Lorentzian components located symmetrically with respect to ω_o. But in the intermediate case, the spectrum becomes very complex and the analysis of the experimental spectrum requires a prior knowledge of the exact spectral shape.

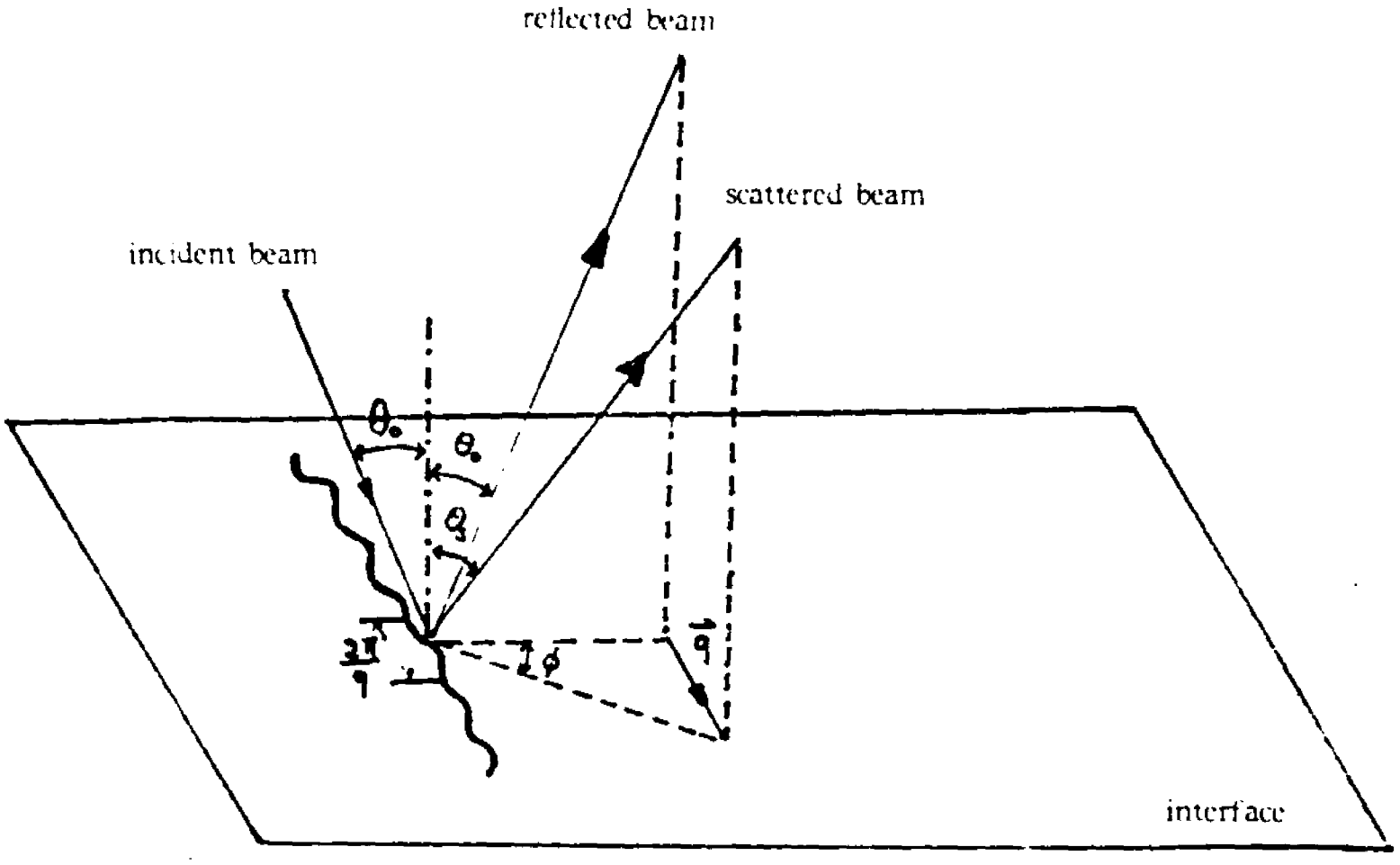

Figure 3.1 Geometry of a light scattering experiment

The intensity of the light scattered by the surface waves was first calculated by Mandelstam (22), and Andronov, Leontovich and Gans (23). In the early investigations of liquid surfaces the studies were limited to the scattered intensity. With the appearance of the laser it became possible to define accurately the surface wavevector q; also the intensity per spectral range is much higher than for classical sources. This allows the performance of very high resolution spectral analysis by means of the Intensity Fluctuation Spectroscopic Technique. The angular study of the scattered intensity reflects the spatial distribution of the fluctuations, ζ, while the spectral analysis reflects their temporal evolution.

The scattered intensity with wavevector $\mathbf{k}'$ and frequency ω is given by (24):

$$I(\mathbf{k}', \omega') = F \cdot S(\mathbf{q}, \omega) \qquad \omega = \omega' - \omega_o \qquad [3.2]$$

Where ω_o is the frequency of the incident light. F depends only on the properties of the incident beam and on the geometrical factors such as the size of the collection aperture, etc., and S only on those of the scattering system; S is the space-time Fourier transform of the correlation function of $\zeta(r,t)$. The vertical displacement of the surface point, $\zeta(\mathbf{r},t)$, due to a single wavevector whose projection on the horizontal plane has the coordinates r(x,y,0) can be expressed as $\zeta(\mathbf{r},t) = \zeta_q e^{i\mathbf{q}\cdot\mathbf{r}}$. Where q is the wavevector of the surface fluctuation.

These surface fluctuations scatter a monochromatic incident light beam with a small frequency shift (tens to thousands of Hertz) which can be detected and studied by measuring the statistical properties of light scattered from the fluctuating interface by either homodyne or heterodyne light scattering spectroscopy (25). One measures the photocurrent of the scattered light and processes it

statistically either in the frequency or time domain. The spectrum or autocorrelation function of the photocurrent is then used to infer the dynamic properties of the liquid interface.

In the analysis of the experiment, the temporal statistics of the scattered electric field has to be related to the statistics of the surface. The statistics of the electric field are then related to the detected photocurrent.

In a heterodyne experiment the scattered electric field is mixed with unshifted light from the same source; which serves as a local oscillator or reference signal. In early studies using heterodyne spectroscopy, the reference field was generated by dust particles or from rough optical elements causing parasitic scattering of light. In more recent experiments, the reference field is generated from the reflected beam by means of a diffraction grating (26, 27, 28).

In general, one cannot select just one surface wave with a perfectly defined wavevector. The detected signal, instead, contains overlapping signals from the nearby wavevectors causing an increase in the width of the spectrum over that expected from a single wave vector. The contribution of these overlapping signals to the width of the experimental spectrum is instrument dependent. Therefore, to calculate the width from a single wavevector, the overlap from the nearby wavevectors has to be substracted.

The present derivation of the surface waves and light scattering properties follows that given by Meunier (29). In deriving the properties of the surface fluctuations we start from an intuitive simple description of the hydrodynamic problem; the parameters which play a basic role are introduced (3.2.1). Statistical properties of the surface fluctuation is discussed (3.2.2). A method for calculating the surface correlation function is presented (3.2.3) and it is shown to

be consistent by deriving the response function at the interface when acted on by an external sinusoidal force (3.2.4). The expression obtained is shown to be equivalent to a harmonic oscillator in one dimension in the case of low damping and high damping conditions (3.2.5). The mean square amplitude of the surface fluctuations is calculated in (3.2.6) and finally the absence of correlation between the vertical displacement of the interface and the the velocity of the fluid underneath this interface is demonstrated in (3.2.7).

In relating the scattered light to the fluctuations at the surface, some general characteristics of the scattered light are explained (3.3.1). This is followed by a study of the intensity of scattered light (3.3.2), and a comparison of the intensity of the light scattered from reflected and refracted beam (3.3.3). The relation of the spectrum of the scattered light to the fluctuations at the interface is then given in (3.3.4).

Finally the broadening of the detected photocurrent power spectrum due to the finite resolution of the experimental apparatus is explained in (3.4) followed by a description of the experiment (3.5)

3.2 THEORY OF THE THERMAL FLUCTUATIONS AT THE INTERFACE

The equilibrium position of the interface between two fluids is given by the coordinates X,Y,0. The amplitude of the thermal undulations are assumed to be small compared to wavelength. $\zeta(\mathbf{r},t)$ is a vertical displacement at time t of an element of surface with its projection on the surface defined by the vector $\mathbf{r}$. For a liquid at equilibrium, $\zeta(\mathbf{r},t)$ is a macroscopic variable, such that the average of the surface displacement, $\overline{\zeta(\mathbf{r},t)}$, is equal to 0. The choice of the initial conditions, $\zeta(\mathbf{r},0)$, and boundary conditions of the surface waves at the interface, together with the hydrodynamic equations determine the probability of subsequent values of the fluctuations at any point on the surface, $\zeta(\mathbf{r}+\mathbf{R},t)$. The surface correlation function is, therefore, obtained by constructing $\overline{\zeta(\mathbf{r},0)\zeta(\mathbf{r}+\mathbf{R},t)}$ and applying thermodynamic and hydrodynamic theories.

3.2.1 QUALITATIVE DESCRIPTION OF THE HYDRODYNAMIC PROBLEM

Because of thermal agitation, the surface of a liquid is constantly displaced from its point of equilibrium and shows, as a consequence, asperities whose amplitudes are small compared to their wavelength. This surface disturbance is damped completely at a distance of 1/q within the bulk (30). Figure 3.2 shows a typical surface wave, $\zeta(x,t)$, displaced vertically from its equilibrium point (X,Y,0) with dimensions ΔX ,L, and q^{-1} ($\Delta X \ll q^{-1}$) in the direction of 0X, 0Y and 0Z respectively. The deformation of the surface is brought back toward equilibrium by capillary and gravitational forces.

$$(\gamma_i q^2 + \Delta\rho g)\,\zeta\,\Delta X\,L \qquad [3.3]$$

where

γ_i is the surface tension

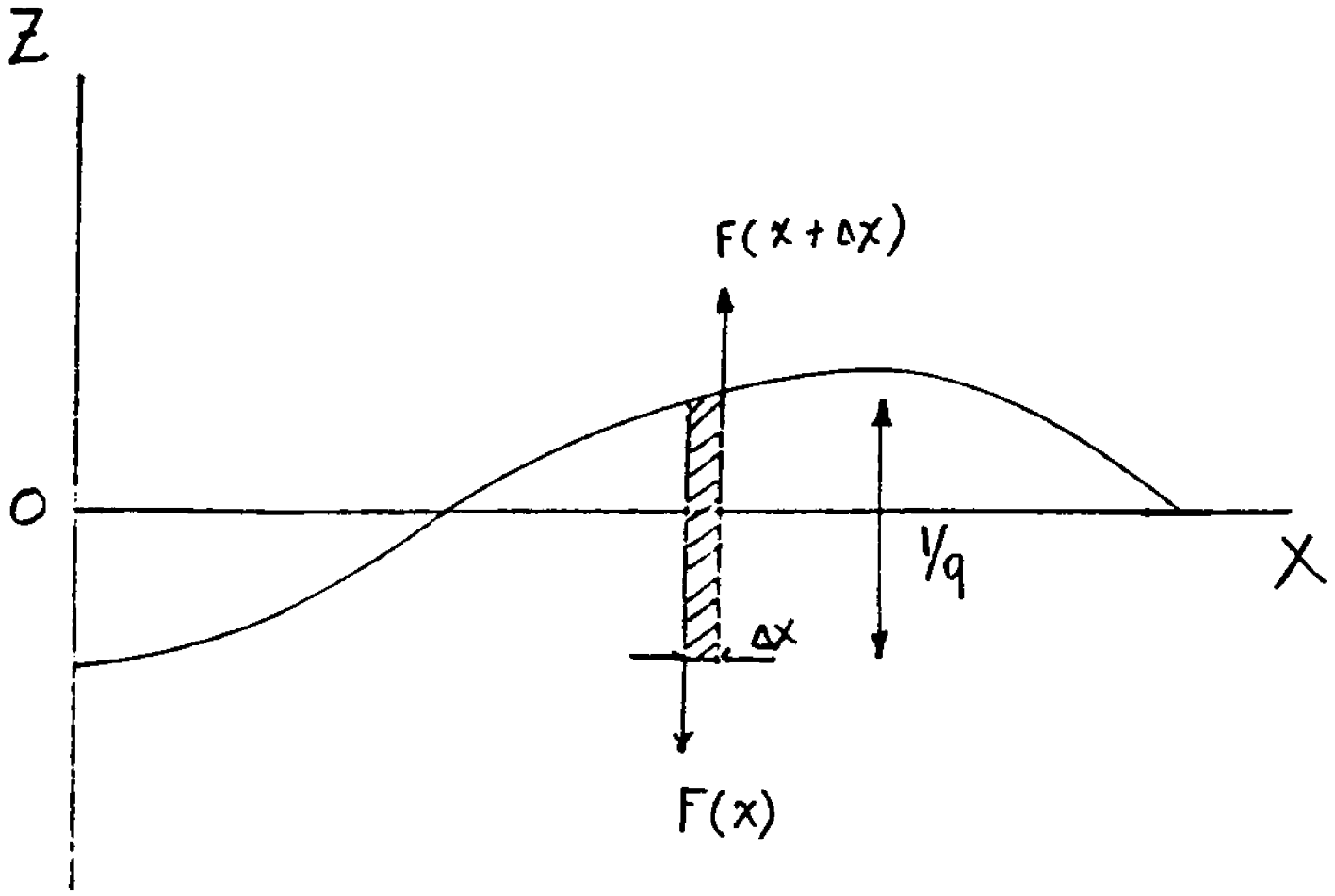

Figure 3.2 Plane section of a surface wave displaced vertically from its equilbrium point.

$\Delta\rho$ is the difference in density of the fluids

and

$\frac{\partial^2\zeta}{\partial X^2} = -q^2\zeta$ is the curvature of the surface waves.

The frictional forces of the fluid layer, F(X) and F(X + ΔX), act against neighboring layers in the opposite direction.

$$F(X) = \int_{-1/q}^{0} \eta L \left|\frac{\partial^2 V_Z}{\partial X^2}\right| dZ \qquad [3.4]$$

η = viscosity of the fluid

V_Z = the velocity of the fluid

$$F(X+\Delta X) - F(X) = \eta L \Delta X \int_{-1/q}^{0} \frac{\partial^2 V_Z}{\partial X^2}\, dZ \qquad [3.5]$$

Taking the velocity of the fluid, $d\zeta/dt$, at the interface to be near 0 at the depth of 1/q, we have

$$F(X+\Delta X) - F(X) \approx \eta q \Delta X L \frac{d\zeta}{dt} \qquad [3.6]$$

This reasoning leads to an equation of motion of a layer of fluid projected over 0Z that is qualitatively correct at high and low viscosities. Following Newton's law,

$$\rho \Delta X \frac{L}{q} \frac{d^2\zeta}{dt^2} = -\left(\gamma_i q^2 + \Delta\rho g\right) \Delta X L \zeta - \eta q \Delta X L \frac{d\zeta}{dt} \qquad [3.7]$$

$$\frac{\rho}{q} \frac{d^2\zeta}{dt^2} + \eta q \frac{d\zeta}{dt} + \left(\gamma_i q^2 + \Delta\rho g\right)\zeta = 0 \qquad [3.8]$$

This is a differential equation of an harmonic oscillator. The form of the temporal evolution which this equation describes depends on the dimensionless parameter:

$$y = \frac{\gamma_i \rho}{4\eta^2 q} = \frac{(\textit{Force of capillary}) \times (\textit{Force of inertia})}{(\textit{Force of viscosity})^2} \qquad [3.9]$$

When $y \ll 1$, The surface wave is damped exponentially as $e^{-\mu}$ with the damping coefficient

$$\mu = \frac{\gamma_i}{2\eta} q \qquad [3.10]$$

This corresponds to the surface wave being damped without propagating. The second coefficient,

$$\mu = \frac{\eta}{\rho} q^2 \qquad [3.11]$$

corresponds to a motion which is damped too rapidly to be observed.

When $y \gg 1$ the surface wave propagates as capillary waves in the form $e^{(i\omega_q - \mu)t}$. The dispersion characteristic of this wave is

$$\omega^2_q = \frac{\gamma_i}{\rho} q^3 \qquad [3.12]$$

The role of the viscosity is to dampen the propagation of the waves, therefore the damping coefficient is related to the viscosity by

$$\mu = 2 \left| \frac{\eta}{\rho} \right| q^2 \qquad [3.13]$$

The damping coefficient not only includes the viscosity, but also the wavevector **q**. Therefore, in the case of large wavevectors the undulations are damped quickly. Those of small wavevectors, the damping coefficient is relatively small even in the case of a highly viscous fluid.

A complete derivation of the dynamics of the thermal waves shows that the dispersion equation is not an harmonic oscillator, but this approximation is an excellent one when $y \gg 1$ and $y \ll 1$. For $y \simeq 1$, the evolution of the fluctuations deviate from that of the harmonic oscillator.

The gravitational and capillary forces acting on the surface waves are weak forces in comparison to the elastic forces which occur in sound waves. Therefore, the frequency of the surface wave is very small compared to that of the sound wave of equal wavevector (approximatedly 1000 times). This results in the two types of waves being totally decoupled from each other.

3.2.2 GENERAL PROPERTIES OF THE SURFACE CORRELATION FUNCTION.

The correlation function of surface fluctuations in general is $\overline{\zeta(\mathbf{r},t')\zeta(\mathbf{r}+\mathbf{R},t+t')}$. Since the thermal fluctuations at the interface are stationary, the correlation function is independent of t'. Since the surface wave is translationally invariant, it is independent of r. It depends, instead, on $|\mathbf{R}|$, the distance between two points at the interface. Therefore,

$$\overline{\zeta(\mathbf{r},t')\zeta(\mathbf{r}+\mathbf{R},t+t')} = \overline{\zeta(0,0)\zeta(\mathbf{R},t)} \qquad [3.14]$$

$$= \overline{\zeta(\mathbf{r},0)\zeta(\mathbf{r}+\mathbf{R},t)}$$

Furthermore, by the linear regression hypothesis, the initial value $\zeta(\mathbf{r},0)$ evolves in time according to the hydrodynamic equations:

$$\zeta(\mathbf{r}+\mathbf{R},t) = \zeta(\mathbf{r},0)\, f(\mathbf{r},t) \qquad [3.15]$$

Thus,

$$\overline{\zeta(\mathbf{r},0)\zeta(\mathbf{r}+\mathbf{R},t)} = \overline{\zeta(\mathbf{r},0)\zeta(\mathbf{r},0)} f(\mathbf{r},t) \qquad [3.16]$$

And the correlation function separates into an equilibrium (equal time) correlation function multiplied by the time-dependent solution to the hydrodynamic equation. Therefore,

$$f(R,t) = \overline{\zeta(\mathbf{r},0)\,\zeta(\mathbf{r}+\mathbf{R},t)} \qquad [3.17]$$

expressing $\zeta(\mathbf{r},0)$ in terms of wavevector $\mathbf{q}$.

$$\zeta_{\mathbf{q}}(0) = A^{-1}\int \zeta(\mathbf{r},0)\exp(i\,\mathbf{q}\cdot\mathbf{r})\,d^2\mathbf{r} \qquad [3.18]$$

where A is the area of the interface.

The surface wave correlation function can then be calculated

$$\overline{\zeta_{\mathbf{q}}(0)\,\zeta^{*}_{\mathbf{q}'}(t)} = A^{-2}\int\int \overline{\zeta(\mathbf{r},0)\,\zeta(\mathbf{r}+\mathbf{R},t)}\exp i[\mathbf{q}\cdot\mathbf{r} - \mathbf{q}'\cdot(\mathbf{r}+\mathbf{R})]\,d^2\mathbf{r}\,d^2(\mathbf{r}+\mathbf{R}) \qquad [3.19]$$

$$= A^{-2}\int f(R,t)\exp[-i\,(\mathbf{q}+\mathbf{q}')\cdot\tfrac{\mathbf{R}}{2}]\,d^2\mathbf{R}\int \exp[i\,(\mathbf{q}-\mathbf{q}')\cdot(\mathbf{r}+\tfrac{\mathbf{R}}{2})]\,d^2(\mathbf{r}+\tfrac{\mathbf{R}}{2}) \qquad [3.20]$$

Since the waves are translationally invariant at the interface, the surface correlation function becomes consequently

$$\overline{\zeta_{\mathbf{q}}(0)\,\zeta^{*}_{\mathbf{q}'}(t)} = 4\pi^2 A^{-2}\int f(R,\tau)\exp[-i\,(\mathbf{q}+\mathbf{q}')\cdot\tfrac{\mathbf{R}}{2}]\delta(\mathbf{q}-\mathbf{q}')\,d^2\mathbf{R} \qquad [3.21]$$

This correlation function is nonzero only if $\mathbf{q} = \mathbf{q}'$. The correlation function of wavevector $\mathbf{q}$ is then

$$F_{\mathbf{q}}(t) = A\ \overline{\zeta_{\mathbf{q}}(0)\,\zeta^{*}_{\mathbf{q}'}(t)} \qquad [3.22]$$

$$= 4\pi^2 A^{-1}\int f(R,t)\exp(-i\,\mathbf{q}\cdot\mathbf{R})\,d^2\mathbf{R}$$

Thus the translational invariance of the waves on the surface leads to the conclusion that the surface waves due to different wavevectors are not correlated. The correlation function is then written as the sum of the correlation functions of each mode.

The correlation function of the scattered light electric field due to the undulations of the surface waves of wavevector $\mathbf{q}$, $F_{\mathbf{q}}(t)$, is proportional to the

latter; its Fourier transformation with respect to time is:

$$P_q(\omega) = (2\pi)^{-1} \int_{-\infty}^{+\infty} F_q(t)\, e^{i\omega t}\, dt \qquad [3.23]$$

This is the calculated surface correlation function due to one wavevector **q**.

3.2.3 CALCULATION OF THE SURFACE CORRELATION FUNCTION

The surface correlation function is calculated by taking the average value of $\zeta_q(t)$ from a large number of samples whose initial states are known and fixed. In an incompressible liquid, the surface waves are completely specified if the vertical displacement at the interface, $\zeta_q(t)$, and the velocity component in the Z direction are known at the initial time.

Consider an ensemble of system in thermal equilibrium. Dividing it in several classes, putting those systems having the same fluctuations $(\zeta(0), V_z(Z,0))$ at a given time, t=0, in the same class, and taking the hydrodynamic solution $\zeta_q(t)$ to represent the average value of $\zeta_q(t)$ for the systems in this particular class:

$$\zeta_q(0)\zeta_{q_i}(t) = |\zeta_q(0)|^2 f_q(t) + \zeta_q(0) V_{zq}(Z,0)\, h_q(Z,t) \qquad [3.24]$$

for $t > 0$

Here, f_q and h_q are functions of the time interval, t, and do not depend on the initial conditions. Consider all the different classes; from one class to another $\zeta_q(0)$ and $V_{Zq}(Z,0)$ vary randomly, but f_q and h_q remain unchanged. Performing the averaging on the whole ensemble, we can write:

$$\overline{\zeta_q(0)\zeta_q^*(t)} = \overline{|\zeta_q(0)|^2}\, f_q(t) + \int_{-\infty}^{+\infty} \overline{\zeta_q(0) V_{Zq}^*(Z,0)}\, h_q(Z,t)\, dZ \qquad [3.25]$$

for $t > 0$

For $t < 0$ the above equation is also applicable since the correlation function $\overline{\zeta_q(0)\zeta_q^*(t)}$ is an even function of τ as a result of the stationarity of the random process.

The average value is then obtained by applying the principle of statistical mechanics to a system at equilibrium:

$$\overline{|\zeta_q(0)|^2} = \frac{k_B T}{[\gamma_i q^2 + g\,(\rho - \rho')]\,A} \qquad [3.26]$$

and

$$\overline{\zeta_q(0)\, V^*_{zq}(Z,0)} = 0 \qquad [3.27]$$

The first relation is justified in section 3.2.6. The second relation is calculated in section 3.2.7. The correlation function, therefore, depends on $f_q(t)$.

$$\overline{\zeta_q(0)\, \zeta^*_q(t)} = \overline{|\zeta_q(0)|^2} f_q(t) \qquad [3.28]$$

This is obtained by calculating the evolution of a fluctuation having its initial conditions, $\zeta_q(0)$, fixed and $V_{zq}(Z,0) = 0$. The solution of the hydrodynamic equations having these initial conditions can be obtained through its Laplace transform in the time domain and the introduction of the initial values (31).

$$\tilde{\zeta}_q(s) = \int_0^\infty \zeta_q(t) e^{-st}\, dt \qquad [3.29]$$

The problem can also be treated through the fluctuation-dissipation theorem which states that if one applies to the liquid surface a pressure force which is periodic, a deformation of the surface occurs. The corresponding change in energy on the surface is

$$-\int \zeta(\mathbf{r})\, \Psi(\mathbf{r}, t)\, d^2\mathbf{r} \qquad [3.30]$$

where Ψ is an oscillating exterior pressure.

The response of the surface acted on by the exterior pressure is described by the sum of the displacement at different points $(\mathbf{r} - \mathbf{r}')$ of the surface, caused by the exterior pressure.

$$\zeta(\mathbf{r}, 0) = \int_S d^2\mathbf{r} \int_0^\infty [\chi(\mathbf{r} - \mathbf{r}', t)\, \Psi(\mathbf{r}', t)\, d^2\mathbf{r}'\, dt]\, dt \qquad [3.31]$$

or in a vector mode

$$\zeta_q(0) = \int_0^\infty x_q(t)\, \Psi_q(t)\, dt \qquad [3.32]$$

If Ψ_q is of the form of $\Psi_q^\omega e^{-i\omega}$, $\zeta_q(0)$ will have a similar form and :

$$\tilde{\zeta}_q(\omega) = \tilde{x}_q(\omega)\, \Psi_q^\omega \qquad [3.33]$$

with

$$\tilde{x}_q(\omega) = \int_0^\infty x_q(t)\, e^{i\omega}\, dt \qquad [3.34]$$

In the classical limit of $\hbar\omega \ll k_B T$, the fluctuation-dissipation theorem states the thermal fluctuation power spectrum, $P(\omega)$, is related to the response function $\tilde{x}_q(\omega)$ by:

$$P_q(\omega) = \frac{k_B T}{\pi\omega} \mathrm{Im}(\tilde{x}_q(\omega)) \qquad [3.35]$$

It is therefore necessary to search for the response $\tilde{x}_q(\omega)$ of a system due to an exterior pressure of frequency ω.

3.2.4 RESPONSE OF A SYSTEM TO AN EXTERIOR PRESSURE, DERIVATION OF THE SPECTRAL WAVES.

Taking $\rho, \eta, \mathbf{V}, P$ as the density, viscosity, velocity and pressure of the lower phase fluid, respectively, and $\rho', \eta', \mathbf{V}', P'$ the same parameters in the upper phase fluid. (ρ', η' is not defined if the upper phase refers to the free surface of a liquid), g as the gravitational acceleration and γ_i as the interfacial tension at the interface, The hydrodynamic equations are

1) The equation of conservation of mass

2) The equation of conservation of momentum

for the lower phase and for an incompressible liquid, we have

$$div\ \mathbf{V} = 0 \qquad [3.36]$$

$$\frac{\partial \mathbf{V}}{\partial t} + (\mathbf{v}\cdot\nabla)\mathbf{V} = -\frac{1}{\rho}\nabla p + \frac{\eta}{\rho}\Delta \mathbf{V} + \mathbf{g} \qquad [3.37]$$

Let us estimate the order of magnitude of the term (V•grad)V. The fluid particles in the wave travel a distance of the order of the amplitude a during the time interval of the order of the period τ; the period of oscillation of the fluid particles in the wave. Although the velocity of the particles varies considerably over the range of τ and the wavelength λ, the average velocity is of the order of a/τ. The time derivative and the space derivative of the velocity are then of the order of V/τ and V/λ respectively. Obviously

$$(\mathbf{V}\cdot\mathbf{grad})\mathbf{V} \sim \frac{V^2}{\lambda} \sim 1/\lambda\,(a/\tau)^2 \qquad [3.38]$$

$$\frac{\partial V}{\partial t} \sim \frac{V}{\tau} \sim \left|\frac{a}{\tau}\right| \left|\frac{1}{\tau}\right| \qquad [3.39]$$

(V•grad)V is small in comparison to $\frac{\partial \mathbf{V}}{\partial t}$ if

$$(\mathbf{V}\cdot\mathbf{grad})\mathbf{V} \ll \frac{\partial \mathbf{V}}{\partial t} \qquad [3.40]$$

$$\frac{1}{\lambda}\left|\frac{a}{\tau}\right|^2 \ll \left|\frac{a}{\tau}\right| \left|\frac{1}{\tau}\right| \qquad [3.41]$$

or

$$\frac{a}{\lambda} \ll 1 \qquad [3.42]$$

$$a \ll \lambda \qquad [3.43]$$

Thus if the amplitude of the surface waves is small in comparison with the wavelength, the hydrodynamic equations can be linearized.

$$div\ \mathbf{V} = 0 \qquad [3.44]$$

$$\frac{\partial \mathbf{V}}{\partial t} = -\frac{1}{\rho}\nabla p + \frac{\eta}{\rho}\Delta \mathbf{V} + \mathbf{g} \qquad [3.45]$$

Consider a wave-vector directed toward 0X (figure 3.2). The hydrodynamic equation becomes:

$$\frac{\partial V_Z}{\partial Z} + \frac{\partial V_X}{\partial X} = 0 \qquad [3.46]$$

$$\frac{\partial V_X}{\partial t} = \frac{\eta}{\rho}\left|\frac{\partial^2 V_X}{\partial X^2} + \frac{\partial^2 V_X}{\partial Z^2}\right| - \frac{1}{\rho}\frac{\partial P}{\partial X} \qquad [3.47]$$

$$\frac{\partial V_Z}{\partial t} = \frac{\eta}{\rho}\left|\frac{\partial^2 V_Z}{\partial X^2} + \frac{\partial^2 V_Z}{\partial Z^2}\right| - \frac{1}{\rho}\frac{\partial P}{\partial Z} + g \qquad [3.48]$$

The boundary conditions at the interface, Z=0, are

$$\eta\left|\frac{\partial V_X}{\partial Z} + \frac{\partial V_Z}{\partial X}\right| = \eta'\left|\frac{\partial V'_X}{\partial Z} + \frac{\partial V'_Z}{\partial X}\right| \qquad [3.49]$$

$$-P + 2\eta\frac{\partial V_z}{\partial Z} + \Delta\rho\, g - \gamma_i\frac{\partial^2 \zeta}{\partial X^2} = -P' + 2\eta'\frac{\partial V'_Z}{\partial Z} + \Psi_q^{\omega} \qquad [3.50]$$

$$V_Z = V'_Z \qquad [3.51]$$
$$V_X = V'_X$$

$$\mathbf{V} \to 0 \qquad when \qquad Z \to -\infty \qquad [3.52]$$

Conditions 3.46 and 3.47 expresses the normal and tangential constraints, Applied on both sides of the surface and acted upon by a force of external pressure. Condition 3.48 expresses the continuity of V and 3.49 refers that the thickness of the liquid is assumed to be large in comparison to q^{-1}. $\Delta\rho$ is the difference in density between the two phases (ρ - ρ'), and $V_z|_{z=0} = \frac{\partial \zeta}{\partial t} + \frac{\partial \zeta}{\partial X}\frac{dX}{dt} \approx \frac{\partial \zeta}{\partial t}$ is an approximation of the amplitude of a wave

that is very small compared to its wavelength.

The equation of motion of the surface due to an oscillating exterior pressure, $\Psi_q^{\omega} e^{-i\omega t}$, and parallel to OX is written in the most general way as:

$$V_X = e^{iqX} e^{-i\omega t} \sum_{m_i} e^{m_i(\omega)Z} A_i(\omega) \qquad [3.53]$$

From equations 3.46, 3.47, 3.48 it can be deduced that

$$m_1 = q \qquad [3.54]$$

$$m_2 = {}^{+}\sqrt{q^2 - \frac{i\omega\rho}{\eta}} \qquad [3.55]$$

where $+\sqrt{}$ is taken as the square root of a positive rational number

Substituting $m = m_2$, we have,

$$\begin{aligned} V_X &= e^{iqX} e^{-i\omega t} [A e^{qZ} + B e^{mZ}] \\ V_Z &= -ie^{iqX} e^{-i\omega t} [A e^{qZ} + B \frac{q}{m} e^{mZ}] \\ \frac{P}{\rho} &= e^{iqX} e^{-i\omega t} A \frac{\omega}{q} e^{qZ} \end{aligned} \qquad [3.56]$$

For the upper phase

$$\begin{aligned} m' &= {}^{+}\sqrt{q^2 - \frac{i\omega\rho'}{\eta'}} \\ V'_X &= e^{iqX} e^{-i\omega t} [A' e^{-qZ} + B' e^{m'Z}] \\ V'_Z &= +ie^{iqX} e^{-i\omega t} [A' e^{-qZ} + \frac{q}{m'} B' e^{-m'Z}] \\ \frac{P'}{\rho'} &= e^{iqX} e^{-i\omega t} [A' \frac{\omega}{q}] e^{-qZ} \end{aligned} \qquad [3.57]$$

The coefficients A, B, A', B' are determined from the boundary conditions satisfying:

$$2\eta A + \eta\left(\frac{m}{q}+\frac{q}{m}\right)B + 2\eta' A' + \eta'\left(\frac{m'}{q}+\frac{q}{m'}\right)B' = 0 \qquad [3.58]$$

$$\left(2\eta\omega q + i(\gamma_i q^2 + \Delta\rho g) - i\omega^2\frac{\rho}{q}\right)A + \left(2\eta\omega q + i\gamma_i\frac{q^3}{m}\right)B - \left(2\eta'\omega q - \frac{i\omega^2\rho'}{q}\right)A' - 2\eta'\omega q\, B' = -i\omega\Psi_q^{\omega}$$

$$A + B - A' - B' = 0$$

$$A + \frac{q}{m}B + A' + \frac{q}{m'}B' = 0$$

This is a linear system of 4 equations with 4 unknowns and with the second member having an unique solution. The response ζ_q due to a perturbation $\Psi_q{}^{\omega}$ is

$$\zeta_q = e^{iqX}\, e^{-i\omega t}\,\frac{1}{\omega}\left[A(\omega) + \frac{q}{m}B(\omega)\right]\Pi_q{}^{\omega} \qquad [3.59]$$

$$\tilde{x}_q(\omega) = \frac{1}{\omega}\left[A(\omega) + \frac{q}{m}B(\omega)\right] \qquad [3.60]$$

In the case of a free surface the fluctuation of a fluid assumes $\rho' = 0$ and $\eta' = 0$. The system then reduces to two equations with two unknowns because the last two equations depend on the velocity on both sides of the surface (equation 3.51). In this case it is not a valid condition. The solution of the set of equations and the application of the theorem of fluctuation-dissipation lead to the spectrum of thermal fluctuation:

$$P_q(\omega) = \frac{\tau_o{}^2}{2\eta q}\,\frac{kT}{\pi\omega\tau_o}\,\mathrm{Im}\frac{1}{y + (1 - i\omega\tau_o)^2 - + \sqrt{1 - 2i\omega\tau_o}} \qquad [3.61]$$

where

$$\tau_o = \frac{\rho}{2\eta q^2} \qquad [3.62]$$

$$y = \frac{\rho(\gamma_i + \rho g/q^2)}{4\eta^2 q} \qquad [3.63]$$

The parameter y corresponds to that which was introduced in section 3.2.1.

$$y = \frac{(\rho/q)\times(\gamma_i q^2 + \rho g)}{(2\eta q^2)^2} = \frac{(\textit{force of inertia})\times(\textit{force of balance})}{(\textit{force of friction})^2} \qquad [3.64]$$

and τ_o has a time dimension and is inversely related to the viscosity of the liquid.

Taking $\tilde{x}_q^{\omega}$ as an analytical function of the complex variable ω, the poles of this function corresponds to the roots of the dispersion equation

$$y + (1 - i\omega\tau_o)^2 - {}^{+}\sqrt{1 - 2i\omega\tau_o} = 0 \qquad [3.65]$$

A closer look to this equation shows that with $Im(\omega) < 0$ its two roots have a dependence on y. When $y \gg 1$, both roots are complex conjugates. The surface waves propagate at the frequency ν and the damping of the wave determines the spectral linewidth centered at $\pm\nu$. When $y \ll 1$, the surface waves are damped without propagating. The spectrum has a maximum value at zero frequency. The transition from a damped surface wave to a propagating surface wave is continuous with $y = 0.145$ being the critical point and with equation 3.65 having a double root.

The spectrum of an interfacial wave, between two liquid phases, shows greater complexity than that of a free surface wave. Its power spectra, $P_q(\omega)$, includes ρ', η', and ρ, η the upper phase and lower phase density and viscosity respectively and γ_i, the interfacial tension. The power spectrum function is given as:

$$P_q(\omega) = (y\tau/\alpha_q q^2)(k_b T/\pi\omega\tau)\,\mathrm{Im}\,[D(i\omega\tau)]^{-1} \qquad [3.66]$$

$$\tau = (\rho + \rho')/2(\eta + \eta')q^2 \quad , \quad \alpha_q = \gamma_i + (\rho - \rho')g/q^2$$

and

$$y = \alpha_q(\rho + \rho')/\ 4(\eta + \eta')^2 q$$

$$D(S) = y + \frac{(\rho - \rho'^2 + 2R\rho\rho')}{(\rho + \rho')^2}\ \frac{\eta(m-1) - \eta'(m'-1)}{\eta(m+1) + \eta'(m'+1)}\ S$$

$$+ \frac{\rho\dfrac{\eta(m^2+1) + \eta'[m-1+m'(m+1)]}{m-1} + \rho'\dfrac{\eta'(m'^2+1) + \eta[m'-1+m(m'+1)]}{m'-1}}{(\rho+\rho')[\eta(m+1) + \eta'(m'+1)]} S^2$$

$$m = +\sqrt{1 + 2\frac{\rho + \rho'}{\rho + \rho' + R\rho'}S} \qquad m' = +\sqrt{1 + 2\frac{\rho + \rho'}{\rho + \rho' - R\rho}S}$$

$$R = \frac{\eta/\rho - \eta'/\rho'}{(\eta + \eta')/(\rho + \rho')}$$

$+\sqrt{}$ = positive rational number

g = gravity accéleration constant

q = wave-vector of the scattered light

T = temperature

k_b = Boltzman constant

3.2.5 COMPARISON OF THE SURFACE WAVE TO A HARMONIC OSCILLATOR.

When an oscillating perturbation of wave-vector **q** is applied at the interface at time t' = 0, it induces in the fluid a vertical displacement, $U_q(t)$, at depth z, which at time t' > 0, is related to $\zeta_q(t)$ by

$$U_q(Z,t) = \int_o^\infty K(Z, t'-t))\,\zeta_q(t)\,dt \qquad [3.67]$$

from equation 3.56 and 3.59 $U_q(Z,t)$ and $\zeta_q(t)$ can be written as

$$\zeta_q(t) = \int e^{-i\omega(t)}\,\frac{1}{\omega}\,[A(\omega) + \frac{q}{m(\omega)}\,B(\omega)]\,d\omega \qquad [3.68]$$

$$U_q(Z,t) = \int e^{-i\omega}\ \frac{1}{\omega}\,[A(\omega)e^{qZ} + \frac{qe^{mZ}}{m(\omega)}\,B(\omega)]\,d\omega \qquad [3.69]$$

Taking the Fourier transformation of equation 3.67 and taking into account equations 3.68 and 3.69, we obtain:

$$\frac{1}{\omega}\left[A(\omega)e^{qZ} + \frac{qe^{m(\omega)Z}}{m(\omega)}B(\omega)\right] = \frac{1}{\omega}\left[A(\omega) + \frac{q}{m(\omega)}B(\omega)\right]\int_o^\infty K(Z,t)e^{i\omega t}\,dt \quad [3.70]$$

For the case of a free surface (the case of an interface between two fluids is analogous), equation 3.58 becomes

$$m\,A(\omega) + q(1 - i\omega\tau_o)B(\omega) = 0 \quad [3.71]$$

and from equation 3.70 and 3.71 :

$$\tilde{K}(Z,\omega) = (2\Psi)^{-1}\int_o^\infty K(Z,t)e^{i\omega t}\,dt \quad [3.72]$$

$$= e^{qZ} + \frac{i}{\omega\tau_o}\left(e^{qZ\sqrt{1 - 2i\omega\tau_o}} - e^{qZ}\right) \quad [3.73]$$

The first term, e^{qZ}, is independent of ω and corresponds to a potential flow induced by a pressure variation. In an incompressible liquid, as the surface is displaced, the pressure variation is transmitted instantaneously into the bulk. The second term is characterized by a retardation of the order of τ_o and corresponds to the a rotational flow. In a viscous fluid ($rot\ \mathbf{V} \neq 0$) the surface displacement creates horizontal vortex lines perpendicular to q, which diffuse inside the liquid with a time constant τ_o, and progressively excites a retarded displacement under the surface.

Defining ω_1, ω_2 as the frequencies where $P_q(\omega)$ assumes significant values, in low and high damping conditions $\tilde{K}(z,\omega)$ may be simplified within the range (ω_1, ω_2). In the case of low damping $(\omega_1, \omega_2 \gg 1/\tau_o)$ and $\tilde{K}(z,\omega) \approx e^{qZ}$. For the high damping case $(\omega_1, \omega_2 \ll 1/\tau)$, $\tilde{K}(Z,\omega) \approx e^{qZ}(1 + qZ)$. In both cases $\tilde{K}$ is frequency independent in the range (ω_1, ω_2). For low damping the rotational flow has no time to set in before the surface wave has completely decayed. For high damping the rotational flow sets in faster than the wave decay. In both cases

the surface wave is not perturbed by the dispersion process associated with the transmission of a motion from the surface to the bulk. The surface response is analogous to that of a resonant system. The interface then acts like a thin membrane with the surface wave behaving like a harmonic oscillator having the same frequencies as the roots of the calculated dispersion equation.

A dissipation process in the liquid under the surface is always present but it modifies the spectrum only when its characteristic time is of the order of the time decay of the surface waves $\omega_1 < 1/\tau_0 < \omega_2$; the wave decay and the transmission of motion under the surface take place simultaneously. Therefore, the corresponding bulk dissipation process appears on the spectrum. The transition from underdamped to overdamped surface wave ($y = 0.145$) occurs near the critical damping.

3.2.6 AMPLITUDE OF THE SURFACE WAVES.

The mean square amplitude of the waves can be obtained without resorting to hydrodynamic calculations since the amplitude of the waves does not depend on their temporal evolution (22). The calculation assumes Boltzmann statistics at room temperature, $T \sim 300°K$. The region of frequency is limited to $0 < \omega < 10^{15}$ Hz because of the requirement that $\hbar\omega \ll k_B T$.

If ΔS is the variation in entropy in the liquid due to the surface fluctuations, statistical mechanics shows that the probability $\bar{\omega}$ of the fluctuations is proportional to $e^{-\Delta S / k_B}$. This variation in entropy is bounded by the minimum work required to create a reversible fluctuation at the interface.

$$\Delta S = \frac{W_{min}}{T} \qquad [3.74]$$

Where T is the absolute temperature, W_{min} is the potential energy at the interface. The deformation is done infinitely slowly. Therefore work done against the force of viscosity is negligible. The potential energy is in two parts:

1- The energy of surface tension is proportional to the increase in area, ΔA, of the interface due to deformation ($E_{p,1} = \gamma_i \cdot \Delta A$, where γ_i is the surface tension).

2- The energy required to overcome gravity.

$$E_{p,2} = \int\int (\rho - \rho') g \, \zeta \, d\zeta \, dA = \frac{A}{2}(\rho - \rho') g \, \overline{|\zeta|^2} \qquad [3.75]$$

where ρ' and ρ are respectively the densities of the upper and lower phases, g the gravitational acceleration, $\overline{|\zeta|^2}$ is the average of the squared value of $|\zeta|$ in the portion of the interface considered.

$$\Delta A = \int_A \sqrt{1 + \left|\frac{\partial \zeta(\mathbf{r},t)}{\partial x}\right|^2 + \left|\frac{\partial \zeta(\mathbf{r},t)}{\partial y}\right|^2}\, dx\, dy - A \qquad [3.76]$$

Taking the amplitude of the waves to be very small compared to the wavelength, the expression can be simplified to

$$\Delta A = \frac{1}{2}\int_A \left[\left|\frac{\partial \zeta(\mathbf{r},t)}{\partial x}\right|^2 + \left|\frac{\partial \zeta(\mathbf{r},t)}{\partial y}\right|^2\right] dx\, dy \qquad [3.77]$$

The potential energy of the waves at the interface is then

$$E_p = \frac{1}{2}\int_A \left[\gamma_i \left[\left|\frac{\partial \zeta}{\partial x}\right|^2 + \left|\frac{\partial \zeta}{\partial y}\right|^2\right] + g(\rho - \rho')\,\zeta^2\right] dx\, dy \qquad [3.78]$$

As previously stated, the surface waves can be expressed as:

$$\zeta(\mathbf{r},t) = \sum_q \zeta_q(t)\, e^{i\mathbf{q}\cdot\mathbf{r}} \qquad [3.79]$$

Since each mode of ζ_q is not correlated with other modes, the potential energy of the waves is then the sum of the energy potential of each of the modes.

$$E_p = \frac{A}{2}\sum_q [\gamma_l q^2 + g(\rho - \rho')]|\zeta_q(t)|^2 d^2q$$

$$= \sum_q E_p(\mathbf{q}) \qquad [3.80]$$

The probability $\bar{\omega}$ of a wave is obtained as the product of the probabilities relative to each mode.

$$\bar{P} = \frac{e^{-E_p/kT}}{\int e^{-E_p/kT} dE_p} = \prod_q \frac{e^{-E_p(\mathbf{q})/kT}}{\int e^{-E_p(\mathbf{q})/kT} dE_p(\mathbf{q})} \qquad [3.81]$$

The average value of $|\zeta_q(t)|^2$ can then be calculated from the probability $\bar{\omega}(\mathbf{q})$

$$|\zeta_q(t)|^2 = \frac{\int e^{-E_p(\mathbf{q})/kT} |\zeta_q|^2 dE_p(\mathbf{q})}{\int e^{-E_p(\mathbf{q})/kT} dE_p(\mathbf{q})} \qquad [3.82]$$

$$|\zeta_q(t)|^2 = \frac{kT}{[\gamma_l q^2 + g(\rho - \rho')]A} \qquad [3.83]$$

Because the process is stationary the average value of $\overline{|\zeta_q(t)|^2}$ is independent of time.

From the average of the square of the surface waves of wave-vector $\mathbf{q}$, the average squared of the amplitude of the waves is calculated.

$$\overline{|\zeta|^2} = \sum_q \overline{|\zeta_q|^2} \qquad [3.84]$$

If the interface is of dimension L × L, the wave-vector then satisfies the relation

$$q^2 = \frac{\pi^2}{L^2}(n^2 + m^2) \qquad [3.85]$$

where n and m are integers. It follows

$$\overline{|\zeta|^2} = \sum_m \sum_n \frac{k_B T}{(\gamma_l \frac{\pi^2}{A}(n^2 + m^2) + \Delta\rho g)A} \qquad [3.86]$$

replacing the sum for an integral we have

$$\overline{|\zeta|^2} = \int_{q_0}^{q_1} \frac{1}{2\pi} \frac{k_B T}{(\gamma_i q^2 + \Delta\rho \cdot g)} q \, dq \qquad [3.87]$$

$$\overline{|\zeta|^2} = \frac{kT}{4\gamma_i \pi} Log \left| \frac{\gamma_i q_1^2 + \Delta\rho \cdot g}{\gamma_i q_0^2 + \Delta\rho \cdot g} \right| \qquad [3.88]$$

where q_0 is a very small wave-vector.

$$q_0 = \frac{\pi}{L} \qquad [3.89]$$

Because the dimension of the interface increases as $q_0 \rightarrow 0$, the lower limit of the integral is determined by the term $\Delta\rho \cdot g$. This is due to the fact that the amplitude of the undulations of large wavelengths is small.

If q_1 is the upper limit wave-vector of the integral, when $q_1 \rightarrow \infty$ the integral diverges. As the wave-vector q_1 approaches infinity, the wavelength approaches the intermolecular distance. Since only those surface waves having a wave length longer than that of the wave length of light are detectable by the incident light beam, $q_1 \approx 2\pi/\lambda$. The waves which are of interest are, therefore, those with wave-vectors that lies between $1/\lambda$ and 0.

$$\overline{|\zeta|^2} = \frac{kT}{4\gamma_i \pi} Log \frac{\gamma_i (2\pi/\lambda)^2}{\Delta\rho \cdot g} \qquad [3.90]$$

3.2.7 CORRELATION BETWEEN THE VERTICAL DISPLACEMENT OF THE INTERFACE AND THE VELOCITY OF THE FLUID BENEATH.

It should be noted that for a single wave ζ_q, the solution to the hydrodynamic equations give a definite velocity field in the fluid adjacent to the surface. In fact, the surface wave has a penetration depth of the order of 1/q and a displacement at the surface cannot be dissociated from the liquid flow underneath and viceversa. The present derivation applies to the overall fluid in thermal equilibrium. Here, there is no correlation between the vertical displacement of the interface and the velocity of the fluid below this interface, considered at the same time.

$$\overline{V_Z(X,Z,t)\zeta(X_o,t)} = 0 \qquad [3.91]$$

Where the average is taken over an ensemble of systems in thermal equilibrium.

Expressing $V_z(X,Z)\zeta(X_o)$, For each system, as a function of position q_i and momentum p_i of the individual particles, we have

$$V_z(X,Z)\zeta(X_o) = \sum_i \frac{1}{N} \frac{p_{z,i}}{m_i} \times \sum_j \frac{1}{N'} q_{z,j} = A\,(p_i q_j) \qquad [3.92]$$

Where N and N' are the number of particles inside small volume elements V and V' around the points X, Z and X_o, Z_o=0. If N and N' are large and if the volume elements have dimensions that are small compared to 1/q, the final result will be independent of their choice. The average quantity can then be written as:

$$\overline{V_Z(X,Z)\zeta(X_o)} = \bar{A} \propto \int_{-\infty}^{\infty} dp_i \ldots \int_{V'} dq_j \ldots A\,(p_i,q_j)\, e^{-\beta H(p_i,q_j)} \qquad [3.93]$$

where **H** is the Hamiltonian of the microscopic system. In the absence of a magnetic field, it is time reversal invariant. When time is reversed the position of the particle is unchanged and its momentum is reversed:

$\mathbf{H}(p_i, q_j) = -\mathbf{H}(-p_i, q_j)$. Using the definition of A

$$A(p_i, q_j) = -A(-p_i, q_j). \qquad [3.94]$$

the result is

$$\bar{A} = -\bar{A} \quad or \quad \bar{A} = 0. \qquad [3.95]$$

The result holds for any X and X_o, therefore:

$$\int \overline{V_z(X_o, Z)\,\zeta(X - X_o)}\, dX_o = 0 \qquad [3.96]$$

or taking the Fourier transform with respect to x:

$$V_{z,q}(Z)\cdot\zeta_q^* = 0. \qquad [3.97]$$

A similar proof could be used to show the absence of correlation between two different physical quantities considered at the same time, providing their product is an odd function of time.

3.3 SCATTERED LIGHT CAUSED BY THERMAL WAVES AT THE INTERFACE

3.3.1 CHARACTERISTICS OF SCATTERED LIGHT

Consider an interface between two liquids covered by a set of waves of different phase shift and amplitude and with a range of wavelengths which covers a large range of the spectrum. The amplitude of the surface fluctuations, ζ_q, is assumed to be very small compared to the wavelength of light, λ.

$$\frac{\zeta_q}{\lambda} \ll 1 \qquad [3.98]$$

In this approximation, the surface waves of wave-vector **q** can be treated independently of each other. The interface can then be treated from the viewpoint of optics as a superposition of waves with phases of periodicity $2\pi/q$. When a beam reaches the interface, it is reflected (spectrum of zero order) and also diffracted by each of the waves at the interface. J.W. Rayleigh (33) has shown that the intensity of the spectrum of order n is scattered from the interface proportionally to $(\zeta_q/\lambda)^n$. Therefore only first order scattering has a non-neglegible intensity, thus establishing a relation between the angle of observation, and the wave-vector **q**. At a defined direction of observation the spectrum of the scattered light is associated to one and only one surface wave-vector whose intensity is at a maximum, corresponding to a first order scattering intensity.

Assume a scattered beam in the direction of θ_s, ϕ, originated from a point P on the interface. ν_q is the frequency of the surface wave responsible for the scattering at point P. The incident light beam with frequency ν_o undergoes a Doppler effect on its scattered beam with a frequency shift of $\pm\nu$ from a first

order scattering of the light.

$$\nu_o - \nu_s = \pm \nu_q \qquad [3.99]$$

This can also be looked at as an annihilation or creation of surface phonons.

Incident photon + surface phonon $\longrightarrow$ scattered photon

Incident photon - surface phonon $\longrightarrow$ scattered photon

The frequency relation may also be treated from the energy conservation perspective. Taking $1/\tau$, the life span of a surface phonon, the scattered beam shows two peaks with frequency $\nu_s = \nu_o \pm \nu_q$ with linewidth of τ/π. The wave-vector q, and the direction of the scattered light are related through the principle of momentum conservation. Taking $(\mathbf{K}_o)_{plane}$ and $(\mathbf{K}_s)_{plane}$ as the projection of the reflected, $\mathbf{K}_o$, and scattered, $\mathbf{K}_s$, beams wave-vector on the surface plane (figure 3.1)

$$(\mathbf{K}_o)_{plane} - (\mathbf{K}_s)_{plane} = \pm \mathbf{q} \qquad [3.100]$$

Transforming the relation in scalar terms

$$q^2 = K_s^2 \sin^2\theta_o + K_o^2 \sin^2\theta_o - 2K_s K_o \sin\theta_o \sin\theta_s \cos\phi \qquad [3.101]$$

where

θ_o = angle of incidence at the interface

θ_s = angle between the scattered ray and the normal

ϕ = angle defined by the plane of reflection and the plane of scattering

The frequency shift is small compared to the frequency of the scattered light (the frequency of the incident light is $\simeq 10^{15}$ Hertz).

$$K_s \approx K_o \qquad [3.102]$$

therefore:

$$q^2 = K_o^2 (\sin^2\theta_o + \sin^2\theta_s - 2\sin\theta_s \sin\theta_o \cos\phi) \qquad [3.103]$$

3.3.2 INTENSITY OF THE SCATTERED LIGHT

The intensity of scattered light due to the fluctuations at the interface of two liquids or at a free surface of a liquid have been studied by Mandelstam(22). The assumptions involved in his calculations were:

1.- $\zeta_q / \lambda \ll 1$, the amplitude of the fluctuations of the surface or interface is very small compared to the wavelength of the incident light. The interface can be taken as a superposition of waves with wavelength $2\pi/q$. These waves scatter light independently of each other and only in the first order scattering spectrum.

2.- $qD \gg 2\pi$, the diameter of the light beam, D, on the liquid surface is large compared to the wavelength of the surface fluctuations. This allows the assumption of light scattered from an incident beam of infinite diameter.

3.- The thickness of the interface (zone where the refractive index varies appreciably) is small compared to the wavelength of light.

First Mandelstam, then Andronov, Leontovich and Gans (23) determined the scattered beam intensity to be

$$\frac{dI}{d\Omega}(q) = I_o \frac{16\pi^2}{\lambda^2} \left| \frac{A}{A'} \right| \frac{\overline{|\zeta_q|^2}}{\lambda^2} f(\theta_o, \theta_s, \phi, N) \qquad [3.104]$$

where

I_o is the intensity of the incident beam on the surface A at the interface, A' is the projection of A on a plane normal to the direction of observation, N

$= n_r / n_i$, where n_i and n_r are the refractive index of the media of the reflected and refracted light respectively, and $\overline{|\zeta_q|^2}$ is the average of the squared of the amplitude of the surface fluctuations of wave-vector q

$$\overline{|\zeta_q|^2} = \frac{k_B T}{\gamma_i q^2 + \Delta\rho \cdot g} \qquad [3.105]$$

Experimentally, usually $\gamma_i q^2 > \Delta\rho \cdot g$. $\overline{|\zeta_q|^2}$ then varies proportional to $1/q^2$. Therefore the scattered light will have non-neglegible intensity in the neighborhood of the reflected and refracted beam, where the magnitude q of is small. The geometry of a reflected and a refracted light on an interface with their respective scattered beams is shown in figure 3.3, where θ_o and θ_s are defined as the angle of reflection and the angle of scattering on reflection respectively, θ'_o and θ'_s are the angle of refraction and the angle of scattering on refraction, and the angles ϕ and ϕ' are defined between the plane of reflection and the plane of scattering on reflection and the plane of scattering on refraction, respectively.

The function $f(\theta_o, \theta_s, \phi, N)$ is tabulated on table 3.1. The distinction between light scattered on reflection and light scattered on refraction is provided by the upper indices R and T respectively. The polarization of the incident beam is assumed to be paralled ($\parallel$) or normal ($\perp$) to the plane of incidence. The function $f(\theta_o, N)$, on table 3.1, represents $f(\theta_o, \theta_s, \phi, N)$ by a small scattering angle ($\phi = 0, \theta_s \approx \theta_o, \theta' \approx \theta'_o$).

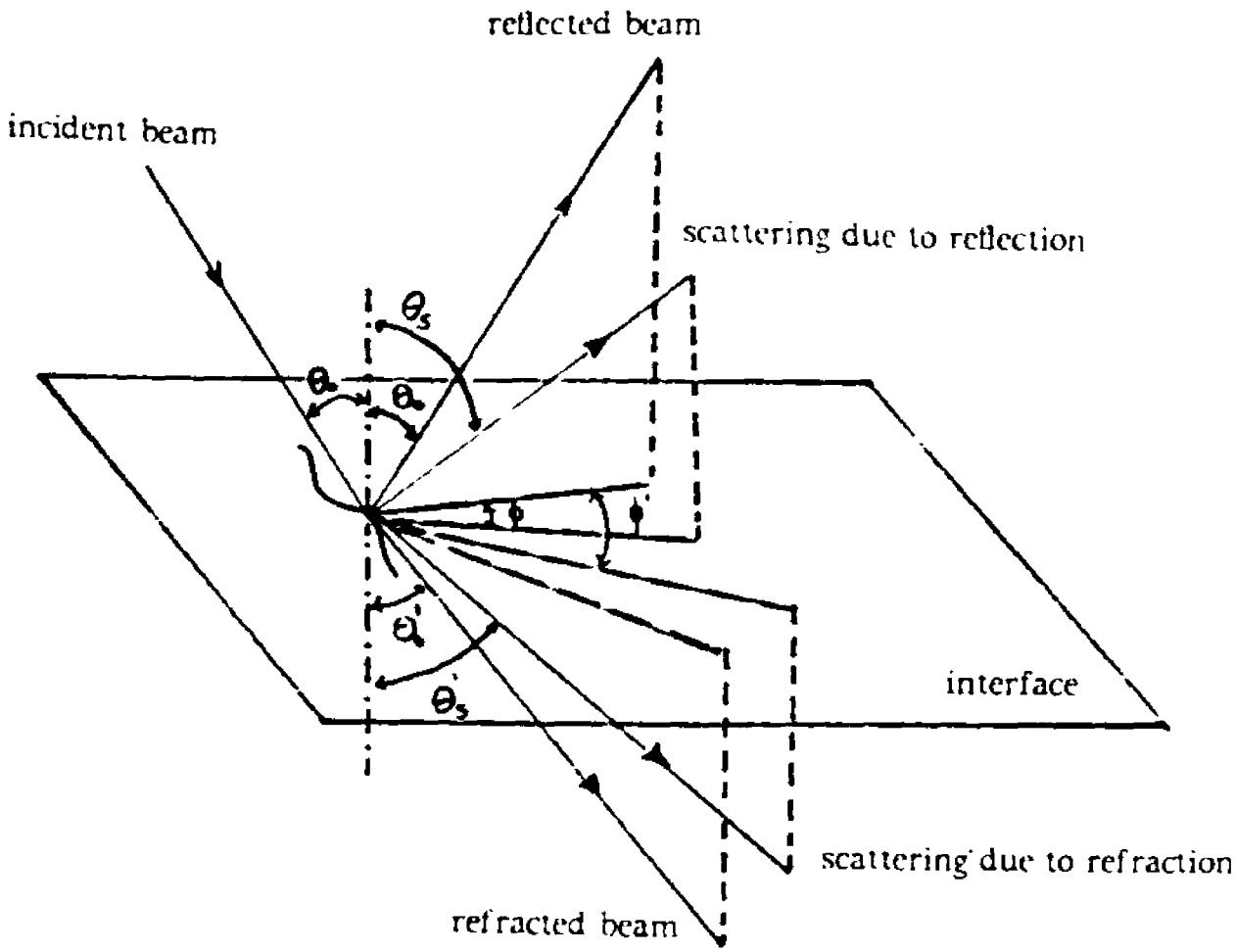

Figure 3.3 Geometry of a reflected and scattered light due to reflection, a refracted and scattered light due to refraction from an incident light at an interface.

TABLE 3.1: Angular dependency of the intensity of the scattered reflected beam and the scattered refracted beam. The function $f(\theta_o, N)$ represents $f(\theta_o, \theta_s, \phi, N)$ by a small scattering angle and $\phi=0$.

TABLE 3.1

3.106	$f^R_{\parallel}(\theta_o, \theta_s, \phi, N)$	$\left\| \frac{(N^2-1)\,[\cos\theta_o \cos\theta_s\, \xi]}{\delta} \right\|^2 + \ldots$
3.107	$f^R_{\perp}(\theta_o, \theta_s, \phi, N)$	$\left\| \frac{(N^2-1)\,[\cos\theta_o \cos\theta_s \cos\phi]}{\beta} \right\|^2 + \ldots$
3.108	$f^T_{\parallel}(\theta_o, \theta_s, \phi, N)$	$N^3 \left\| \frac{(N^2-1)\,[\cos\theta_o \cos\theta'_s\, \psi]}{\delta} \right\|^2 + \ldots$
3.109	$f^T_{\perp}(\theta_o, \theta_s, \phi, N)$	$N^3 \left\| \frac{(N^2-1)\,[\cos\theta_o \cos\theta'_s \cos\phi]}{\beta} \right\|^2 + \ldots$
3.110	$f^R_{\parallel}(\theta_o, N)$	$\left\| \frac{\tan(\theta_o-\theta'_o)}{\tan(\theta_o+\theta'_o)} \right\|^2 \cos^4\theta_o$
3.111	$f^R_{\perp}(\theta_o, N)$	$\left\| \frac{\sin(\theta_o-\theta'_o)}{\sin(\theta_o+\theta'_o)} \right\|^2 \cos^4\theta_o$
3.112	$f^T_{\parallel}(\theta_o, N)$	$N^3 \left\| \frac{\tan(\theta_o-\theta'_o)}{\sin(\theta_o+\theta'_o)} \right\|^2 \cos^2\theta_o \cos^2\theta_o$
3.113	$f^T_{\perp}(\theta_o, N)$	$N^3 \left\| \frac{\sin(\theta_o-\theta'_o)}{\sin(\theta_o+\theta'_o)} \right\|^2 \cos^2\theta_o \cos^2\theta_o$

where

$\xi = (\cos\theta'_o \cos\theta'_s \cos\phi - \sin\theta_o \sin\theta_s)$ $\qquad$ $\delta = (N\cos\theta_o + \cos\theta'_o)(N\cos\theta_s + \cos\theta'_s)$

$\psi = (\cos\theta'_o \cos\theta_s \cos\phi + \sin\theta'_o \sin\theta_s)$ $\qquad$ $\beta = (\cos\theta_o + N\cos\theta'_o)(\cos\theta_s + N\cos\theta'_s)$

R = scattered light from a reflected beam
T = scattered light from a refracted beam
$\parallel$ = polarization of the beam normal to the surface
$\perp$ = polarization of the beam parallel to the surface

3.3.3 COMPARISON OF THE INTENSITY OF THE LIGHT SCATTERED ON REFLECTION AND ON REFRACTION

In order to compare both intensities, the solid angle of the light scattered on reflection, $d\Omega$, in the direction of θ_s, ϕ, and the light scattered on refraction, $d\Omega'$, in the direction θ'_s, ϕ' should be such that the scattered light in $d\Omega$ and $d\Omega'$ is due to the same fluctuation at the interface. In the range of the surface waves of wavevector $\mathbf{q}$ within the interval $q_x, q_x + dq_x ; q_y, q_y + dq_y$, the wavevectors and their scattered angles are related according to

$$-\sin\theta_0 + \sin\theta_s \cos\phi = \frac{\lambda q_x}{2\pi} \qquad [3.114]$$

$$\sin\theta_s \sin\phi = \frac{\lambda q_y}{2\pi} \qquad [3.115]$$

$$-\sin\theta'_0 + \sin\theta'_s \cos\phi' = \frac{\lambda' q_x}{2\pi} \qquad [3.116]$$

$$\sin\theta'_s \sin\phi' = \frac{\lambda' q_y}{2\pi} \qquad [3.117]$$

The intensity of the scattered light in the solid angle $d\Omega = \sin\theta_s\, d\theta_s\, d\phi$ and $d\Omega' = \sin\theta'_s\, d\theta'_s\, d\phi'$ is from to the same wavevector $\mathbf{q}$ if we approximate $\phi \simeq 0$ and $\phi' \simeq 0$. The relation then becomes

$$d\Omega' = \left|\frac{\lambda'}{\lambda}\right|^2 \frac{\cos\theta_s}{\cos\theta'_s}\, d\Omega \qquad [3.118]$$

$$d\Omega' = \frac{1}{N^2}\frac{\cos\theta_s}{\cos\theta'_s}\, d\Omega \qquad [3.119]$$

This study of the intensity of the scattered light by surface waves with a constant relative index, N, and incident angle θ_0 is reduced to a study of the

angular factors (equations 3.104 and 3.118)

$$F^R = f^R / \cos\theta_o \qquad [3.120]$$

due to scattering on reflection, and

$$F^T = f^T \left| \frac{1}{N^2 \cos\theta'_o} \right| \frac{\cos\theta_o}{\cos\theta'_o} \qquad [3.121]$$

due to scattering on refraction.

Table 3.2 shows the expression of F^R and F^T when the polarization of the incident beam is either parallel or normal to the incident plane. These formulas is summarized into the following expressions:

light scattered on reflection

$$\frac{dI(q)}{d\Omega} = \frac{16\pi^2}{\lambda^2} \frac{\overline{|\zeta_q|^2}}{\lambda^2} I_R \cos^3\theta_o \qquad [3.126]$$

where I_R is the intensity of the reflected beam.

light scattered on refraction

$$\frac{dI(q)}{d\Omega} = \frac{16\pi^2}{\lambda^2} \frac{\overline{|\zeta_q|^2}}{\lambda^2} I_T \frac{\sin^2(\theta_o - \theta'_o)}{\sin^2\theta'_o} \frac{N}{4} \cos\theta_o \qquad [3.127]$$

I_T is the intensity of the transmitted beam.

When the coefficient N is equal to 1, equations 3.123 and 3.125 are identical. The intensity of the light scattered on reflection and the light scattered on refraction, with a polarization normal or on the plane of incidence, is proportional to 1/N. Thus, if N is close to 1, the intensity of the light scattered on refraction is independent of the polarization of the incident beam and is practically equal to the intensity of the light scattered on reflection, polarized normal

TABLE 3.2: Intensity of the scattered light by surface fluctuation with a constant relative index N, and incident angle θ_o.

TABLE 3.2		
3.122	$F^R_{\parallel} = R_{\parallel} \cos^3\theta_o$	$R_{\parallel} = \left\lvert \frac{\tan(\theta_o - \theta'_o)}{\tan(\theta_o + \theta'_o)} \right\rvert^2$
3.123	$F = R_{\perp} \cos^3\theta_o$	$R_{\perp} = \left\lvert \frac{\sin(\theta_o - \theta'_o)}{\sin(\theta_o + \theta'_o)} \right\rvert^2$
3.124	$F^T_{\parallel} = (N/4)\, T_{\parallel} \frac{\sin^2(\theta_o - \theta'_o)}{\sin^2\theta'_o} \cos\theta_o$	$T_{\parallel} = \left\lvert \frac{2 \sin\theta'_o \cos\theta_o}{\sin(\theta_o + \theta'_o)\cos(\theta_o - \theta'_o)} \right\rvert$
3.125	$F^T_{\perp} = (N/4)\, T_{\perp} \frac{\sin^2(\theta_o - \theta'_o)}{\sin^2\theta'_o} \cos\theta$	$T_{\perp} = \left\lvert \frac{2 \sin\theta'_o \cos\theta_o}{\sin(\theta_o + \theta'_o)} \right\rvert$

where

Index $\parallel$ = polarization parallel to the plane of incidence

index $\perp$ = polarization normal to the plane of incidence

Index R = light scattered from a to reflected beam

Index T = light scattered from a refracted beam

R = reflection coefficient

T = refraction coefficient

to the plane of incidence.

Introducing the notation

$$N^* = n_i / n_r = N^{-1} \qquad \text{if } n_i > n_r$$

$$N^* = n_r / n_i = N \qquad \text{if } n_i < n_r$$

If N^* and θ_o are fixed, the intensity of the light scattered on reflection is maximized when the light is polarized normal to the plane of incidence. In fact, the intensity of this scattered light is proportional to the reflected light. This is at a maximum when the polarization is normal to the surface because of the inequality (equations 3.122, 3.123, 3.126, 3.127)

$$\left[\frac{\sin(\theta_o - \theta'_o)}{\sin(\theta_o + \theta'_o)}\right]^2 \geq \left[\frac{\tan(\theta_o - \theta'_o)}{\tan(\theta_o + \theta'_o)}\right]^2 \qquad [3.128]$$

Keeping N^* constant, the intensity of the scattered light is then a function of θ_o. This presents a very pronounced maximum when the incident light is propagated in the medium of higher refractive index and around $\theta_o = (\theta_o)_{crit}$, corresponding to the critical angle. In this case, the maximum is then independent on the direction of polarization.

3.3.4 SPECTRUM OF THE SCATTERED LIGHT

We have yet to relate the thermal waves at the interface to the intensity of the scattered light. The scattered light is subject to a Doppler effect from the fluctuations. The spectrum of the scattered light then reflects the temporal evolution of the amplitudes of the waves at the interface. The objective is to relate the spectrum of the scattered light to that of the power spectrum, $P_q(\omega)$ of the fluctuations at the interface.

Defining E_o as the amplitude of the electric field of the incident beam with frequency ν_o, and assuming, for the moment that the fluctuations at the interface are motionless, the electric field $E_s(K_s, t)$ scattered in the direction K_s by the fluctuations ζ_q is a function of the incident and the scattering angles, the relative refractive index between both phases ($N = n_r/n_i$) and the wavelenght of the incident light beam.

$$E_s(\mathbf{K}_s, t) = E_o\, e^{-i\omega_o t}\, H(\mathbf{K}_o, \mathbf{K}_s, \lambda, N, \zeta_q) \qquad [3.129]$$

The function H is zero if $\zeta_q = 0$, except in the direction of the reflection. Taking $\zeta_q / \lambda \ll 1$, H can be expanded in a polynomial series. The zero order term is zero, except in the direction of the regular reflection. Only the first order term in ζ_q / λ is important.

$$E_s(\mathbf{K}_s, t) = E_o e^{-i\omega_o t} H_1(\mathbf{K}_o, \mathbf{K}_s, \lambda, N)\, \frac{\zeta_q}{\lambda} \qquad [3.130]$$

Since the amplitudes of the surface waves fluctuate with time, the electric field of the scattered light, $E_s(\mathbf{K}_s, t)$, at any point in its line of propagation depends on the state of the fluctuations at the time (t-a/c), where a/c is the time of propagation of the scattered light between the interface and the point of

observation.

$$E_s(\mathbf{K}_s, t) = E_o e^{-i\omega_o t} H_1(\mathbf{K}_o, \mathbf{K}_s, \lambda, N) \frac{\zeta_q(t - a/c)}{\lambda} \qquad [3.130A]$$

The power spectrum of the electromagnetic field is given by (32)

$$P_s(\mathbf{K}_s, \omega) = \lim_{T \to \infty} \frac{\overline{|E_s^T(\mathbf{K}_s, \omega)|^2}}{2T} \qquad [3.131]$$

with

$$E_s^T(\mathbf{K}_s, \omega) = \frac{1}{2\pi} \int_{\infty}^{-\infty} E_s^T(\mathbf{K}_s, t) e^{i\omega t} dt \qquad [3.132]$$

$$E_s^T(\mathbf{K}_s, t) = E_s(\mathbf{K}_s, t) \qquad if \ |t| < T \qquad [3.133]$$

$$E_s^T(\mathbf{K}_s, t) = 0 \qquad if \ |t| > T \qquad [3.134]$$

The average is a statistical average of an ensemble of systems from a thermodynamic point of view.

From equations 3.130A, 3.131 and 3.132

$$P_s(\mathbf{K}_s, \omega) = \lim_{T \to \infty} \left| \frac{1}{2T} \frac{E_o^2}{\lambda^2} K_1 K_1^* \int_{-\infty}^{\infty} \int_{-\infty}^{\infty} e^{-i(\omega_o - \omega)(t' - t'')} \right. \qquad [3.135]$$

$$\left. \overline{\zeta_q^T(t') \zeta_q^{T*}(t'')} \, dt' dt'' \right|$$

with

$$\zeta_q^T(t) = \zeta_q(t) \qquad if \ |t| < T \qquad [3.136]$$

$$\zeta_q^T(t) = 0 \qquad if \ |t| > T \qquad [3.137]$$

from

$$\tau = t' - t''$$

$$2t = t' + t''$$

$$P_s(\mathbf{K}_s, \omega) = \lim_{T \to \infty} \left| \frac{1}{2T} \frac{E_o^2}{\lambda^2} K_1 K_1^* \int_{-\infty}^{\infty} \int_{-\infty}^{\infty} e^{-i(\omega_o - \omega)\tau} \overline{\zeta_q^T(t - \tau/2)\, \zeta_q^T(t + \tau/2)}\, d\tau\, dt \right| \qquad [3.138]$$

Since the fluctuations are stationary

$$\overline{\zeta_q^T(t - \tau/2)\, \zeta_q^T(t + \tau/2)} = 0 \qquad [3.139]$$

if $|t - \tau/2|$ and $|t + \tau/2| > T$

and if $|t - \tau/2|$, $|t + \tau/2| < T$, and $\tau/t \ll 1$ when $t \to \infty$, it is equal to $F_q(\tau)$, where

$$\lim_{T \to \infty} \frac{1}{2T} \int_{-\infty}^{\infty} \overline{\zeta_q^T(t - \tau/2)\, \zeta_q^T(t + \tau/2)}\, dt = \overline{\zeta_q(0)\, \zeta_q(\tau)} = F_q(\tau) \qquad [3.140]$$

The power spectrum becomes

$$P_s(\mathbf{K}_s, \omega) = \frac{E_o^2}{\lambda^2} K_1 K_1^* \int_{-\infty}^{\infty} e^{-i(\omega_o - \omega)\tau} F_q(\tau)\, d\tau \qquad [3.141]$$

The spectrum of the scattered light then reflects the spectrum of the surface waves displaced from ω_o (frequency of the incident beam) in the frequency domain. From relation 3.101, the cross-section of the scattered light is

$$\frac{d^2 I(\omega + \omega_o, q)}{d\omega\, d\Omega} = \left| I_o \frac{16\pi^2}{\lambda^2} \left(\frac{A}{A^*}\right) \frac{f(\theta_o, \theta, \Phi, N)}{\lambda^2} \right| P_q(\omega) \qquad [3.142]$$

the first term refers to the properties of the incident beam and the refractive indices of both phases; the second term represents the power spectrum of the surface waves.

3.4 BROADENING OF THE EXPERIMENTAL SPECTRUM BECAUSE OF INSTRUMENTAL FACTORS

experimentally one can never select just one surface wave so that the detected signal contains overlap of several spectra from wavevectors near the desired one. The shift in the peak frequency of the various spectra overlapping the detected signal causes an increase in width of the measured power spectrum over that expected from a single wavevector. This excess broadening of the power spectrum is attributed to several instrumental effects.

1) Because of convergence of the laser beam, the angle of reflection at the interface is not $\Delta\theta$, but a set of angles within the interval $\Delta\theta \pm \delta(\Delta\theta)$. The finite radius of the laser beam, thus, illuminates a finite number of waves with different wavevectors q.

2) The width of the pinhole aperture at the photomultiplier limits the sets of angles, $\Delta\theta \pm \delta(\Delta\theta)$, of the scattered light detected by the photomultiplier. It allows the detection of the scattered light falling within the aperture and truncates those falling beyond the aperture.

3) The circuitry at the detector introduces noise with a characteristic decay time.

The measured power spectrum is, thus, a superpositioning of several spectras of wavevectors inside a finite range $q_o \pm \Delta q$. The portion of the instrument effect due to the narrowing and truncation of the beam is independent of time. Therefore, the experimental power spectrum, $P(\omega)$, is a convolution of a wavenumber dependent instrumental function and the theoretical power spectrum, $P_q(\omega)$, of a single wave vector of the surface fluctuations (in the case of a liquid/liquid interface it refers to equation 3.66).

$$P(\omega) = \sum_{\Delta q = -N}^{N} F(\Delta q / \sigma) \times P_q(\omega, q_o + \Delta q) \qquad [3.143]$$

where

$F(\Delta q / \sigma)$ = intensity distribution of the various spectra of different wavevectors superimposed on the measured power spectrum.

$P_q(\omega, q_o + \Delta q)$ = theoretical power spectrum of a single wavevector of the surface fluctuation

N = spread of wavenumbers

σ = width of the instrument function, F,to be optimized

q_o = magnitude of the experimentally determined wave-vector - equation 3.103.

The instrumental response function can be estimated by comparing the power spectrum predicted by equation 3.143 with various trial functions F with an experimentally obtained power spectrum of a fluid whose properties are well known. Such comparisons have been made with a spectrum obtained from the carbon tetrachloride/air interface. In our determination of the instrument function a fixed spread of wavenumbers, N, was used and σ was optimized for each trial function F. Through fitting of several spectra of different wavenumbers, we found that the instrumental response was best represented by a Lorentzian squared function which, when inserted in equation 3.143, gives

$$P(\omega) = \sum_{\Delta q = -N}^{N} (1/ [(\Delta q / \sigma)^2+1]^2) \times P_q(\omega, q_o + \Delta q) \qquad [3.144]$$

Figure 3.4 shows a calibration spectrum of carbon tetrachloride. The continuous line was obtained by fitting the convoluted function to the dots (data points). The spectrum was obtained at q_o = 196.42 cm^{-1}, with the assumed spread of wavenumbers N = 50. The best fit was obtained at σ = 15.62 . Although other

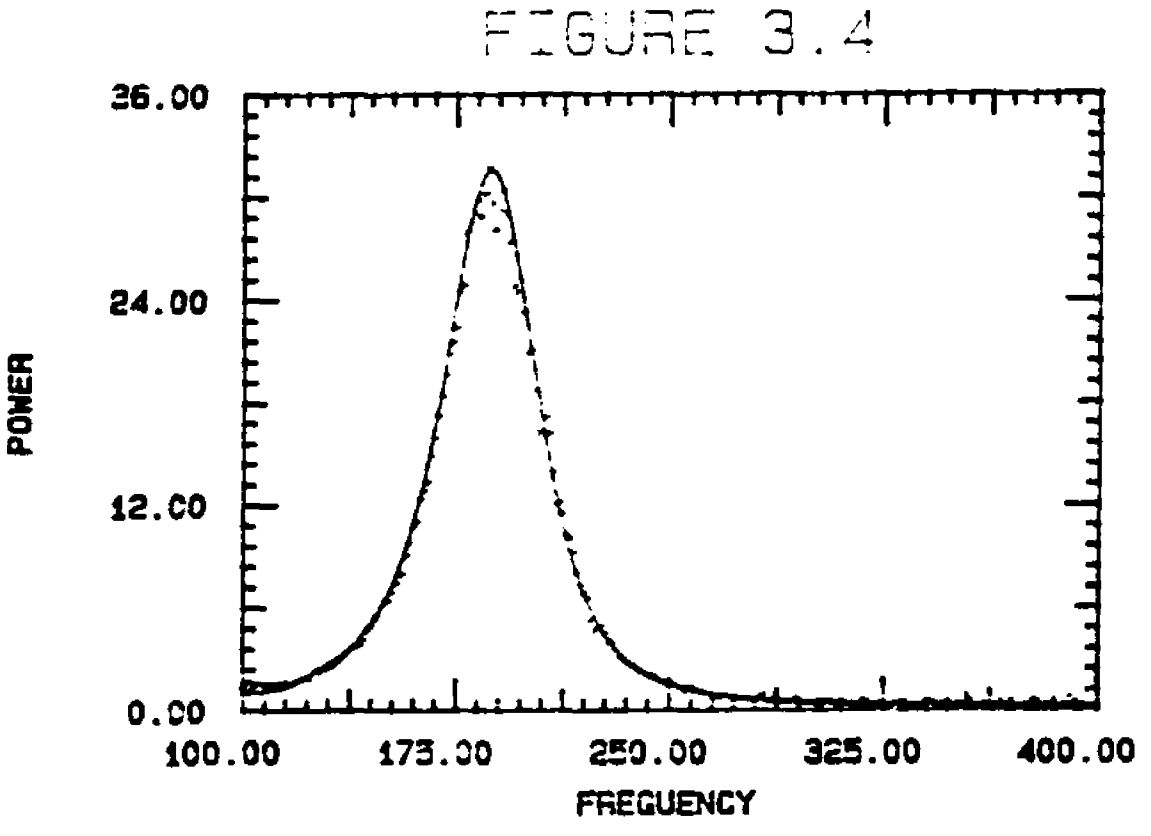

Figure 3.4 Experimental spectrum of light scattered by the free surface of carbon tetracloride recorded at 23 °C for a wave vector of 196.42 cm^{-1}. The solid line is the result of a fit performed with equation 3.141 having N = 50 and σ = 15.62.

investigators have found that a Gaussian instrumental function gives a good fit to their spectra (6, 13, 28), in our analysis the Gaussian function gave a poor fit.

3.5 EXPERIMENTAL

3.5.1 THEORY OF HETERODYNE PHOTON SPECTROSCOPY

The surface wave fluctuations were studied using Heterodyne Optical Intensity Fluctuation Spectroscopy. A review and detailed analysis of the technique is given by Cummins and Swinney (25). The capillary waves of the liquid interface act as an extremely weak oscillating diffraction grating. When illuminated by a laser beam, they give rise to a weak, modulated light beam scattered by a small angle from the reflected main beam. The intensity (10^{-15}) of the diffracted beam is, however, too small to be analyzed directly. Therefore, the scattered light is mixed coherently on the photocathode of the detector with a stronger light beam which acts as the local oscillator. Incident Laser Light reflected from the interface and diffracted by a diffraction grating, as first implemented by Hård (28), acts as a local oscillator. The scattered beams mixing with the much stronger local oscillator beam from the diffraction grating on the photocathode of the detector will cause a modulation of the amplitude, I(t), of the detector current. The power spectrum of this modulation depicts the amplitude modulation of the capillary waves and is recorded with a spectrum analyzer.

Semiquantitatively, the electric field at the photocathode surface is made up of two components. One is due to the diffraction grating and is expressed as $E_o \cos\omega_o t$, where ω_o is the incident light frequency and E_o is the time independent amplitude. The second component is due to diffraction from the liquid interface

waves and is expressed as $E_1(t)\cos\omega_o t$ and $E_2(t)\sin\omega_o t$, where the amplitude $E_1(t)$ and $E_2(t)$ are related to the instantaneous amplitude and phase of the surface waves and are functions of time.

The photocurrent I(t) is proportional to the square of the total electric amplitude integrated over the detector surface.

$$I_o + I(t) \alpha \int_s [E_o \cos\omega_o t\ E_1 \cos\omega_o t + E_2 \sin\omega_o t]^2 dS \qquad [3.145]$$

$$= 1/2 \int_s [E_o^2 + 2E_o E_1(t) + E_1^2(t) + E_2^2(t)] dS \qquad [3.146]$$

+ light frequency terms which are not detected.

The "local oscillator field" E_o has a greater intensity than $E_1(t)$ and $E_2(t)$ so that the last terms in equation 3.146 can be neglected. The recorded signal is the remaining time-dependent signal I(t) of the current, $\int_s E_o E_1(t) dS$. Half of the information $E_2(t)$ is thus lost in the detection process.

The field E_o, due to the grating, is concentrated within a diffraction spot which is displaced at an angle $(\theta_o - \theta_s) \sim \lambda/a$ from the main beam, where a is the spacing of the grating. Thus only those liquid surface waves which form diffraction spots overlapping the diffraction spot due to the grating contribute significantly to the signal. This condition is only fulfilled by surface waves in the X direction (figure 3.5) with wavelength $2\pi/k \sim a/\cos\theta$.

Since $E_1(t)$ is proportional to the corresponding instantaneous surface amplitude, the current I(t) gives the time variation of the surface waves of wavelength $a/\cos\theta$. Thus with this simplified picture of the apparatus the power spectrum of I(t) equals the power spectrum of the surface waves, apart from a constant factor. A more thorough development of the diffraction grating

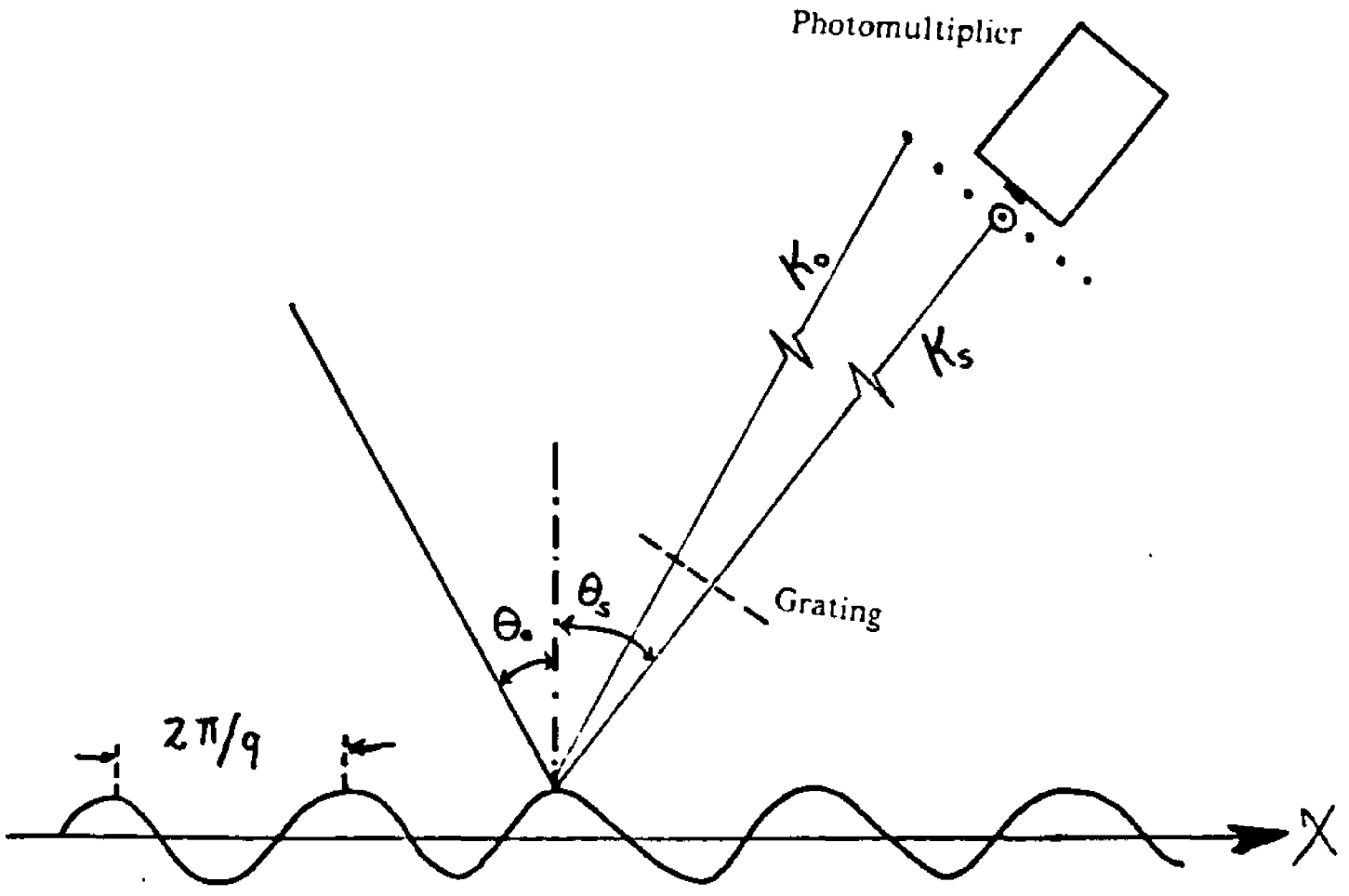

Figure 3.5 The principle of operation of a diffraction grating. One diffraction order is selected by an aperture and beats with scattered light coincident with it on the detector. • Local oscillator light. O scattered light.

is given by Hård (28).

There are several practical advantages to using a diffraction grating to select a surface wave number.

1) It is easier to measure accurately the grating spacing than to measure the small angle ($\theta_o - \theta_s$).

2) Large-scale shaking of the liquid surface due to external vibrations is minimized and no longer becomes a major problem.

3) The well-controlled local oscillator (the diffracted light from the grating) makes the measurements easily reproducible.

3.5.2 INSTRUMENTAL SETTING OF THE EXPERIMENT

The arrangement of the experimental equipment for the laser light scattering experiments is shown schematically in figure 3.6. The laser beam was spatially filtered and expanded with a focusing lens of 2.9 cm focal length before being focused on the detector. In the experiment, the beam was directed to the sample interface at an angle of 22°, measured from the horizontal in the air medium, by means of mirrors. The beam was directed to the interface from the phase of higher refractive index to obtain total reflection. The cell containing the two phases was mounted on a movable platform which could be moved in each of the three orthogonal directions.

In the experiment, light scattered in the plane of incidence, $\phi = 0$, was selected for analysis of the power spectrum. The reflected beam was intercepted by a diffraction grating located about 2 cm from the point of reflection at the interface. After the beam traveled 275 cm in length (measured from the point of reflection at the interface to the photomultiplier), one of the diffraction

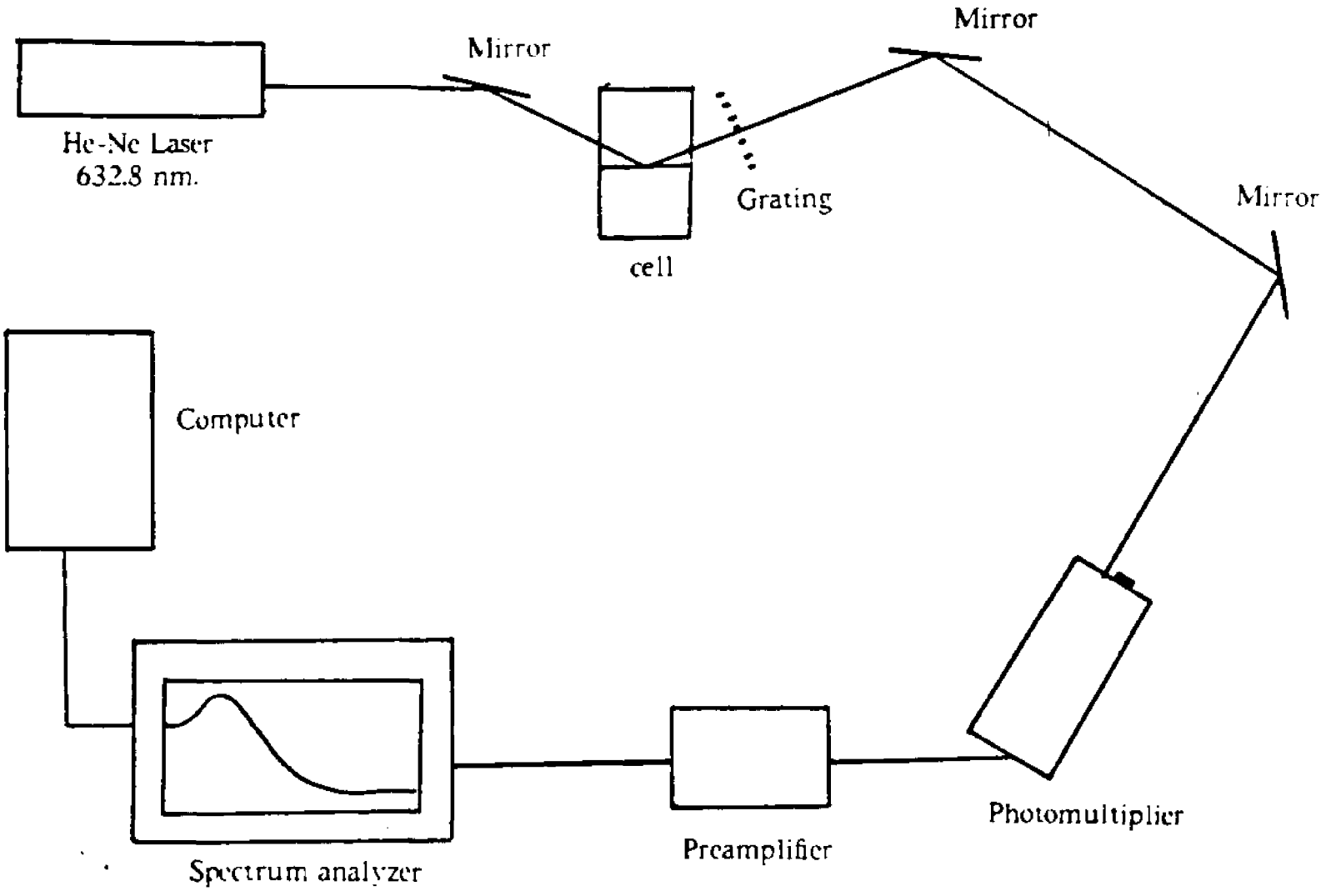

Figure 3.6 Equipment setup of the laser light scattering experiment.

orders was selected by an aperture in front of the photomultiplier detector. The diffracted light beat with light scattered by capillary waves of a particular wavevector falling on the same area (figure 3.5). The aperture for the photomultiplier was selected such that the size of the pinhole would be the same as the diffraction spot due to the grating. The photodetector current was amplified by a low-noise preamplifier which also rejected low frequency noise before the signal reached the spectrum analyzer. From the spectrum analyzer the data was transferred to a PDP 8 computer and then to the VAX 11/780 for analysis. The analysis of the data was performed with a nonlinear Least-Squares fitting procedure (appendix E and F) with the theoretical equation 3.144 representing the power spectrum.

3.5.3 EXPERIMENTAL DETERMINATION OF WAVEVECTOR q

The magnitude of wavevector q was determined using equation 3.103. The angle of reflection, θ_o, was determined as follow: the angle ϕ (figure 3.7) of the reflected beam was measured normal to the wall of the cell. This angle was related to ϕ', the angle of incidence at the wall of the cell in the liquid phase, by Snell's law:

$$n \sin\phi = n' \sin\phi' \qquad [3.147]$$

where

n = refractive index of the air medium

ϕ= angle of refraction in the air medium, measured normal to the cell wall.

n'= refractive index of the liquid phase.

ϕ'= angle of incidence in the liquid phase measured normal to the cell wall.

From the complementary angle of ϕ' the angle of reflection was then calculated.

In determining the angle of scattering the relation $\theta_s = \theta_o + d\theta$ was used. Starting from Snell's law, equation 3.147, with n=1 and $\phi' = 90 - \theta_o$ (figure 3.7).

$$\sin\phi = n\,'\sin\phi' = n\sin(90-\theta_o) \qquad [3.148]$$

From the derivative of equation 3.148

$$\cos\phi\, d\phi = n\,'\cos(90-\theta_o)(-d\theta) \qquad [3.149]$$

Therefore,

$$-d\theta = \frac{1}{n'}\frac{\cos\phi}{\cos\phi'}d\phi \qquad [3.150]$$

$d\phi$ is equivalent to the distance from the reflected beam to the aperture on the photomultiplier over the distance the beam traveled from the cellto the photomultiplier.

The wavevector of the reflected light beam was taken as $\mathbf{k}_o/n'$.

3.5.4 INSTRUMENTS

In our laser light scattering investigation of the temporal evolution of the capillary waves the following instruments were used:

1) A 35 mW, 632.8 nM Helium-Neon laser (Spectra-Physics, model 124, 1250 W. Middlefield Road, Mountain View, CA. 94042).

2) A FFT computing Spectrum Analyzer from Nicolet Scientific Co., 446B Mini-Ubiquitous (245 Livingston Street, Northvale, N.J., 07647).

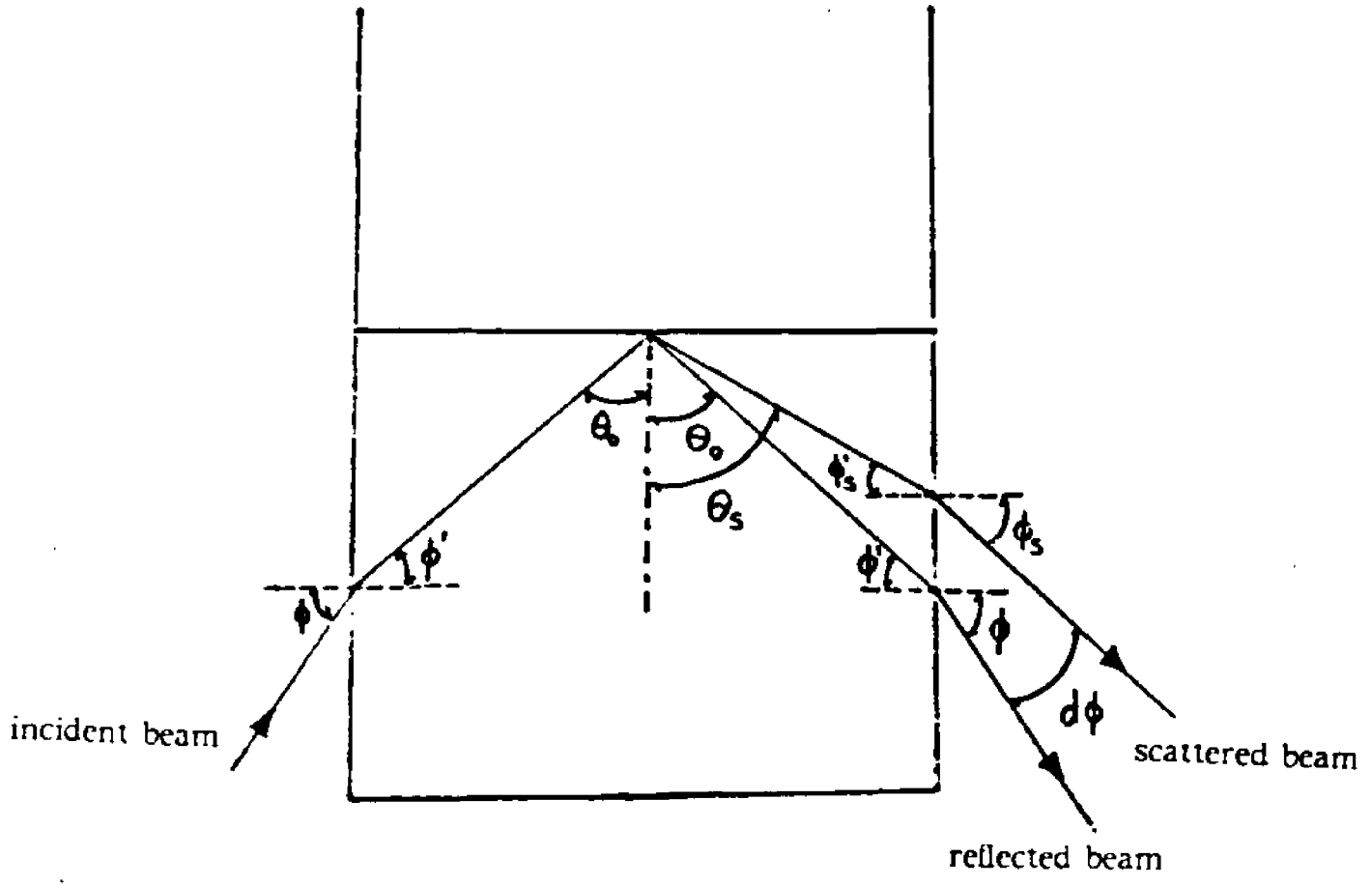

Figure 3.7 Definition of the measured reflected and scattered angles at the cell to obtain the experimentally determined q wave vector.

3) A Calibrated High Voltage Source from Power Designs Inc., Model 2K20, 1-202 VDC, 0-20 mA (1700 Shames Drive, Westbury, N.Y. 11590).

4) A EG & G Park model 113, Low-Noise Preamplifier (P.O. Box 2565, Princeton, N.J. 08540).

5) A Hamamatsu PM-R550, photomultiplier and a PDP 8 computer.

6) A focusing lens of 2.9 cm focal length.

7) A set of diffraction gratings made by photographing a computer generated set of parallel lines.

CHAPTER 4

SYSTEMS STUDIED IN MEASURING LOW AND ULTRALOW INTERFACIAL TENSION

4.1 INTRODUCTION

In the investigation of the laser light scattering technique as a method for measuring low, and ultralow interfacial tension, three systems were selected and studied.

1) Toluene / water / 1-propanol

2) 46.35% toluene / 1.95% sodium dodecyl sulfate / 3.75% 1-butanol / 47.95% Saline NaCl

3) Carbon tetrachloride

In systems of toluene/water/1-propanol change in the concentration of 1-propanol provided a range of interfacial tensions of 35 mN/M (toluene/water interface) to 0.3 mN/M. In the quaternary systems change in the concentration of NaCl in saline furnished a range of interfacial tensions of 10^{-1} mN/M (4% NaCl) to 10^{-3} mN/M (7% NaCl). The density, viscosity, and refractive index of each of the phases of the systems studied were measured at various temperatures, and their values were fitted to linear equations as a function of temperature with a Linear Least Squares program. The density was measured with a 10 ml picnometer and the viscosity was determined with an Ostwald viscometer. A thermostated refractometer, Fisher Scientific Co., was used to measure the refractive index.

4.2 CHEMICALS

Toluene, propanol, butanol and NaCl were all reagent grade and distributed by Fisher Scientific Co., Pittsburg, P.A. 15219. Sodium dodecyl sulfate was also reagent grade and produced by J.T. Baker Chemical Co., Phillipsburg, P.A. 08865. Carbon tetrachloride was also reagent grade and produced by Amend Drug and Chemical Co., Irvington, N.J. 07111. Freshly distilled water was used in all preparations.

4.3 TOLUENE / WATER / 1-PROPANOL SYSTEM

1-Propanol acts as a solubilizing agent for toluene and water. Upon addition of sufficient 1-propanol to a toluene/water system, 1-propanol is partially hydrated/solvated by water and toluene molecules and the interface eventually disappears. This is seen in the ternary phase diagram of water/toluene/1-propanol system at 21.5 °C, shown in figure 4.1. Mixtures of equal volumes of water and toluene in different amounts of 1-propanol were selected for the study. Because of the change in density due to variations in temperature, the solutions were prepared by weight. The density of toluene, water and 1-propanol were selected from the *CRC Handbook of Chemistry and Physics* 38th edition and are given as follows:

Toluene = 0.86694 gm/mL

1-Propanol = 0.8044 gm/mL

water = 0.9982 gm/mL

In this investigation, solutions containing 5 ml of toluene, 5 ml of water and various volumes of 1-propanol were made. The desired volumes were converted into weights using the selected density values. The proper amount were then

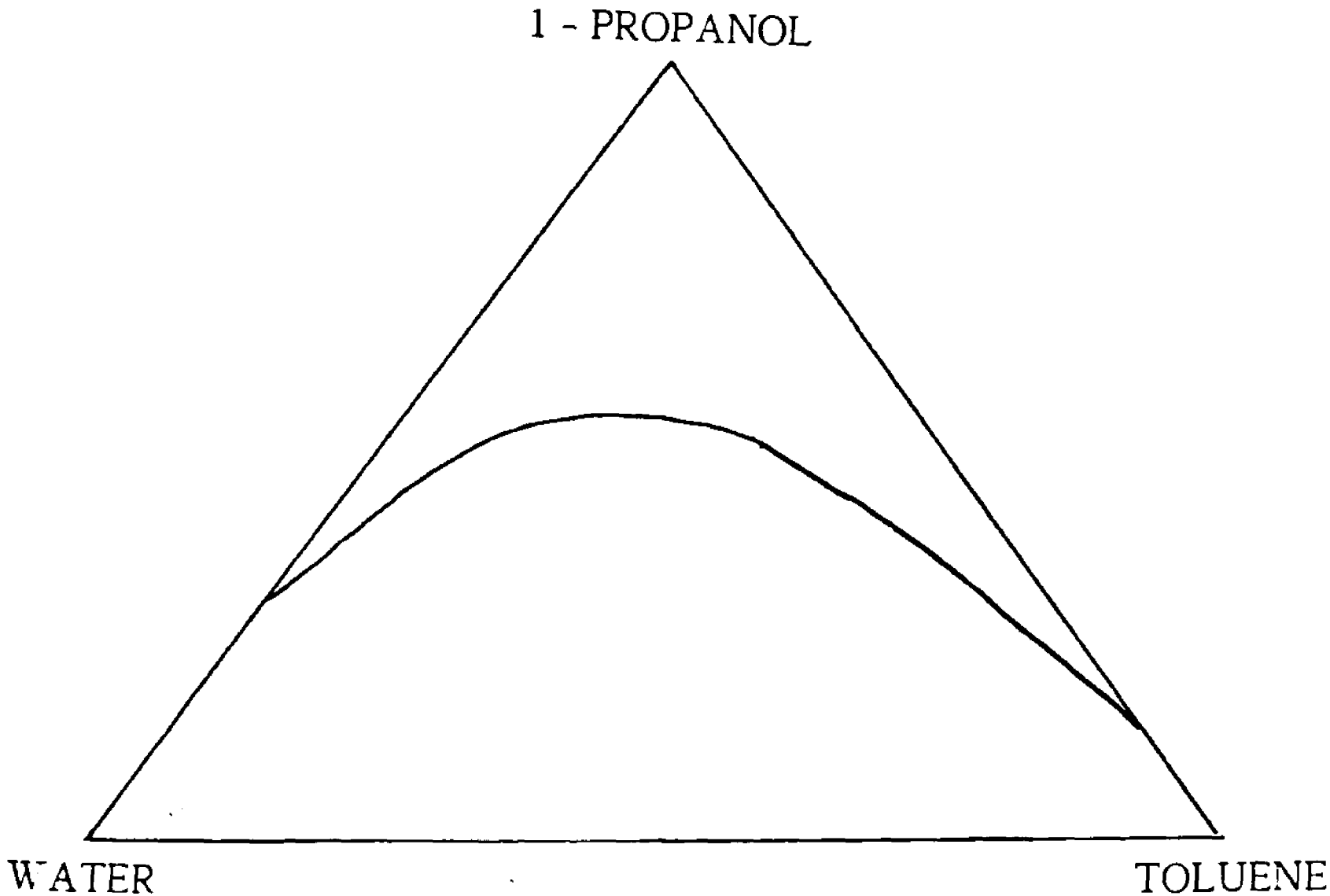

Figure 4.1 Ternary phase diagram of toluene, water, 1-propanol system at temperature 21.5 °C.

weighed out and mixed. Following each addition of alcohol, the solutions were thoroughly shaken and left overnight in an air conditioned room. The lower phase volume of the cosolubilized systems was plotted against the amount (mL) of 1-propanol added. This is shown in figure 4.2. It is seen from the figure that the toluene/water interface dissappears and the system becomes solubilized after the addition of 15.6 ml of 1-propanol.

In addition, the density, viscosity and refractive index of each of the phases were measured at 5 ml of toluene and 5 ml of water with the concentration of 1-propanol at 0, 3, 5, 6, 7, 8, 10, 12, 14 mL. The measurements were performed at various temperature ranging from 15 to 30 °C. The interfacial tension of these solutions over the same temperature range were also measured. Table 4.1 shows the linearlized equations representing the behavior of each physical property as a function of temperature. The temperatures measured were in degrees Celsius, the densities were in gm/ml, the viscosities were determined in centipoise and the interfacial tensions in mN/M. Figure 4.3 illustrates the change in interfacial tension at 21°C, as 1-propanol (mL) was added. The left ordinate curve shows the values of interfacial tension measured in the region from 0 to 10 mL. The interfacial tension (left hand side ordinate mN/M) measurements were made using a sandblasted Teflon blade. The right ordinate curve shows the measurements obtained in the region from 8 to 18 mL of added 1-propanol. The interfacial tension in this curve (right hand side ordinate in 10^{-3} mN/M) was measured with the spinning drop method. The apparent change in slope of the curves in these figures is due to a change in scale of ordinate axis. Extrapolation of the right hand curve to $\gamma = 0$ yields a 1-propanol volume of 17.6 mL. Note that this volume is different from the amount necessary to solubilize the system to a monophasic state (figure 4.2).

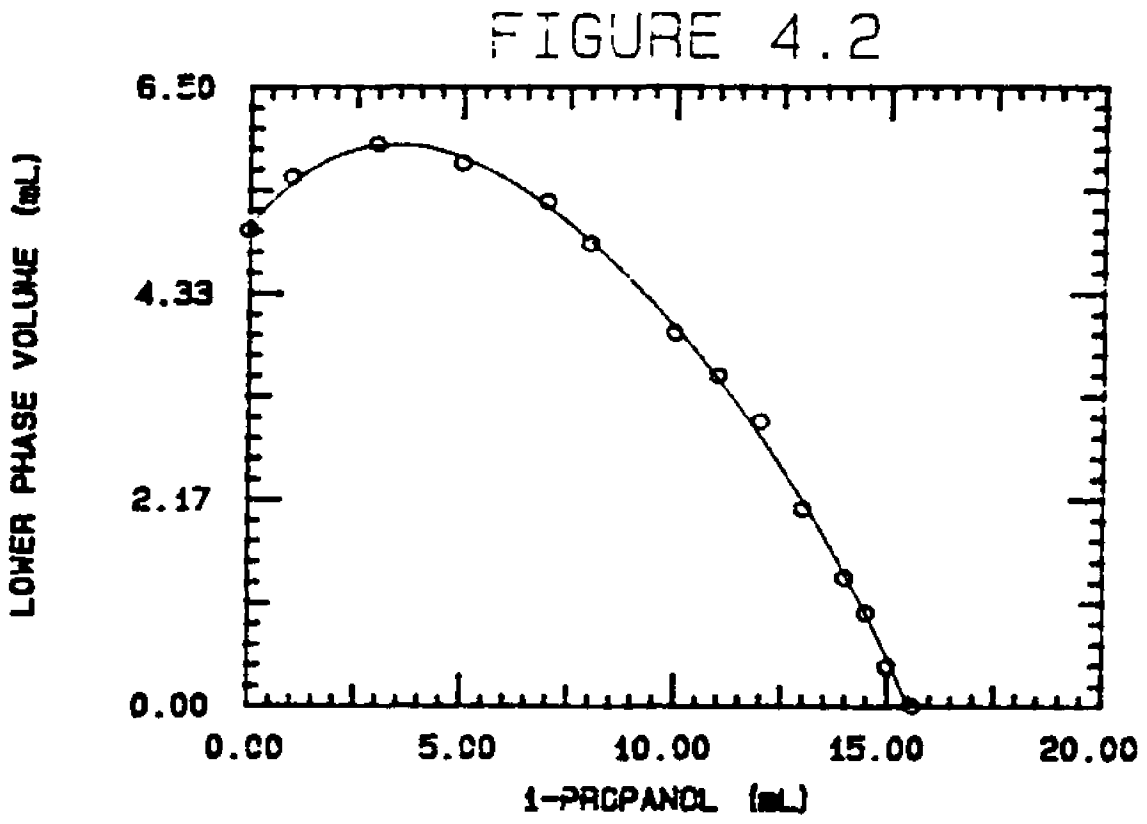

Figure 4.2 Lower phase (aqueous) volume as a function of solubilizing agent 1-pentanol. Initial system 5 mL toluene/5 mL water. The lower phase disappeared after addition of 15.6 ml of 1-Propanol. Temperature 21.5 °C.

TABLE 4.1: Linear fit of the bulk thermodynamic properties as a function of temperature of 5 mL water, 5 mL toluene, at different volumes of 1-propanol. Temperature unit, degrees Celsius; viscosity, Centipoise; density, gm/mL; and interfacial tension, mN/M.

TABLE 4.1			
y = mT + b			
	phase	m	b
5 water, 5 toluene, 3 1-propanol system			
refractive index	upper	-5.484×10^{-4}	1.4734
	lower	-1.564×10^{-4}	1.3511
density	upper	-6.571×10^{-4}	0.8661
	lower	-3.549×10^{-4}	0.9831
viscosity	upper	-1.157×10^{-2}	1.0414
	lower	-5.096×10^{-2}	3.0166
interfacial tension		-1.986×10^{-2}	2.9805
5 water, 5 toluene, 5 1-propanol system			
refractive index	upper	-4.797×10^{-4}	1.4521
	lower	-2.002×10^{-4}	1.3530
density	upper	-9.620×10^{-4}	0.8717
	lower	-4.395×10^{-4}	0.9839
viscosity	upper	-1.831×10^{-2}	1.4490
	lower	-5.372×10^{-2}	3.1438
interfacial tension		-1.718×10^{-2}	2.0788

TABLE 4.1 *(continued)*

$y = mT + b$

	phase	m	b
5 water, 5 toluene, 6 1-propanol system			
refractive index	upper	-4.896×10^{-4}	1.4448
	lower	-2.410×10^{-4}	1.3552
density	upper	-3.276×10^{-4}	0.8722
	lower	-5.151×10^{-4}	0.9883
viscosity	upper	-2.786×10^{-2}	1.8550
	lower	-7.018×10^{-2}	3.5801
interfacial tension		-5.514×10^{-3}	1.3906
5 water, 5 toluene, 7 1-propanol system			
refractive index	upper	-4.333×10^{-4}	1.4328
	lower	-2.396×10^{-4}	1.3571
density	upper	-7.912×10^{-4}	0.8705
	lower	-4.425×10^{-4}	0.9867
viscosity	upper	-3.313×10^{-2}	2.0663
	lower	-8.633×10^{-2}	3.9549
interfacial tension		-1.158×10^{-2}	1.5640
5 water, 5 toluene, 8 1-propanol system			
refractive index	upper	-4.476×10^{-4}	1.4281
	lower	-2.308×10^{-4}	1.3567
density	upper	-1.023×10^{-3}	0.8691
	lower	-7.828×10^{-4}	0.9911
viscosity	upper	-3.244×10^{-2}	2.1214
	lower	-6.574×10^{-2}	3.4725
interfacial tension		-1.320×10^{-2}	1.4047

TABLE 4.1 *(continued)*

$y = mT + b$

	phase	m	b
5 water, 5 toluene, 10 1-propanol system			
refractive index	upper	-4.903×10^{-4}	1.4182
	lower	-2.235×10^{-4}	1.3567
density	upper	-6.411×10^{-4}	0.8633
	lower	-4.555×10^{-4}	0.9723
viscosity	upper	-3.801×10^{-2}	2.4832
	lower	-6.429×10^{-2}	3.4592
interfacial tension		-1.520×10^{-2}	1.1867
5 water, 5 toluene, 12 1-propanol system			
refractive index	upper	-4.711×10^{-4}	1.4133
	lower	-2.573×10^{-4}	1.3580
density	upper	-7.458×10^{-4}	0.8689
	lower	-3.981×10^{-4}	0.9717
viscosity	upper	-4.259×10^{-2}	2.7391
	lower	-6.914×10^{-2}	3.6431
interfacial tension		-1.105×10^{-2}	0.7511
5 water, 5 toluene, 14 1-propanol system			
refractive index	upper	-4.524×10^{-4}	1.4118
	lower	-2.637×10^{-4}	1.3597
density	upper	-7.721×10^{-4}	0.8680
	lower	-5.589×10^{-4}	0.9712
viscosity	upper	-4.984×10^{-2}	3.0988
	lower	-6.539×10^{-2}	3.5548
interfacial tension		-7.839×10^{-3}	0.5665

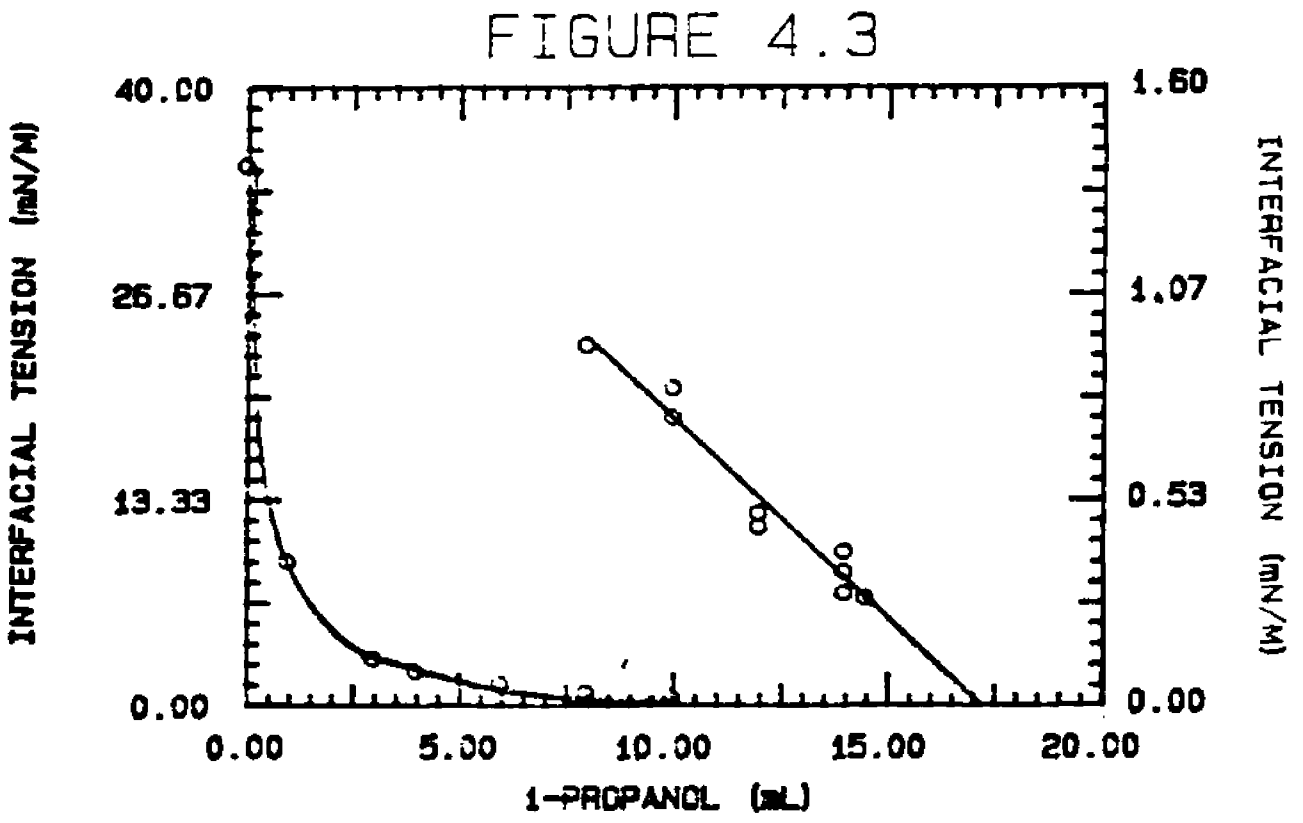

Figure 4.3 Change in interfacial tension as a function of volume of 1-propanol added to 5 ml water, 5 ml toluene. Left side ordinate shows the region from 0 to 10 mL of added 1–propanol. Right side ordinate shows the region from 8 to 18 mL. The apparent change in slope of the curve in these figures is due to a change in scale of the ordinate axis. Temperature 21.5 °C.

4.4 46.35% TOLUENE / 1.95% SODIUM DODECYL SULFATE / 3.75% 1-BUTANOL / 47.95% NACL (AQUEOUS) SYSTEM

Mixtures of water, oil, alcohol, and surfactant can give rise to stable, transparent or translucent solutions. Figure 4.4 relates to this type of complicated emulsion system. 1.95% Na dodecyl sulfate, 3.75% 1-butanol, 46.35% toluene were mixed with a 47.95% saline solution at different concentration of NaCl. The concentration of NaCl was calculated as grams of NaCl in 100 grams of solution. Each NaCl system was thoroughly shaken in a graduated cylinder and left in an air conditioned room at 21.5 °C for several days until the volumes of each phase remained constant, indicating a state of equilibrium. The total volume of each solution and the total volume in each phase was measured. It can be seen that between 4.0% and 5.5% sodium chloride, a two phase system was formed with the upper layer clear and the lower layer milky indicating an oil in water dispersion. Above 5.5% and below 7.5% NaCl three phases were observed, an upper clear phase, a milky middle phase and a lower clear phase. Above 7.5% sodium chloride a two phase region again occurred. This time, the upper was milky and the lower phase was clear, indicating a complete inversion of water and oil. Plotted on the same curve are the measurements of the interfacial tension at the upper phase and lower phase interfaces. As the concentration of sodium chloride increases, the interfacial tension of the upper phase decreases, while that of the lower phase increases. It can be seen from the graph, there is at least a two order of magnitude change, from 10^{-1} to 10^{-3} mN/M, in the value of interfacial tension as the concentration of NaCl is increased. This system was previously studied by Pouchelon *et al* (34).

The density, viscosity, refractive index in each phase were measured, in solutions containing different concentrations of NaCl, at various temperature in

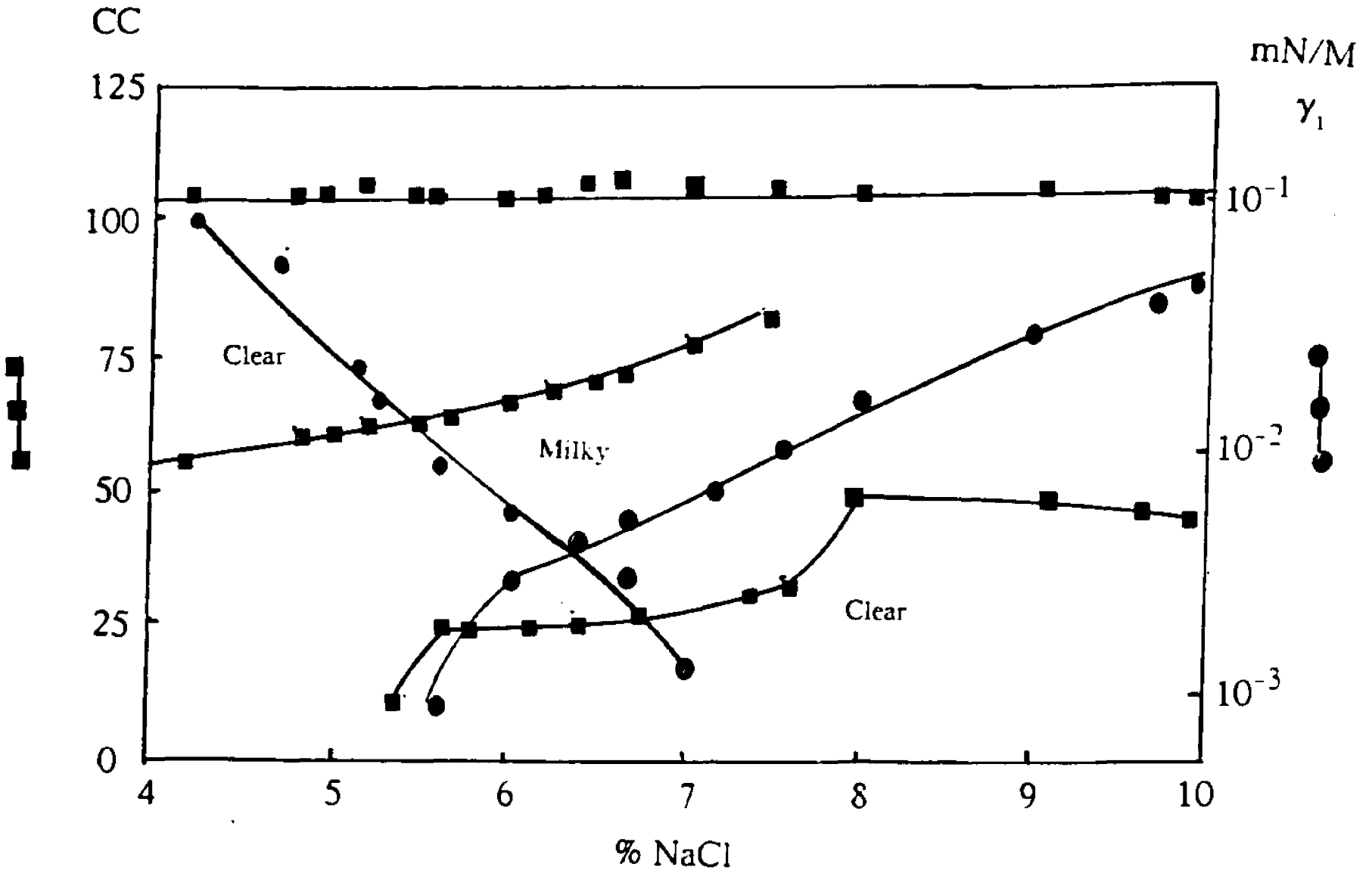

Figure 4.4 Change in interfacial tension (O) and phase volume (■) as a function of weight percent of NaCl for the dispersion of toluene / 1-butanol / Na dodecylsulfate / aqueous NaCl. Temperature 21.5 °C.

the range of 15 to 30 °C. The interfacial tension of mixtures of components similar to the previous solutions was measured with the spinning drop method. In the case of a three phase system, the interfacial tension between the upper phase and the lower phase was also measured. The calculated values were then fitted to a straight line equation, and it is shown in table 4.2. The temperatures were measured in degrees Celsius, the densities were in gm/ml, the viscosities were determined in centipoise and the interfacial tensions were determined in mN/M.

TABLE 4.2: Linear fit as a function of temperature of the bulk thermodynamic properties of 46.35% toluene/1.95% SDS/3.75% 1-butanol/47.95% saline NaCL systems at different concentrations of NaCl in saline. Temperature units, degrees Celsius; viscosity, centipoise; density, gm/mL; and interfacial tension, mN/M.

TABLE 4.2

$y = mT + b$

	phase	m	b
4.0% NaCl brine solution			
refractive index	upper	-5.429×10^{-4}	1.5030
	lower	-1.572×10^{-4}	1.3663
density	upper	-1.009×10^{-3}	0.8831
	lower	-5.375×10^{-4}	1.0168
viscosity	upper	-7.533×10^{-3}	0.7469
	lower	-1.631×10^{-2}	2.4999
interfacial tension	upper/lower	-1.727×10^{-3}	0.1242
4.5% NaCl brine solution			
refractive index	upper	-5.409×10^{-4}	1.5030
	lower	-2.207×10^{-4}	1.3712
density	upper	-6.779×10^{-4}	0.8715
	lower	-6.783×10^{-4}	1.0170
viscosity	upper	-6.638×10^{-3}	0.7276
	lower	9.352×10^{-3}	2.5307
interfacial tension	upper/lower	-1.247×10^{-3}	0.0806
5.0% NaCl brine solution			
refractive index	upper	-7.931×10^{-4}	1.5083
	lower	-2.467×10^{-4}	1.3761
density	upper	-1.307×10^{-3}	0.8927
	lower	-8.632×10^{-4}	1.0267
viscosity	upper	-7.935×10^{-3}	0.7657
	lower	7.428×10^{-3}	3.3606
interfacial tension	upper/lower	-1.247×10^{-3}	0.0614

TABLE 4.2 *(continued)*

$y = mT + b$

	phase	m	b
5.5% NaCl brine solution			
refractive index	upper	-5.571×10^{-4}	1.5029
	middle	-3.500×10^{-4}	1.4057
	lower	-1.953×10^{-4}	1.3501
density	upper	-9.150×10^{-4}	0.8794
	middle	-4.359×10^{-4}	1.0021
	lower	-3.228×10^{-4}	1.0386
viscosity	upper	-7.317×10^{-3}	0.7440
	middle	-4.491×10^{-2}	3.3653
	lower	-2.464×10^{-2}	1.7249
interfacial tension	upper/lower	-2.431×10^{-3}	0.0735
	middle/lower	4.604×10^{-4}	0.0103
	upper/middle	-4.409×10^{-4}	0.0246
6.0% NaCl brine solution			
refractive index	upper	-5.569×10^{-4}	1.5032
	middle	-2.564×10^{-4}	1.4119
	lower	-1.572×10^{-4}	1.3498
density	upper	-9.053×10^{-4}	0.8777
	middle	-9.028×10^{-4}	0.9842
	lower	-4.310×10^{-4}	1.0482
viscosity	upper	-7.422×10^{-3}	0.7486
	middle	-2.410×10^{-2}	3.7488
	lower	-2.646×10^{-2}	1.7317
interfacial tension	upper/lower	-3.391×10^{-3}	0.1038
	middle/lower	8.383×10^{-4}	0.0204
	upper/middle	-1.251×10^{-4}	0.0109

TABLE 4.2 *(continued)*

$y = mT + b$

	phase	m	b
6.5% NaCl brine solution			
refractive index	upper	-5.524×10^{-4}	1.5029
	middle	-2.987×10^{-4}	1.4305
	lower	-1.682×10^{-4}	1.3508
density	upper	-8.506×10^{-4}	0.8781
	middle	-7.619×10^{-4}	0.9643
	lower	-4.431×10^{-4}	1.0534
viscosity	upper	-6.973×10^{-3}	0.7300
	middle	-6.612×10^{-2}	4.7458
	lower	-2.532×10^{-2}	1.7017
interfacial tension	upper/lower	-1.301×10^{-3}	0.0410
	middle/lower	9.908×10^{-4}	0.0187
	upper/middle	-7.845×10^{-5}	0.0059
7.0% NaCl brine solution			
refractive index	upper	-5.199×10^{-4}	1.5019
	middle	-3.888×10^{-4}	1.4482
	lower	-1.382×10^{-4}	1.3507
density	upper	-8.521×10^{-4}	0.8804
	middle	-7.972×10^{-4}	0.9484
	lower	-4.939×10^{-4}	1.0575
viscosity	upper	-7.037×10^{-3}	0.7446
	middle	-6.685×10^{-2}	5.0218
	lower	-2.601×10^{-2}	1.7409
interfacial tension	upper/lower	2.611×10^{-3}	-0.0553
	middle/lower	1.729×10^{-3}	0.0329
	upper/middle	-4.689×10^{-6}	0.0019

TABLE 4.2 *(continued)*

$y = mT + b$

	phase	m	b
7.5% NaCl brine solution			
refractive index	upper	-9.626×10^{-4}	1.4867
	lower	-1.414×10^{-4}	1.3515
density	upper	-7.449×10^{-4}	0.9125
	lower	-3.207×10^{-4}	1.0457
viscosity	upper	-6.911×10^{-3}	2.4055
	lower	-2.596×10^{-2}	1.7402
interfacial tension	upper/lower	2.494×10^{-3}	-0.0462
8.0% NaCl brine solution			
refractive index	upper	-4.645×10^{-4}	1.4789
	lower	-1.257×10^{-4}	1.3520
density	upper	-8.126×10^{-4}	0.9110
	lower	-3.782×10^{-4}	1.0592
viscosity	upper	-9.270×10^{-3}	2.0350
	lower	-2.551×10^{-2}	1.7310
interfacial tension	upper/lower	4.024×10^{-3}	0.0683
9.0% NaCl brine solution			
refractive index	upper	-4.537×10^{-4}	1.4835
	lower	-1.300×10^{-4}	1.3536
density	upper	-9.673×10^{-4}	0.9097
	lower	-4.232×10^{-4}	1.0685
viscosity	upper	-1.288×10^{-2}	1.5075
	lower	-2.372×10^{-2}	1.7054
interfacial tension	upper/lower	5.019×10^{-3}	0.0652

4.5 CARBON TETRACHLORIDE

The density, viscosity and refractive index were measured as a function of temperature in the range of 15 to 30 °C. The surface tension of carbon tetrachloride versus air was also determined at various temperatures within the same range. The measurements were done with a sandblasted platinum blade. The fitted values obtained as a function of temperature are shown in table 4.3. The temperatures were in degrees celsius, the densities in gm/ml, the viscosities in centipoise and the interfacial tension in mN/M.

TABLE 4.3: Linear fit of the bulk thermodynamic properties of CCl_4 versus air system as a function of temperature. Temperature unit, degrees Celsius; viscosity, centipoise; density, gm/mL; and interfacial tension, mN/M.

TABLE 4.3		
$y = mT + b$		
	m	b
refractive index	-6.1072×10^{-4}	1.4732
density	-1.9127×10^{-3}	1.6317
viscosity	-1.1262×10^{-2}	1.1932
interfacial tension	-1.1384×10^{-2}	29.179

CHAPTER 5

RESULTS OF THE MEASUREMENTS OF INTERFACIAL TENSION

5.1 INTRODUCTION

The interfacial tension of various systems of

1) Toluene/Water/1-Propanol

2) 46.35% toluene/1.95% SDS/3.75% 1-butanol/47.95% saline NaCl

were measured with several methods.

Solutions composed of 5 ml of water, 5 ml of toluene, and different volumes (3, 5, 7, 10, 12, 14 mL) of 1-propanol were measured with the laser light scattering, spinning drop and pendant drop methods. These solutions were made in the manner described in chapter 4. The measurements were taken within the range of 22.5 ± 1.5°C, by keeping the ambient temperature of the experimental room constant with an air conditioner.

The interfacial tension of solutions made of 46.35% toluene/1.95% SDS/3.75% 1-butanol/47.95% of different weight per cent (4, 5, 6, 7) of Nacl (aqueous) were also measured with the laser light scattering and the spinning drop methods.

Because of poor precision at low values of interfacial tension, the blade method was not used in these measurements.

5.2 RESULTS OBTAINED FROM THE LASER LIGHT SCATTERING METHOD

5.2.1 TOLUENE / WATER / 1-PROPANOL SYSTEM

In the spectral analysis of the scattered light, the instrumental broadening was first determined with several spectra of CCl_4 vs air. A series of spectra were obtained for each diffraction order under similar optical conditions to the spectrum obtained from the liquid/liquid system. The density, viscosity, interfacial tension and refractive index (needed to calculate the experimentally determined q value) of carbon tetrachloride were measured at 22.5 °C. Using equation 3.144, the density, viscosity, interfacial tension, refractive index and the magnitude of the measured wavevector q_o of the spectrum of carbon tetrachloride were inserted into the equation. Using an assumed value for N, which was kept constant for each diffraction order, σ was then optimized. The result of this calculation is given in table 5.1. About 6 spectra per wave-vector were analyzed and averaged. Each wave-vector represents a different diffraction order of the grating at the photomultiplier. It can be seen that, at higher diffraction order the value of σ increases. These values of σ and N were subsequently applied to the spectral analysis of the liquid/liquid systems for which the parameters γ and η (or η') were then optimized by the same equation. The density, viscosity, and refractive index of each phase were measured at 22.5 °C. Using equation 3.144 again, the density and viscosity of the upper phase, the density of the lower phase, the interfacial tension, refractive index of the upper phase and the magnitude of the measured wavevector q_o of the spectrum were inserted into the equation. σ and N were given the values in table 5.1 according to the scattered angle of the recorded spectrum. Figures 5.1 and 5.2 show typical spectra obtained at two different q values. Figure 5.1 shows a nearly symmetric spec-

TABLE 5.1: Measurement of the instrumental width, σ, from the spectras of CCl_4 vs air at 23 °C.

TABLE 5.1

Wave-vector (cm^{-1})	Order	σ	N
199.317	2	16.61 ± 1.26	50
294.793	3	26.67 ± 1.53	70
398.633	4	49.25 ± 2.25	95

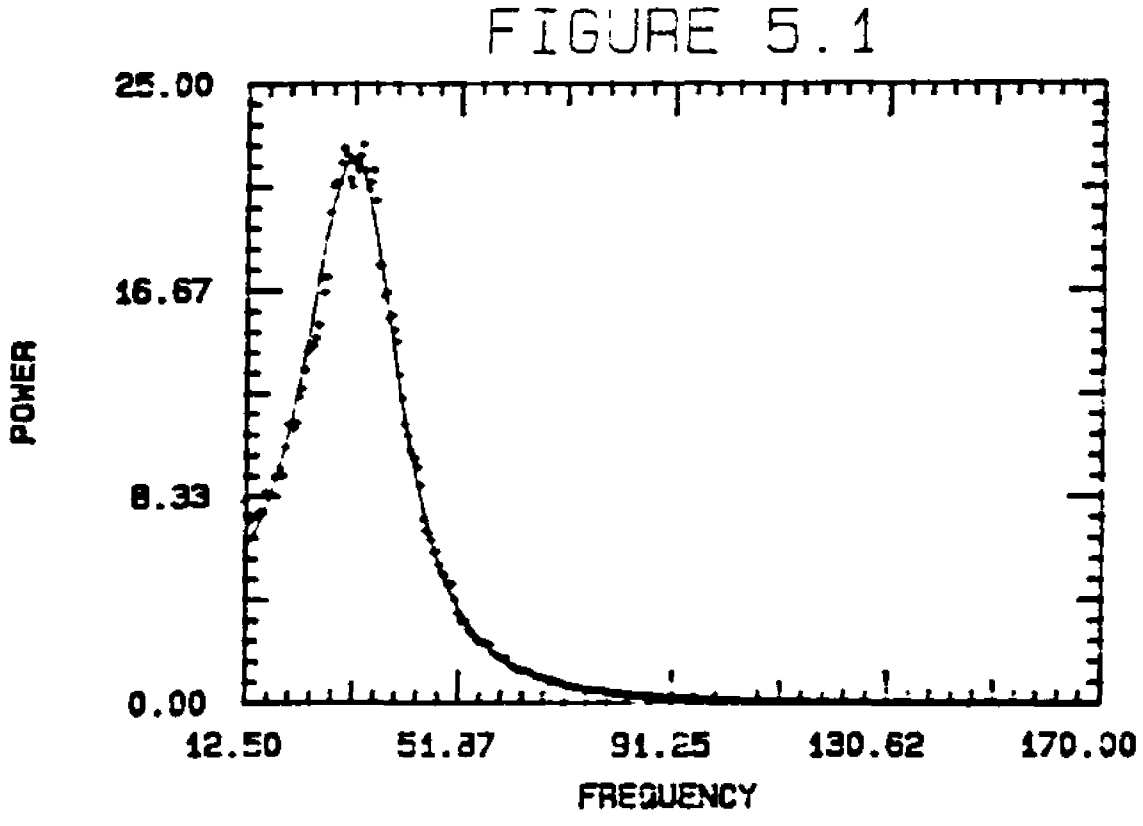

Figure 5.1 Experimental spectrum (points) of light scattered by toluene/water interface at 23°C for q = 193.39 cm^{-1}. The solid line represents the best fit obtained with equation 3.141 with N = 50, σ = 16.61. The values obtained were γ_1 = 1.72 dynes/cm and η = 1.86 cp. The sample was 5 ml water, 5 ml toluene, 5 ml 1-propanol.

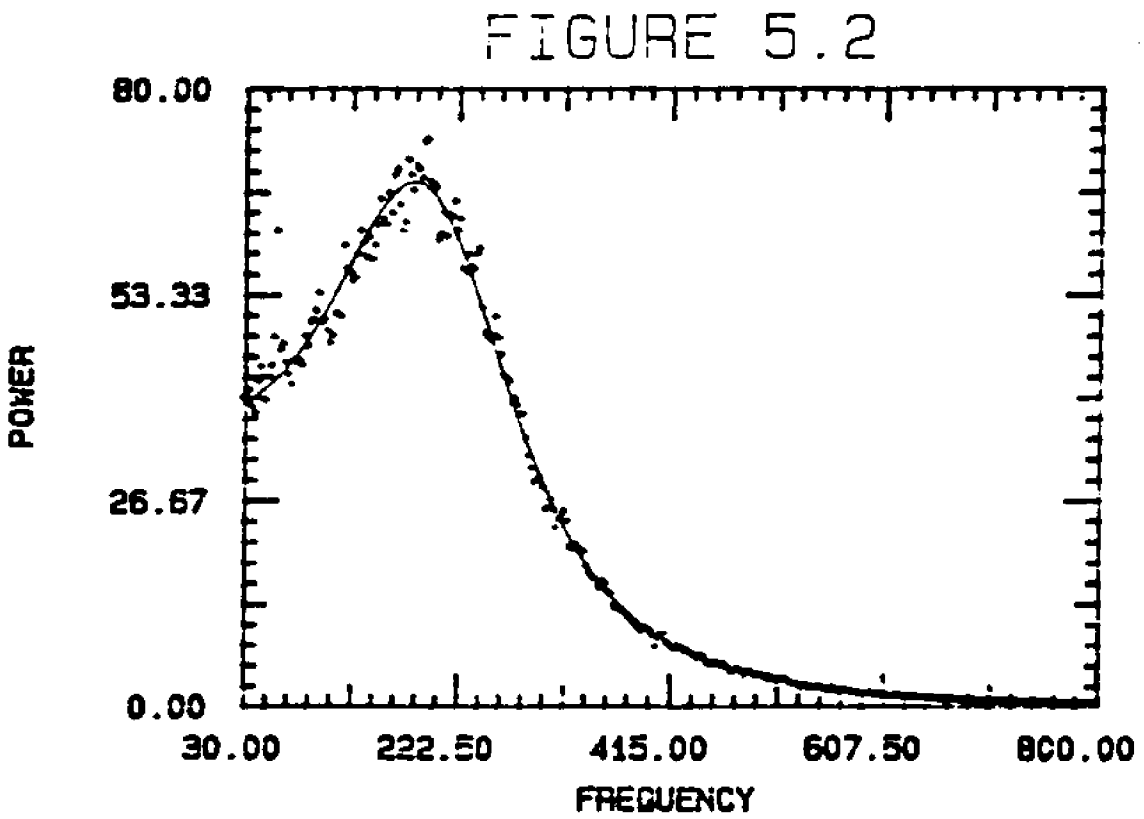

Figure 5.2 Experimental spectrum (points) of light scattered by a toluene/water interface at 22°C for q = 207.18 cm^{-1}. The solid line represents the best fit obtained with equation 3.144 with N=50 and σ=16.61. The values obtained were γ_i = 0.699 dynes/cm and η = 2.09 cp. The sample was 5 ml water, 5 ml toluene, 12 ml 1-propanol.

trum of the light scattered at the liquid/liquid interface of a solution of 5 ml of water, 5 ml toluene, 5 ml 1–Propanol. Figure 5.2 is a strongly asymmetric spectrum of the scattered light at the interface of a solution of 5 ml water, 5 ml toluene, 12 ml 1–propanol. Both spectra were analyzed using the values of $N = 50$ and $\sigma = 16.61$. The agreement between the experimentally measured spectrum and the computer fitted one using equation 3.144 is seen to be good over the whole spectral range. The values of interfacial tension found for the various water/toluene/propanol systems are shown in table 5.2. The interfacial tension value at each wave-vector q represents the average of the analysis of 3 spectra. The average interfacial tension was obtained by averaging all the values obtained with different wavevectors q in that particular system. Table 5.3 shows the calculated viscosities obtained from the spectral analysis of the set of water/toluene/1-propanol systems. The third column in the table shows the calculated viscosities obtained after correcting for the instrumental broadening. The next column shows the values obtained by fitting equation 3.66 to the experimental spectrum. The bulk shear viscosities of the lower phase were measured with an Ostwald viscometer.

5.2.2 46.39% TOLUENE / 1.95% SDS / 3.75% 1-BUTANOL / 47.95% SALINE NACL SYSTEM

Figures 5.3 and 5.4 show typical spectra obtained from 1.95% SDS, 3.75% butanol, 46.39% toluene, 47.95% saline NaCl. Figure 5.3 shows a spectrum of light scattered at the liquid/liquid interface of a solution containing 47.95% saline with 4.0% NaCl. Figure 5.4 shows a spectrum of light scattered at the liquid/liquid interface defined by the middle phase and lower phase of a solution containing 47.95% saline with 7.0% NaCl. In the analysis of these spectra the density, viscosity and refractive index of each of the phases were obtained

TABLE 5.2: Measurements of interfacial tension by laser light scattering, spinning drop, pendant drop methods of 5 ml water, 5 ml toluene, x ml 1-propanol

TABLE 5.2

1-propanol x ml	Q (cm^{-1})	laser light scattering (dynes/cm)	spinning drop (dynes/cm)	pendant drop (dynes/cm)	temperature °C
3 ml	196.36	2.52 ± 0.04			
	203.50	2.62 ± 0.05			
	396.54	2.63 ± 0.02			
	average	2.59 ± 0.07	2.65 ± 0.02	2.54 ± 0.09	24
5 ml	193.39	1.72 ± 0.01			
	291.59	1.79 ± 0.02			
	average	1.76 ± 0.04	1.74 ± 0.01	1.71 ± 0.06	23
7 ml	206.89	1.13 ± 0.04			
	311.88	1.22 ± 0.01			
	417.90	1.33 ± 0.01			
	average	1.23 ± 0.09	1.20 ± 0.02	1.11 ± 0.02	23
10 ml	207.71	0.758 ± .013			
	313.11	0.757 ± .024			
	419.44	0.754 ± .030			
	average	0.756 ± .020	.759 ± .007	.748 ± .006	22
12 ml	207.18	0.718 ± .022			
	312.35	0.733 ± .028			
	average	0.726 ± .025	.735 ± .010	.702 ± .005	22
14 ml	203.50	0.357 ± 0.026	.332 ± .004	.349 ± .003	22

TABLE 5.3: Measurements of the viscosity by laser light scattering, and by Ostwald viscometer of 5 ml water, 5 ml toluene, x ml 1-propanol

TABLE 5.3

1-propanol x ml	Q (cm^{-1})	Light scattering (cp)	Bulk Shear viscosity* (cp)	Temperature °C
3 ml	196.36	1.67 ± .04		
	203.50	1.68 ± .05		
	396.54	1.67 ± .08		
	average	1.68 ± .05	1.69 ± .01	24
5 ml	193.39	1.89 ± .07		
	291.59	1.97 ± .06		
	average	1.93 ± .07	1.88 ± .01	23
7 ml	206.89	1.90 ± .01		
	311.88	2.11 ± .03		
	417.90	2.11 ± .13		
	average	2.04 ± .12	1.91 ± .01	23
10 ml	207.71	2.08 ± .05		
	313.11	2.22 ± .06		
	419.44	2.15 ± .15		
	average	2.14 ± .10	2.05 ± .01	22
12 ml	207.18	2.15 ± .06		
	312.35	2.14 ± .19		
	average	2.14 ± .13	2.06 ± .01	22
14 ml	203.50	2.08 ± .19	2.14 ± .01	22

* Bulk shear viscosity measurements of the lower phase

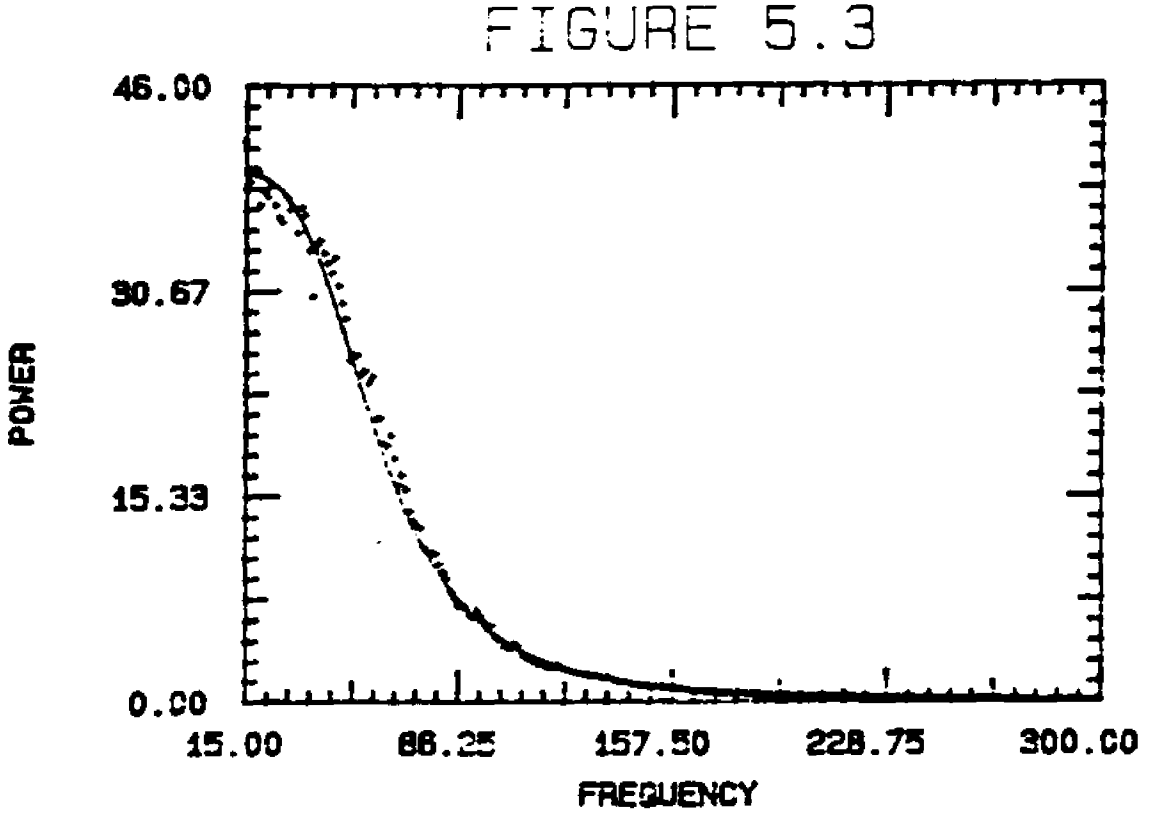

Figure 5.3 Experimental spectrum (points) of light scattered by a toluene/water interface for q = 166.84 cm^{-1}. The solid line represents the best fit obtained with equation 3.141. The best values obtained were γ_i = 8.23 × 10^{-2} mN/M. The sample was 46.39% toluene, 1.95% SDS, 3.75% 1-butanol, 47.95% NaCl (aqueous) with a 4% NaCl brine system.

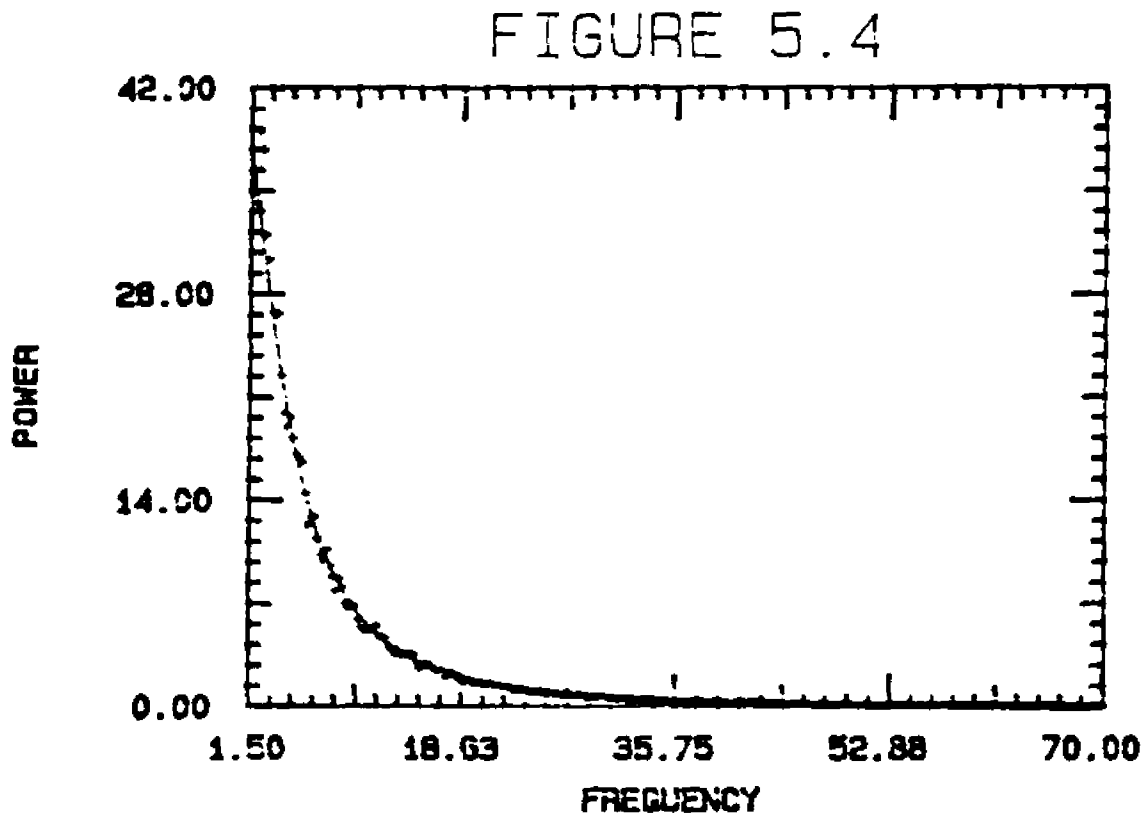

Figure 5.4 Experimental spectrum (points) of light scattered by a toluene/water interface (middle/lower phases) for q = 114.69 cm^{-1}. The solid line represents the best fit obtained with equation 3.141. The best values obtained were γ_1 = 1.12 × 10^{-2} mN/M. The sample was 46.39% toluene, 1.95% SDS, 3.75% 1-butanol, 47.95% NaCl (aqueous) with a 7% NaCl brine system.

by interpolating from the linearized equation shown in table 4.2, at the respective temperature of the experiment. Because of the low interfacial tension and high viscosity of these systems, the surface waves are damped without propagating. Thus, the power spectrum approximates a Lorentzian curve centered at zero frequency. The experimental power spectrum comprises of many spectra due to single wavevectors within a range of $q - \Delta q/2$ to $q + \Delta q/2$. But in this case, the spectra comprising the experimental power spectrum are all centered at zero frequency. Consequently, the instrumental broadening is not expected to contribute significantly to the power spectrum of these highly damped waves and only one parameter (the ratio of the interfacial tension to the viscosity, γ_i / η) can be obtained from the spectrum. (35) Thus, the spectra of these systems were analyzed by optimizing the interfacial tension, γ_i, without subtracting for the instrumental broadening contribution. This was done by setting N=0 and σ=1 in equation 3.144. The values of interfacial tension measured at different concentration of NaCl in saline solution are shown in table 5.4. The interfacial tension value represents the average of the analysis of 5 spectra at three different q values.

5.3 RESULTS OBTAINED FROM THE SPINNING DROP METHOD

5.3.1 TOLUENE / WATER / 1-PROPANOL SYSTEM

The interfacial tension measurements performed with the spinning drop method were done on the same solutions that were prepared for the laser light scattering method. The procedure followed is described in chapter 2. Equation 2.8 was used to calculate the interfacial tension. The measurements were performed at the same temperature as the laser light scattering experiments. The measured radius of the drop was always larger than the true radius of the drop

TABLE 5.4: Measurements of interfacial tension by laser light scattering and spinning drop methods of 1.95% SDS, 3.75% butanol, 46.35% toluene, 47.95% saline NaCl at different concentration of NaCl in saline

TABLE 5.4

Phases	% NaCl	Laser Light Scattering	Spinning Drop	Temperature °C
upper/lower	4.0	$8.09 \times 10^{-2} \pm 2.78 \times 10^{-3}$	$8.16 \times 10^{-2} \pm 8.58 \times 10^{-4}$	24
upper/lower	5.0	$2.98 \times 10^{-2} \pm 1.51 \times 10^{-3}$	$3.15 \times 10^{-2} \pm 5.73 \times 10^{-4}$	24
upper/lower	6.0	$1.51 \times 10^{-2} \pm 2.72 \times 10^{-3}$	$1.65 \times 10^{-2} \pm 1.41 \times 10^{-4}$	24
upper/middle	6.0	$7.58 \times 10^{-3} \pm 4.18 \times 10^{-4}$	$7.50 \times 10^{-3} \pm 1.04 \times 10^{-4}$	24
middle/lower	6.0	$3.23 \times 10^{-3} \pm 3.80 \times 10^{-4}$	$2.88 \times 10^{-3} \pm 1.04 \times 10^{-4}$	27
upper/lower	7.0	$7.65 \times 10^{-3} \pm 3.93 \times 10^{-4}$	$7.40 \times 10^{-3} \pm 4.78 \times 10^{-4}$	24
upper/middle	7.0	$1.91 \times 10^{-3} \pm 1.24 \times 10^{-4}$	$1.98 \times 10^{-3} \pm 4.24 \times 10^{-5}$	24
middle/lower	7.0	$1.10 \times 10^{-3} \pm 6.26 \times 10^{-4}$	$9.89 \times 10^{-3} \pm 1.47 \times 10^{-4}$	24

due to refraction. Because of the design of the spinning drop apparatus, the true radius of the drop was calculated from the ratio of the measured radius of the drop to the refractive index of the lower phase. Table 5.2 shows the calculated values for the various solutions of water/toluene/1-propanol.

5.3.2 46.39% TOLUENE / 1.95% SDS / 3.75% 1-BUTANOL / 47.95% SALINE NACL SYSTEM

The interfacial tensions were determined for samples with similar concentration of NaCl in saline as those prepared for the laser light scattering method. The measurements were performed at the same temperature as those of the laser light scattering method. The procedure followed here in measuring the interfacial tension was similar to that described above. The densities and refractive index of the denser phase taken were from table 4.2, interpolated to the temperature of the experiment. Table 5.4 shows the calculated values at the different concentrations of NaCl.

5.4 RESULTS OBTAINED FROM THE PENDANT DROP METHOD

5.4.1 TOLUENE / WATER / 1-PROPANOL SYSTEM

The interfacial tension measurements were performed in the same room used for the laser light scattering method. Thus allowing for the measurements to be taken at the same temperature range. The solutions used were those used for the laser light scattering method. The procedure followed in determining the interfacial tension was described in chapter 2. Equation 2.16 was used to calculate the interfacial tension. Table 5.2 shows the calculated values for the interfacial tension for the various solutions of water and toluene containing different amounts of 1-propanol.

CHAPTER 6

DISCUSSION OF THE RESULTS

6.1 TOLUENE / WATER / 1—PROPANOL SYSTEM

The results listed in table 5.2 indicate that the laser light scattering optical heterodyne technique is as accurate as the other methods shown in determining low interfacial tension. This supports the conclusion of Löfgren *et al* (13), who found an agreement between the interfacial tension of various liquid/liquid interfaces with high interfacial tension measured by the light scattering technique and by other more conventional methods. The demonstration of the validity of the method was extended to low values of interfacial tension. It was also observed that the light scattering method has a higher standard deviation than the other methods. This could be caused by residual vibrations which could not be eliminated in the experimental setup.

When the surface is not strongly damped, the experimental spectrum is broadened by important instrumental factors. In the spectral analysis, this broadening was corrected through substraction of the contributions due to instrumental effects. Tables 5.1 and 5.3 show that the lorentzian-squared function can be used to represent the instrumental broadening. From table 5.1 a relatively small deviation is seen at each wave-vector of the optimized parameter σ, and from table 5.3, it can be seen that the calculated viscosity from the spectrum of the laser light scattering technique agrees well with the lower phase bulk viscosity within experimental error. Other authors have reported similar agreement between the viscosity measured by the laser light scattering technique and that of the bulk (6, 13, 26, 28, 36).

It has been noted and commented on in chapter 4 that extrapolating the low measured values of interfacial tensions to γ_i=0 yields a 1—propanol volume of 17.6 ml (figure 4.5). This volume of 1—propanol is larger than the volume (15.6 mL) necessary to solubilize the system (figure 4.2). Thus, a smaller volume than what is needed to obtain zero interfacial tension of cosolubilizing agent (1—propanol) is required to produce a 1—phase system. From figure 4.2, it can be seen that to decrease the volume of the bottom aqueous phase an amount greater than 3 mL of 1—propanol was needed with 5 mL of water and 5 mL of toluene. From figure 4.3, it can be seen that alcohol lowers the interfacial tension significantly well before significant reduction of the volume of the lower phase is observed (the pure water/toluene interfacial tension is 35 mN/m). Thus, even if the interfacial tension and the work required for the formation of a one phase system are small, the system still lacks stability. Moreover, a residual positive interfacial tension, γ_i, of 0.2 mN/M seems to be needed for phase separation to occur. These observations are in agreement with previous reports (37-40) in which the work of emulsion formation and of stability are two independent factors. In particular, although the formation of dispersions is enhanced by low γ_i, its stability is related to the interfacial film formed (whether steric or charged) and, in fact, needs a higher γ_i. In the case of toluene, water, and 1—propanol, the film formed is weak and incapable of maintaining a dispersed phase. For this reason, 1—propanol has always been known as a good cosolubilizing agent, but not as an emulsifying agent.

Some authors have suggested the analysis of liquid/liquid interfacial spectra using a dispersion relation similar to that of equation 3.61 (41,42). In this case ρ is taken as the sum of the densities and η as the sum of the viscosities of both phases. We have analyzed some of the liquid/liquid spectra with equation

3.61 representing the dispersion relation. The analysis was undertaken without the utilization of the instrument function. Table 6.1 shows the result of the analysis. The values of the interfacial tension found were close to those obtained with the other methods but were always lower in value. The sum of the upper and lower phase viscosities for the 5 ml water, 5 ml toluene, 10 ml 1—Propanol was calculated to be 3.71 cp. The value obtained in this case was lower than the calculated one.

6.2 46.39% TOLUENE / 1.95% SDS / 3.75% 1—BUTANOL / 47.95% NACL (AQUEOUS) SYSTEM

Because the surface waves in this system are strongly damped, only one parameter, γ_i, can be determined from the analysis. The results of the analysis are shown in table 5.4. They indicate that the laser light scattering method can be applied to measure interfacial tension around 10^{-3} mN/M. This agrees with Pouchelon, *et. al* (34). They also measured similar solutions of quaternary systems with the laser light scattering method. In their papers, they published values of interfacial tension which agree well with those obtained in the experiments.

It is observed that the spinning drop has a greater precision than the laser light scattering method. The range of frequencies where the power spectra has significant value is very low (from 0 to 500 Hz). The contributions of the vibrations to the power spectrum in this frequency range are very strong. Therefore, in the analysis of the power spectrum, the calculated value of interfacial tension is expected to have greater scatter than that obtained from the spinning drop method.

TABLE 6.1: Light scattering measurements of 5 ml water, 5 ml toluene, 10 ml 1−Propanol with equation 3.58 as the dispersion equation.

TABLE 6.1

Q (cm^{-1})	interfacial tension (mN/M)	sum of the viscosity (cp)
207.71	0.646 ± .011	2.983 ± .059
313.11	0.657 ± .019	3.040 ± .047
419.44	0.672 ± .027	3.102 ± .039

CHAPTER 7

CONCLUSIONS

The interfacial tension of the toluene / water / 1-propanol system and 46.35% toluene/1.95% SDS/3.75% 1-butanol/47.95% NaCl (aqueous) has been studied and measured with the spinning drop, pendant drop, and laser light scattering methods. The laser light scattering method is a novel technique which allows the measurement of interfacial tension and interfacial viscosity without perturbing the interface. Until recently, very little work has been published on the validity of this method in measuring interfacial tension of liquid/liquid interfaces. The purpose of this research was to evaluate the method on liquid/liquid interfaces with low and ultralow interfacial tension values, and to correlate the results with conventional methods of measuring interfacial tension.

From the results of this research, it is concluded that the laser light scattering method measures interfacial tension with a precision comparable to the spinning drop and pendant drop methods. A major source of scatter of the values of interfacial tension calculated from the experimental spectrum is due to vibrations. These vibrations causes an imperfect definition of the experimentally determined wave vector **q**, thus increasing the error in the calculation. A diffraction grating helps define the wave vector **q** within one of the diffracted spots, thus minimizing the error caused by vibrations.

The lower limit of interfacial tension which this technique can measure is, theoretically, in the range of 10^{-5} mN/M. This is the region where gravitational forces instead of capillary forces are the dominant force in the surface waves

dynamics. It is seen, from measurements obtained for the quaternary system, that the laser light scattering method can be used to measure interfacial tension as low as 10^{-3} mN/M. This has also been demonstrated in studies of interfacial tension of various liquids near its critical temperature (43,44). In these studies measurements of interfacial tension as low as 0.8×10^{-4} mN/M were performed on carbon dioxide near its critical temperature using the laser light scattering technique (44). At present, the spinning drop method is the other method which can measure such low values with great precision.

The surface waves are damped by viscosity. This damping is related to the width of the power spectrum. The experimental spectra are broadened by the superposition of spectra due to a spread of wavevectors centered on the experimentally determined wavevector due to several instrumental factors. By substracting this instrumental contribution to the observed power spectrum, the interfacial viscosity can be calculated. The contribution of these instrumental factors, it has been found, can be represented by a Lorentzian squared function. From analysis of spectra of the toluene/ water/ 1-propanol system, the interfacial viscosity obtained is found to be equal to the bulk viscosity.

It is seen from the measured interfacial tensions for the various toluene/1—propanol systems that extrapolating these values to the amount of 1—propanol needed to solubilize the system a positive interfacial tension of 0.2 mN/M was still present. Thus a residual interfacial tension of 0.2mN/M is found to be needed to obtain a phase separation. This observation is explained from the fact that emulsification and stability are two independent factors. Although emulsification is enhanced by a low value of interfacial tension, the stability between two phases depends on the interfacial film formed, and therefore requires a higher interfacial tension.

APPENDIX A

DERIVATION OF THE SPINNING DROP METHOD

The present derivation is that of Princen et. al (45). The assumption involved is that the angular velocity of rotation, ω, is sufficiently high that buoyancy due to gravity is neglegible and the drop is aligned on the horizontal axis of rotation. Coordinates (x,y) are chosen with the origin at the left end of the drop. In a cylindrical drop, the angle between the normal to the interface at (x,y) and the negative x direction is θ, and the semiaxes are x_o and y_o. The densities of the drop and of the outerphase are d_1 and d_2 respectively, with d_2 greater than d_1, and the interfacial tension is γ. Because of symmetry, it is only necessary to consider a quarter of the drop, between (0,0) and (x_o,y_o), (figure A1).

The pressure outside of the drop is given by

$$P = P_o + \frac{d_2 \omega^2 y^2}{2} \qquad [A1]$$

and at y = 0, the pressure inside the drop is

$$P'_o = P_o + \frac{2\gamma}{\rho_o} \qquad [A2]$$

where ρ_o is the radius of curvature of the drop surface at the origin. At any y inside the drop, the pressure is

$$P' = P_o + \frac{2\gamma}{\rho_o} - \frac{d_1 \omega^2 y^2}{2} \qquad [A3]$$

so at the surface of the drop, the difference in pressure is

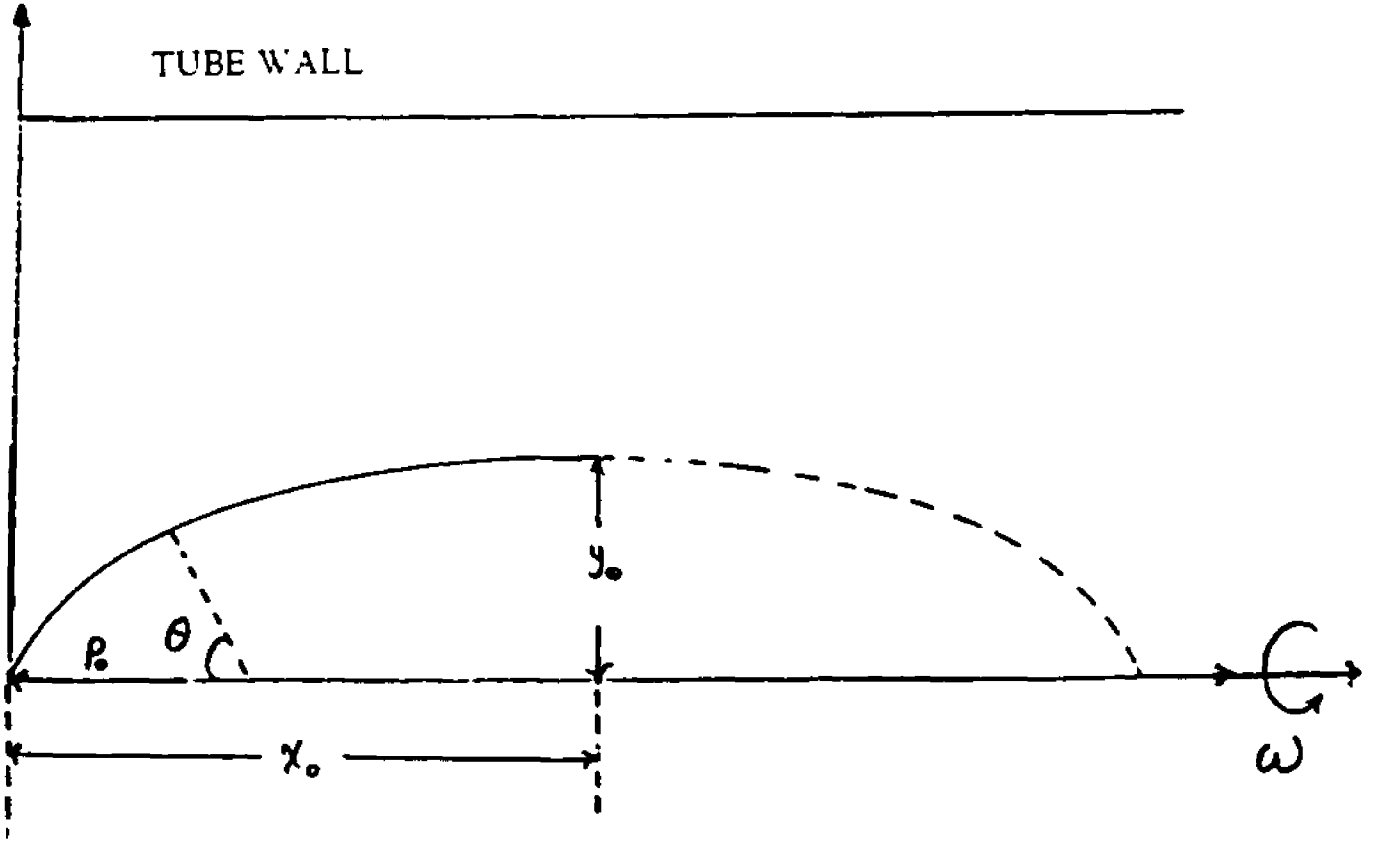

Figure A1 Plane section of a rotating drop with coordinate system to describe the shape.

$$\Delta P = P' - P = \frac{2\gamma}{\rho_o} - \frac{\Delta d\,\omega^2 y^2}{2} \qquad [A4]$$

where Δd is $d_2 - d_1$.

The pressure difference is balanced by the capillary pressure across the interface

$$\Delta P = \gamma \left(\frac{1}{R_1} + \frac{1}{R_2} \right) \qquad [A5]$$

where the principal radius of curvature are

$$\frac{1}{R_1} = \frac{\frac{d^2x}{dy^2}}{\left| + \left| \frac{dx}{dy} \right|^2 \right|^{\frac{3}{2}}} = \frac{d\sin\theta}{dy} \qquad [A6]$$

and

$$\frac{1}{R_2} = \frac{\frac{dx}{dy}}{y\left| 1 + \left| \frac{dx}{dy} \right|^2 \right|^{\frac{1}{2}}} = \frac{\sin\theta}{y} \qquad [A7]$$

equating [A4] and [A5] yields for the equation of interface

$$\frac{d\sin\theta}{dy} + \frac{\sin\theta}{y} = \frac{2}{\rho_o} - \frac{\Delta d\,\omega^2 y^2}{2\gamma} \qquad [A8]$$

expressed in dimensionless form

$$\frac{d\sin\theta}{dY} + \frac{\sin\theta}{Y} = 2 - \alpha Y^2 \qquad [A9]$$

where

$$Y = \frac{y}{\rho_o} \qquad [A9\text{-}1]$$

$$\alpha = \frac{\Delta d\, \omega^2 \rho_o{}^3}{2\gamma} = 2C\rho_o{}^3 \qquad \text{[A9-2]}$$

$$C = \frac{\Delta d\, \omega^2}{4\gamma} \qquad \text{[A9-3]}$$

Integrating equation [A9] gives

$$\sin\theta = Y\left(1 - \frac{\alpha Y^2}{4}\right) \qquad \text{[A10]}$$

In the special case when $Y = Y_o$, $\sin\theta = 1$ hence

$$\alpha Y_o{}^3 - 4Y_o + 4 = 0 \qquad \text{[A11]}$$

one of whose roots gives Y_o as a function of α.

Differentiating [A10] yields

$$d\sin\theta = \left(-\frac{3\alpha Y^2}{4}\right) dY \qquad \text{[A12]}$$

since $\tan\theta = dX/dY$, where $X = x/\rho_o$ and $Y = y/a$. Multiplication on the left hand side by $\tan\theta$ and on the right hand side by dX/dY and integrating between the origin and (X_o, Y_o) yields

$$1 = X_o - \frac{3\alpha}{4}\int_0^{X_o} Y^2\, dX \qquad \text{[A13]}$$

From the relation

$$\frac{V}{\rho_o{}^3} = 2\pi\int_0^{X_o} Y^2\, dX \qquad \text{[A14]}$$

where V is the volume of the drop. One finds from A13

$$\frac{V}{\rho_o{}^3} = \frac{4\pi}{3}\left(\frac{r}{\rho_o}\right)^3 = \frac{8\pi}{3\alpha}\left(X_o - 1\right) \qquad \text{[A15]}$$

where r is the radius of a sphere of the same volume as the drop. Thus equation [A15] reduces to the form

$$\frac{r}{\rho_o} = \left| \frac{2\left(\chi_o - 1\right)}{\alpha} \right|^{\frac{1}{3}} \qquad [A16]$$

which is a relation between r and ρ_o.

At high ω, the drop is closely approximated by a cylinder with rounded ends. In the cylindrical part

$$\frac{d \sin\theta}{dY} = 0 \qquad [A17]$$

with $\theta = 90$ and $Y = Y_o$ and equation [A9] becomes

$$\alpha Y_o^{\,3} - 2Y_o + 1 = 0 \qquad [A18]$$

combining [A18] and [A11] yields for a long cylindrical drop

$$Y_o = \frac{3}{2} \qquad [A19]$$

and the highest possible value of

$$\alpha = \frac{16}{27} \qquad [A20]$$

combining [A9-2], [A19] and [A20] leads to Vonnegut's equation

$$\gamma = \frac{\Delta d\, \omega^2\, y_o^{\,3}}{4} \qquad [A21]$$

for $0 < \alpha < 16/27$, one finds by integrating the relation

$$\tan\theta = \frac{dX}{dY} = \frac{Y\left|1 - \frac{\alpha Y^2}{4}\right|}{\left|-Y^2\left|\frac{\alpha Y^2}{4}\right|^2\right|^{\frac{1}{2}}} \qquad [A22]$$

and by making the substitution

$$q = 1 - \frac{\alpha Y^2}{4} \qquad \text{[A23]}$$

$$q_1 = 1 - \frac{\alpha Y_o^{\,2}}{4}$$

$$dq = \frac{\alpha Y\, dY}{2}$$

that it gives

$$X_o = \frac{1}{\sqrt{\alpha}} \int_{q_1}^{1} \frac{q}{\left| q^3 - q^2 + \frac{\alpha}{4} \right|^{\frac{1}{2}}}\, dq + C \qquad \text{[A24]}$$

If $q_1 > q_2 > q_3$ are the roots of the cubic term in the denominator then (46)

$$q_1 = 1 - \frac{\alpha}{4} Y_o^{\,2} = \frac{2}{3} \cos\left| \frac{\phi}{3} \right| + \frac{1}{3} \qquad \text{[A25]}$$

$$q_2 = \frac{2}{3} \cos\left| \frac{\phi}{3} + \frac{2\pi}{3} \right| + \frac{1}{3} \qquad \text{[A26]}$$

$$q_3 = \frac{2}{3} \cos\left| \frac{\phi}{3} + \frac{\pi}{3} \right| + \frac{1}{3} \qquad \text{[A27]}$$

where $\cos \phi = 1 - 27\alpha/8$

Evaluating the integral in the interval $q_1 \leqslant q \leqslant 1$ the solution is (47)

$$X = -\frac{2}{\sqrt{\alpha}\,(q_1 - q_3)} \left[q_1 F(k, \phi) - (q_1 - q_3) E(k, \phi) \right. \qquad \text{[A28]}$$

$$\left. + \left| q_1 - q_3 \right| \tan\phi \sqrt{1 - K^2 \sin\phi} \right] + C$$

where F and E are the elliptic integrals of the first and second kind.

$$K^2 = \frac{q_2 - q_3}{q_1 - q_3} \qquad [A29]$$

and ϕ is defined by

$$q = \frac{q_1 - q_2 \sin^2\phi}{1 - \sin^2\phi} \qquad 0 \leq \phi \leq \frac{\pi}{2} \qquad [A30]$$

At (X_o, Y_o), q equals q_1, ϕ equals 0 and the bracketed term vanishes so that

$$C = X_o \qquad [A31]$$

At the origin X = 0, Y = 0 and q = 1

$$X_o = \frac{2}{\sqrt{\alpha(q_1 - q_3)}} [\, q_1 F(k, \phi_1) - (q_1 - q_3) E(k, \phi_1) \qquad [A32]$$

$$+ (q_1 - q_3) \tan\phi_1 \sqrt{1 - K^2 \sin^2\phi_1}\,]$$

where $\phi = \phi_1$ and q = 1

These equations allow the drop shape to be computed for any value of α using tables of the elliptic integral (48). Then all dimensions are known in units of ρ_o and can readily be expressed in terms of r using [A16]. Instead of α, the more convenient shape determining factor, Cr^3, can be used by combining [A11] and [A16].

$$Cr^3 = \frac{\alpha}{2} \left(\frac{r}{\rho_o} \right)^3 = X_o - 1 \qquad [A33]$$

Appendix F reports the values of the most important drop parameters for various values of α (49). To obtain a value of γ_i, take a ratio of the length to the width of the drop $\left(\frac{X_o}{Y_o} \right)$. Calculate a value for r and determine the parame-

ter C from appendix F. From equation A9-3 calculate γ_i. At values of α greater than those in appendix F (when the central part of the drop is effectively cylindrical) the following equations apply with sufficient accuracy:

$$\alpha = 16/27 \qquad [A34]$$

$$Y_o = 3/2 \qquad [A35]$$

$$X_o = Cr^3 + 1 \qquad [A36]$$

$$r/a = 3/2(Cr^3)^{\frac{1}{3}} \qquad [A37]$$

$$\frac{x_o}{r} = \frac{2}{3}\frac{Cr^3 + 1}{(Cr^3)^{1/3}} \qquad [A38]$$

$$\frac{y_o}{r} = (Cr^3)^{-1}\frac{}{3} \qquad [A39]$$

$$x_o / y_o = \frac{2}{3}(Cr^3 + 1) \qquad [A40]$$

APPENDIX B

DERIVATION OF THE PENDANT DROP METHOD

B1 - DERIVATION OF THE LAPLACE EQUATION

Consider a curve liquid surface at equilibrium. The pressure is greater on the concave than on the convex side by an amount which depends on the surface or interfacial tension and the curvature. The pressure difference is due to the fact that the displacement of a curved surface along its normal results in an increase in area as the surface moves towards the convex side (figure 2.6). Work must be done to increase the area. The work done by the pressure difference in moving the surface must be exactly equal to the work required to increase the area if the surface is in equilibrium.

The calculation is performed by considering the energy changes involved in the displacement of the surface. In Figure B1, ABCD is a small element of surface with sides at right angles. A'B'C'D' is this area displaced a distance δn, away from the concave side. The normals to the boundaries in the displaced position A'B'C'D' are the same as the normals in the original position ABCD.

The normals at A and B meet at O_1 , and those at B and C at O_2. Letting the radius of curvature of the arc AB be R_1 and that of BC be R_2. The angle AO_1B is AB/R_1 radians and BO_2C is BC/R_2 radians. The area of the element of surface after the displacement is :

$$\left(AB + \frac{AB}{R_1}\delta n\right)\left(BC + \frac{BC}{R_2}\delta n\right) \qquad [B1]$$

Neglecting the second-order terms :

$$ABCD\left(1 + \frac{\delta n}{R_1} + \frac{\delta n}{R_2}\right) \qquad [B2]$$

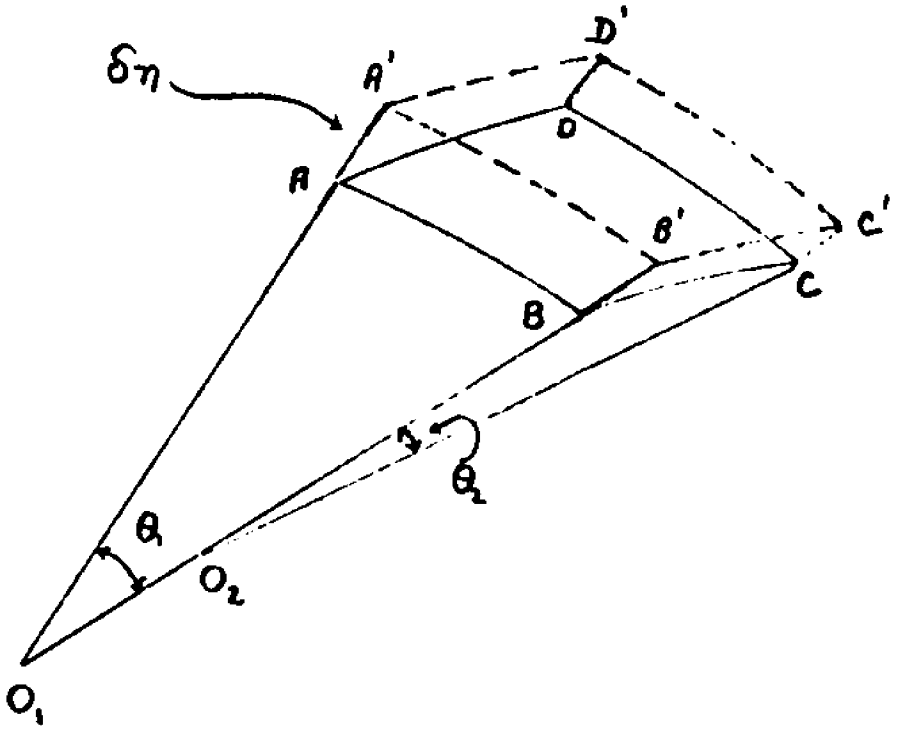

Figure B1 Small section of an arbitrarily curve surface displaced a distance δn

The work done against the interfacial free energy or interfacial tension, γ_i, of the surface is during the expansion therefore :

$$\gamma ABCD\ \delta n \left| \frac{1}{R_1} + \frac{1}{R_2} \right| \qquad [B3]$$

The work done by the pressure difference due to the surface curvature is :

$$\left| \Delta P \right| \delta n\ ABCD. \qquad [B4]$$

No other work is done by any other forces, hence at equilibrium these quantities must be equal, yielding :

$$\Delta P = \gamma \left| \frac{1}{R_1} + \frac{1}{R_2} \right| \qquad [B5]$$

Equation [B5] is the fundamental equation of capillarity and is known as the Laplace equation. Equation [B5] permits the calculation of the shapes of liquid surfaces where the weight of the liquid is neglegible. The difference in pressure can be expressed in terms of the height above a fixed point in the fluid, and the density difference between the two phases on each side of the interface.

B2 - APPLICATION OF THE LAPLACE EQUATION TO A PENDANT DROP

The Laplace equation [B5] relates the pressure difference across a liquid / liquid or liquid / gas interface to the product of the surface (or interfacial) tension and the total curvature ($1/R_1 + 1/R_2$). Note that with a plane surface, $R_1 = -R_2 = \infty$ and ΔP therefore is nil.

Referring to Figure B2 below, and choosing plane 1 (perpendicular to z0x) so that it passes through the axis of revolution (Oz), analytic geometry leads to the following relationship :

FIGURE B2

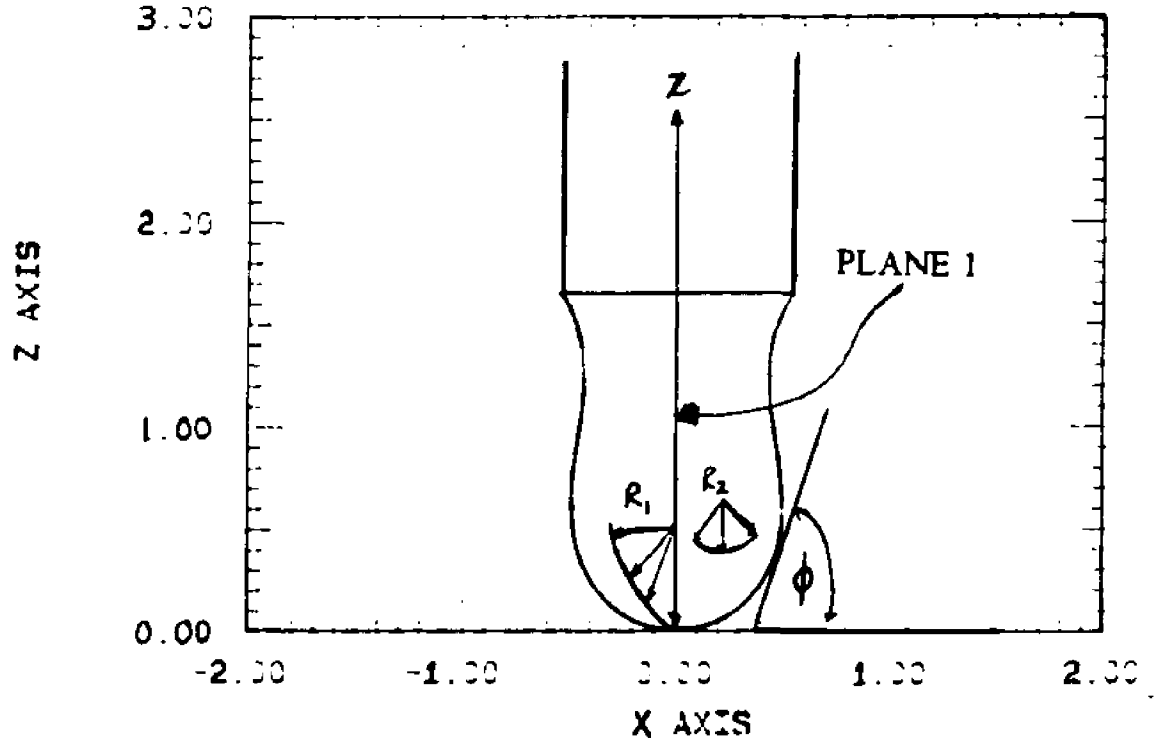

Figure B2 Radii of curvature R_1 and R_2 shown in the pendant drop method.

$$\frac{1}{R_1} = \frac{z''}{(1+(z')^2)^{3/2}} \qquad [B6]$$

where :

$$z' = \frac{dz}{dx}$$
$$z'' = d^2z / dx^2$$

The radius R_2 must then be in the perpendicular plane zOx and is given by the relationship

$$\frac{1}{R_2} = \frac{z'}{x(1+(z')^2)^{1/2}} = \frac{\sin\phi}{x} \qquad [B7]$$

Where ϕ is the angle formed by the tangent at any point on the curvature of the drop (at the intersection of zOx plane and the drop) and the Ox axis.

The pressure difference due to the curvature at any point on the zOx intersection curve equals

$$\Delta P = \frac{2\gamma_i}{b} + \Delta\rho g z \qquad [B8]$$

where :

z is the vertical distance from the origin O.

$\Delta\rho$ is the density difference of the two phases.

g is the gravitational constant.

b is the radius of curvature at the apex of the drop.

and γ_i the surface or interfacial tension.

Substitution of [B6], [B7] and [B8] into equation [B5] and equating :

$$\Delta P = \frac{2\gamma_i}{b} + \Delta\rho g z = \left[\frac{z''}{(1+(z')^2)^{3/2}} + \frac{z'}{x(1+(x')^2)^{1/2}} \right] \gamma_i \qquad [B9]$$

At $z = 0$ the Laplace pressure (ΔP) equals $2\gamma_i / b$ and at any other value of z the

change in the Laplace pressure equals

$$\Delta\rho gz + \frac{2\gamma_l}{b}. \qquad [B10]$$

Equation [B9] may be rearranged to a dimensionless form by utilizing the fact that $R_2 = x/\sin\phi$ and introducing the dimensionless quantities $-\beta$ and α^2 defined as :

$$-\beta = \frac{\Delta\rho g b^2}{\gamma_l} = \frac{2b^2}{\alpha^2} \qquad [B11]$$

and

$$\alpha^2 = \frac{2\gamma_l}{\Delta\rho g} \qquad [B12]$$

where α^2 is known as the capillarity constant.

The dimensionless form of equation [B9] becomes :

$$\frac{b}{R_1} + \frac{b}{x}\sin\phi = \frac{\beta z}{b} + 2. \qquad [B13]$$

β is positive for oblate figures of revolution, (i.e., meniscus in capillary tube or a sessile drop) and is negative for prolate figures (i.e., pendant drop or clinging bubble).

The numerical solution of equation [B13] using the fourth order Runge-Kutta method (50) is presented and explained in section B5.

B3 - THE SHAPE DETERMINING VARIABLES FOR THE ESTIMATION OF SURFACE OR INTERFACIAL TENSION USING PENDANT DROP

It is generally not convenient to measure β directly since it is a function of the shape determining variable b. However, β is related to other variables, H and S, whose determination is easier.

For the pendant drop method Andreas *et al* . (19) felt that the most convenient shape determining quantity is :

$$S = \frac{ds}{de} \qquad [B14]$$

where de is the equational diameter and ds is the diameter of the droplet measured at a vertical distance de from the x-axis parallel to the z-axis as shown in figure 2.6. The radius of curvature b in equation [B11] is combined with β when one defines the quantity :

$$-H = \beta \left| \frac{de}{b} \right|^2 \qquad [B15]$$

Thus from equation [B11]

$$\gamma_i = \frac{-\Delta\rho g b^2}{\beta} = \frac{-\Delta\rho g b^2}{-\left| \frac{b}{de} \right|^2 H} = \frac{\Delta\rho g (de)^2}{H} \qquad [B16]$$

Equation [B16] is the relationship of Andreas *et al* . for the measurement of the surface (or interfacial) tension using pendant drops regardless of size and components. The relationship between the shape dependent correction factor 1/H and the experimentally measurable quantity S was determined empirically by Neuderhauser and Bartell (51), Fordam (52) and Stauffer (53). Various sized

water drops are photographed, where γ_i, $\Delta\rho$ and g are known and de and ds were measured. By rearranging equation [B15], H can be obtained.

$$H = \frac{\Delta\rho(de)^2}{\gamma_i} = \frac{\Delta\rho g(de/ds)^2(ds)^2}{\gamma_i} \qquad [B17]$$

These results are tabulated on table B1.

The relation of 1/H vs S can also be represented with a polynomial within 0.01 percent error and is given by (54)

$$\frac{1}{H} = -118.786759S^{10} + 434.093599S^{9} - 432.601126S^{8} \qquad [B18]$$

$$- 278132760S^{7} + 910.895409S^{6} - 790.791405S^{5}$$

$$+ 341.3744995S^{4} + 138.742343S^{3} - 682.868757S^{2}$$

$$+ 946.6676677S^{1} - 718.068036S^{0} + 324.749083S^{-1}$$

$$- 87.3071898S^{-2} + 13.1715235S^{-3} - 0.832701805S^{-4}$$

B4 ESTIMATION OF SHAPE VARIABLE β AND THE RADIUS OF CURVATURE AT THE APEX OF THE DROP b

Equation [B13] may be solved provided β and b are known. The procedure is as follows:

1) equation [B13] is solved for a given value of β, where β is a function of ϕ, x/b, z/b.

2) A table of ϕ, x/b, z/b is established.

TABLE B1

S	0	1	2	3	4	5	6	7	8	9
0.30	7.09837	7.03966	6.98161	6.92421	6.86746	6.81135	6.75586	6.70099	6.64672	6.59306
0.31	6.53998	6.48748	6.43556	6.38421	6.33341	6.28317	6.23347	6.18431	6.13567	6.08756
0.32	6.03997	5.99288	5.94629	5.90019	5.85459	5.80946	5.76481	5.72063	5.67690	5.63364
0.33	5.59082	5.54845	5.50651	5.46501	5.42393	5.38327	5.34303	5.30320	5.26377	5.22474
0.34	5.18611	5.14786	5.11000	5.07252	5.03542	4.99868	4.96231	4.92629	4.89061	4.85527
0.35	4.82029	4.78564	4.75134	4.71737	4.68374	4.65043	4.61745	4.58479	4.55245	4.52042
0.36	4.48870	4.45729	4.42617	4.39536	4.36484	4.33461	4.30467	4.27501	4.24564	4.21654
0.37	4.18771	4.15916	4.13087	4.10285	4.07509	4.04759	4.02034	3.99334	3.96660	3.94010
0.38	3.91384	3.88786	3.86212	3.83661	3.81133	3.78627	3.76143	3.73682	3.71242	3.68824
0.39	3.66427	3.64051	3.61696	3.59362	3.57047	3.54752	3.52478	3.50223	3.47987	3.45770
0.40	3.43572	3.41393	3.39232	3.37089	3.34965	3.32858	3.30769	3.28698	3.26643	3.24606
0.41	3.22582	3.20576	3.18587	3.16614	3.14657	3.12717	3.10794	3.08886	3.06994	3.05118
0.42	3.03258	3.01413	2.99583	2.97769	2.95969	2.94184	2.92415	2.90659	2.88918	2.87192
0.43	2.85479	2.83781	2.82097	2.80426	2.78769	2.77125	2.75496	2.73880	2.72277	2.70687
0.44	2.69110	2.67545	2.65992	2.64452	2.62924	2.61408	2.59904	2.58412	2.56932	2.55463
0.45	2.54005	2.52559	2.51124	2.49700	2.48287	2.46885	2.45494	2.44114	2.42743	2.41384
0.46	2.40034	2.38695	2.37366	2.36047	2.34738	2.33439	2.32150	2.30870	2.29600	2.28339
0.47	2.27088	2.25846	2.24613	2.23390	2.22176	2.20970	2.19773	2.18586	2.17407	2.16236
0.48	2.15074	2.13921	2.12776	2.11640	2.10511	2.09391	2.08279	2.07175	2.06079	2.04991
0.49	2.03910	2.02838	2.01773	2.00715	1.99666	1.98623	1.97588	1.96561	1.95540	1.94527
0.50	1.93521	1.92522	1.91530	1.90545	1.89567	1.88596	1.87632	1.86674	1.85723	1.84778
0.51	1.83840	1.82909	1.81984	1.81065	1.80153	1.79247	1.78347	1.77453	1.76565	1.75683
0.52	1.74808	1.73938	1.73074	1.72216	1.71364	1.70517	1.69676	1.68841	1.68012	1.67188
0.53	1.66369	1.65556	1.64748	1.63946	1.63149	1.62357	1.61571	1.60790	1.60014	1.59242
0.54	1.58477	1.57716	1.56960	1.56209	1.55462	1.54721	1.53985	1.53253	1.52526	1.51804

TABLE B1 *(Continued)*

S	0	1	2	3	4	5	6	7	8	9
0.55	1.51086	1.50373	1.49665	1.48961	1.48262	1.47567	1.46876	1.46190	1.45509	1.44831
0.56	1.44158	1.43489	1.42825	1.42164	1.41508	1.40856	1.40208	1.39564	1.38924	1.38288
0.57	1.37656	1.37028	1.36404	1.35784	1.35168	1.34555	1.33946	1.33341	1.32740	1.32142
0.58	1.31549	1.30958	1.30372	1.29788	1.29209	1.28633	1.28060	1.27491	1.26926	1.26364
0.59	1.25805	1.25250	1.24698	1.24149	1.23603	1.23061	1.22522	1.21987	1.21454	1.20925
0.60	1.20399	1.19875	1.19356	1.18839	1.18325	1.17814	1.17306	1.16801	1.16300	1.15801
0.61	1.15305	1.14812	1.14322	1.13834	1.13350	1.12868	1.13389	1.11913	1.11440	1.10969
0.62	1.10501	1.10036	1.09574	1.09114	1.08656	1.08202	1.07750	1.07300	1.06853	1.06409
0.63	1.05967	1.05528	1.05091	1.04657	1.04225	1.03796	1.03368	1.02944	1.20522	1.02102
0.64	1.01684	1.01269	1.00856	1.00446	1.00037	0.99631	0.99227	0.98826	0.98427	0.98029
0.65	0.97635	0.97242	0.96851	0.96463	0.96077	0.95692	0.95310	0.94930	0.94552	0.94176
0.66	0.93803	0.93431	0.93061	0.92693	0.92327	0.91964	0.91602	0.91242	0.90884	0.90528
0.67	0.90174	89822	89471	89122	88775	88430	88087	87746	87407	87069
0.68	86733	86399	86067	85736	85407	85080	84755	84431	84110	83790
0.69	83471	83154	82839	82525	82213	81903	81594	81287	80981	80677
0.70	80375	80074	79774	79477	79180	78886	78593	78301	78011	77722
0.71	77434	77148	76864	76581	76299	76019	75740	75463	75187	74912
0.72	74639	74367	74097	73828	73560	73293	73028	72764	72502	72241
0.73	71981	71722	71465	71208	70954	70700	70448	70196	69946	69698
0.74	69450	69204	68959	68715	68472	68230	67990	67751	67513	67276
0.75	67040	66805	66571	66338	66107	65876	65647	65419	65192	64966
0.76	64741	64518	64295	64073	63852	63632	63414	63196	62980	62764
0.77	62550	62336	62123	61912	61701	61491	61282	61075	60868	60662
0.78	60458	60254	60051	59849	59648	59447	59248	59050	58852	58656
0.79	58460	58265	58071	57878	57686	57494	57304	57114	56926	56738
0.80	56551	56364	56179	55994	55811	55628	55446	55264	55084	54904
0.81	54725	54547	54370	54193	54017	53842	53668	53494	53322	53150
0.82	52978	52808	52638	52469	52300	52133	51966	51800	51634	51470
0.83	51306	51142	50980	50818	50656	50496	50336	50176	50018	49860
0.84	49702	49546	49390	49234	49080	48926	48772	48620	48468	48316

TABLE B1 *(Continued)*

S	0	1	2	3	4	5	6	7	8	9
0.85	48165	48015	47865	47716	47568	47420	47272	47126	46980	46834
0.86	46690	46545	46401	46258	46116	45974	45832	45691	45551	45411
0.87	45272	45134	44996	44858	44721	44585	44449	44313	44178	44044
0.88	43910	43777	43644	43512	43380	43249	43118	42988	42858	42729
0.89	42600	42472	42344	42216	42089	41963	41837	41711	41586	41462
0.90	41338	41214	41091	40968	40846	40724	40602	40481	40361	40241
0.91	40121	40001	39882	39764	39646	39528	39411	39294	39178	39062
0.92	38946	38831	38716	38602	38488	38374	38260	38147	38035	37922
0.93	37810	37699	37588	37477	37367	37256	37147	37037	36928	36819
0.94	36711	36603	36495	36387	36280	36173	36067	35960	35854	35749
0.95	35643	35538	35433	35328	35224	35120	35016	34913	34809	34706
0.96	34604	34501	34398	34296	34195	34093	33991	33890	33789	33688
0.97	33587	33487	33386	33286	33186	33086	32986	32887	32787	32688
0.98	32588	32489	32390	32290	32191	32092	31992	31893	31793	31694
0.99	31594	31494	31394	31294	31194	31093	30992	30891	30790	30688
1.00	30586	30483	30379							

TABLE B1: Numerical Tabulation of 1/H versus S Function for Calculation of Interfacial Tension by Pendant Drop Method.

3) From the table when $\phi = 90°$, $\left|\frac{x}{b}\right|_{90°}$ corresponds to the equatorial diameter of the droplet and $2\left|\frac{x}{b}\right|_{90°} = \frac{de}{b}$. The value of $\frac{z}{b} = \frac{de}{b}$ corresponds to a value of $\frac{x}{b}$ equals to $\frac{1}{2}\left|\frac{ds}{b}\right|$, therefore

$$S = \frac{2\left|\frac{x}{b}\right|_{at\ \frac{z}{b} = 2\left|\frac{x}{b}\right|_{90}}}{2\left|\frac{x}{b}\right|_{90°}} \qquad [B19]$$

The calculations are repeated for various values of β , until a table of β vs. S values are established, table B2. From this relation a polynomial representation of β as a function of S has been determined to be (54) :

$$\begin{aligned}\beta = \; & 5.28180041\,S^8 - 34.4163110\,S^7 + 76.773546\,S^6 \\ & - 73.0954332\,S^5 + 25.4482469\,S^4 + 0.00805209381\,S^3 \\ & + 0.176193444\,S^2 - 0.0366337797\,S - 0.0316796537 \\ & - 0.0176872732\,S^{-1} - 2.45519419\,S^{-2} + 2.39538684\,S^{-3} \\ & - 0.615602214\,S^{-4}\end{aligned} \qquad [B20]$$

For a given droplet S is experimentally determined, and 1/H and β can be determined. The corresponding values of b can then be determined :

$$b = \left|\frac{\beta\gamma_i}{\Delta\rho g}\right|^{\frac{1}{2}} \qquad [B21]$$

and equation [B13] can be solved.

TABLE B2: Table of β versus S.

TABLE B2	
β	S
-0.30	0.721953744
-0.31	0.732321225
-0.32	0.742559691
-0.33	0.752678832
-0.34	0.762687711
-0.35	0.772594641
-0.36	0.782407615
-0.37	0.792133990
-0.38	0.801780635
-0.39	0.811354196
-0.40	0.820860779
-0.41	0.830306445
-0.42	0.839696669
-0.43	0.849036704
-0.44	0.848331680
-0.45	0.867586218
-0.46	0.876804840
-0.47	0.885991668
-0.48	0.895150657
-0.49	0.904285197
-0.50	0.913398258
-0.51	0.922492452
-0.52	0.931569280
-0.53	0.940629488
-0.54	0.949677189
-0.55	0.958694269
-0.56	0.976643906
-0.57	0.976643906

B5 DETERMINATION OF THE PROFILE OF THE PENDANT DROP

The profile of a pendant drop is obtained by the solution of equation [B13]. Substituting $1/R_1$ by the relation in [B6] it is obtained

$$\frac{b\,z''}{\left[1+(z')^2\right]^{\frac{3}{2}}} + \frac{b\sin\phi}{x} = \frac{\beta z}{b} + 2 \qquad \text{[B22]}$$

letting :

$$U = \frac{x}{b},\quad Y_1 = \frac{z}{b},\quad Y_2 = \frac{dz}{dx} = \frac{dY}{dU},\quad W = \frac{dU}{dY_1} = \frac{1}{Y_2}$$

applying these relations to [B22] yields :

$$\frac{dY_2}{dU} = \frac{d^2Y_1}{dU^2} = \left[1+Y^2{}_2\right]^{\frac{3}{2}}\left[-\frac{Y_2}{U\,(1+Y_2^2)^{\frac{1}{2}} + \beta Y_1 + 2}\right] \qquad \text{[B23]}$$

then,

$$\frac{d^2U}{dY^2{}_1} = \frac{dW}{dY_1} = \frac{\dfrac{d^2Y_1}{dU^2}}{\left[\dfrac{dY_1}{dU}\right]^3} = \frac{1}{Y_2^3}\frac{d^2Y_1}{dU^2} = -W^3\frac{d^2Y_1}{dU_2} \qquad \text{[B24]}$$

$$= -W^3\left[1+\frac{1}{W^2}\right]^{\frac{3}{2}}\left[\frac{-1}{W\,U\,(1+\frac{1}{W^2})^{\frac{1}{2}} + \beta Y_1 + 2}\right] \qquad \text{[B25]}$$

$$= \left[W^2+1\right]^{\frac{3}{2}} + \left[\frac{1}{U\,(W^2+1)^{\frac{1}{2}} - \beta Y_1 - 2}\right] \qquad \text{[B26]}$$

Now the Runge-Kutta method (50) is incorporated into a fortran program and is used to solve the above differential equation with the initial conditions

$$\begin{array}{ll} 1) & U(0) = 0 \\ 2) & Y_1 = 0 \\ & Y_2 = 0 \end{array}$$

The program solves the differential equation

$$\frac{d^2z}{dx^2} = \mathbf{f}\left[x\ ,z\ ,\frac{dz}{dx}\right] \qquad \text{[B27]}$$

by the Runge-Kutta method. When z is the independent variable, equation [B27] becomes

$$\frac{d^2x}{dz^2} = -\left[\frac{dx}{dz}\right]^3\frac{d^2z}{dx^2} = \left[\frac{dx}{dz}\right]^3 \mathbf{f}_1\left[x\ ,z\ ,(dx\ /\ dz\ )^{-1}\right] \qquad \text{[B28]}$$

$$= \mathbf{f}_2\left[x\ ,z\ ,dx\ /\ dz\ \right] \qquad \text{[B29]}$$

The program operates in mode 1 when equation [B27] is solved and mode 2 when equation [B29] is solved. It switches from one mode to the other whenever dz/ dx |(mode 1) or |dx/ dz|(mode 2) exceeds an input parameter (sw), the switchpoint. A normal switchpoint is 1. when a switch from mode 1 to mode 2 occurs, the current value of x , z , and (dz/ dx)$^{-1}$, become the initial values of x , z and dz/ dx respectively. Likewise, from mode 2 to 1 (dx/ dz)$^{-1}$ becomes initial values of dz/ dx. The functions in this case are

$$\mathbf{f}_1\left[x\ ,z\ ,Y\ \right] = \left[1+Y^2\right]^{\frac{3}{2}}\left[\frac{-Y}{x\ (\ 1+Y^2)^{\frac{1}{2}} + \beta z\ +\ 2}\right] \qquad \text{[B30]}$$

$$\mathbf{f}_2\left[x\ ,z\ ,Y\ \right] = \pm\left[W^2+1\ \right]^{3/\ 2}\left[\frac{\pm 1}{x(\ W^2+1\ )^{\frac{1}{2}} - \beta z\ -\ 2}\right] \qquad \text{[B31]*}$$

$$= \left|W^2+1\right|^{\frac{3}{2}} \left| \frac{1}{x\left|W^2+1\right|^{\frac{1}{2}}} \pm\beta z \pm 2 \right| \qquad [B32]$$

the length of the step (h) and the number of steps to be taken are input parameters. At each step in mode 1, x is incremented by h ; in mode 2, z is incremented by h. Results are printed only when the step number is a multiple of the input parameter IFREQ, or when dz/ dx (mode 1) or dx/ dz (mode 2) exceeds 10 or is less than 10^{-2}. Execution terminates when this derivative exceeds 10^{10}. ϕ is the angle between the tangent to the curve z(x) or x(z) and the positive x-axis. It is given by

$$\phi = \sin^{-1}\left| \frac{\frac{dz}{dx}}{1+\left|\frac{dz}{dx}\right|^2} \right| \qquad (\text{mode } 1) \quad [B33]$$

$$\phi = \cos^{-1}\left| \frac{\frac{dx}{dz}}{1+\left|\frac{dx}{dz}\right|^2} \right| \qquad (\text{mode } 2) \quad [B34]$$

* Where the upper sign is for $x > 0$ and the lower for $x < 0$.

APPENDIX C

TABLE OF CALCULATED SHAPE PARAMETERS OF THE ROTATING DROP

α	r/ρ_0	$C r^3$	x_0/r	y_0/r	x_0/y_0
.00000000	1.000	0.0000	1.000	1.0000	1.000
.01000000	1.003	.0051	1.002	.9992	1.003
.02000000	1.007	.0102	1.003	.9983	1.005
.03000000	1.010	.0155	1.005	.9974	1.008
.04000000	1.014	.0208	1.007	.9965	1.010
.05000000	1.017	.0263	1.009	.9956	1.013
.06000000	1.021	.0319	1.011	.9947	1.016
.07000000	1.025	.0377	1.012	.9939	1.019
.08000000	1.029	.0435	1.014	.9928	1.022
.09000000	1.033	.0495	1.016	.9918	1.025
.10500000	1.039	.0588	1.019	.9903	1.029
.11000000	1.041	.0620	1.020	.9898	1.031
.11500000	1.043	.0652	1.022	.9893	1.033
.12000000	1.045	.0684	1.023	.9888	1.034
.12500000	1.047	.0717	1.024	.9882	1.036
.13000000	1.049	.0750	1.025	.9877	1.038
.13500000	1.051	.0784	1.026	.9872	1.039
.14000000	1.053	.0818	1.027	.9866	1.041
.14500000	1.056	.0853	1.028	.9861	1.043
.15000000	1.058	.0888	1.029	.9855	1.044
.15500000	1.060	.0923	1.030	.9849	1.046
.16000000	1.062	.0959	1.032	.9844	1.048
.16500000	1.065	.0996	1.033	.9838	1.050
.17000000	1.067	.1033	1.034	.9832	1.052

α	r/ρ_0	$C r^3$	x_0/r	y_0/r	x_0/y_0
.17500000	1.069	.1070	1.035	.9826	1.054
.18000000	1.072	.1108	1.036	.9820	1.055
.18500000	1.074	.1147	1.038	.9814	1.057
.19000000	1.077	.1186	1.039	.9808	1.059
.19500000	1.079	.1225	1.040	.9801	1.061
.20000000	1.082	.1265	1.042	.9795	1.063
.20500000	1.084	.1306	1.043	.9789	1.065
.21000000	1.087	.1348	1.044	.9782	1.067
.21500000	1.089	.1390	1.046	.9775	1.070
.22000000	1.092	.1432	1.047	.9769	1.072
.22500000	1.095	.1476	1.048	.9762	1.074
.23000000	1.097	.1520	1.050	.9755	1.076
.23500000	1.100	.1565	1.051	.9748	1.078
.24000000	1.103	.1610	1.053	.9741	1.081
.24500000	1.106	.1656	1.054	.9734	1.083
.25000000	1.109	.1704	1.056	.9727	1.085
.25500000	1.112	.1751	1.057	.9719	1.088
.26000000	1.115	.1800	1.059	.9712	1.090
.26500000	1.118	.1849	1.060	.9704	1.093
.27000000	1.121	.1900	1.062	.9696	1.095
.27500000	1.124	.1951	1.064	.9688	1.098
.28000000	1.127	.2003	1.065	.9680	1.100
.28500000	1.130	.2057	1.067	.9672	1.103
.29000000	1.133	.2111	1.069	.9664	1.106

α	r/ρ_0	$C r^3$	x_0/r	y_0/r	x_0/y_0
.29500000	1.137	.2166	1.070	.9656	1.109
.30000000	1.140	.2222	1.072	.9647	1.111
.30500000	1.143	.2280	1.074	.9638	1.114
.31000000	1.147	.2339	1.076	.9630	1.117
.31500000	1.150	.2398	1.078	.9621	1.120
.32000000	1.154	.2459	1.080	.9611	1.123
.32500000	1.158	.2521	1.082	.9602	1.126
.33000000	1.161	.2585	1.084	.9593	1.130
.33500000	1.165	.2650	1.086	.9583	1.133
.34000000	1.169	.2716	1.088	.9573	1.136
.34500000	1.173	.2784	1.090	.9563	1.140
.35000000	1.177	.2854	1.092	.9553	1.143
.35500000	1.181	.2925	1.094	.9542	1.147
.36000000	1.185	.2998	1.097	.9531	1.150
.36500000	1.190	.3072	1.099	.9520	1.154
.37000000	1.194	.3149	1.101	.9509	1.158
.37500000	1.198	.3228	1.104	.9498	1.162
.38000000	1.203	.3308	1.106	.9486	1.166
.38500000	1.208	.3391	1.109	.9474	1.170
.39000000	1.212	.3476	1.111	.9462	1.175
.39500000	1.217	.3563	1.114	.9449	1.179
.40000000	1.222	.3653	1.117	.9436	1.184
.40500000	1.228	.3746	1.120	.9423	1.188
.41000000	1.233	.3841	1.123	.9409	1.193

α	r/ρ_0	$C r^3$	x_0/r	y_0/r	x_0/y_0
.41500000	1.238	.3940	1.126	.9395	1.198
.42000000	1.244	.4041	1.129	.9381	1.203
.42500000	1.250	.4146	1.132	.9366	1.209
.43000000	1.255	.4254	1.135	.9351	1.214
.43500000	1.261	.4366	1.139	.9335	1.220
.44000000	1.268	.4482	1.142	.9319	1.226
.44500000	1.274	.4603	1.146	.9302	1.232
.45000000	1.281	.4728	1.150	.9285	1.238
.45500000	1.288	.4858	1.154	.9267	1.245
.46000000	1.295	.4993	1.158	.9248	1.252
.46500000	1.302	.5134	1.162	.9229	1.259
.47000000	1.310	.5281	1.167	.9209	1.267
.47500000	1.318	.5435	1.171	.9188	1.275
.48000000	1.326	.5596	1.176	.9166	1.283
.48500000	1.335	.5766	1.181	.9144	1.292
.49000000	1.344	.5944	1.187	.9120	1.301
.49500000	1.353	.6132	1.192	.9095	1.311
.50000000	1.363	.6330	1.198	.9069	1.321
.50500000	1.373	.6541	1.204	.9041	1.332
.51000000	1.384	.6765	1.211	.9012	1.344
.51500000	1.396	.7004	1.218	.8981	1.356
.52000000	1.408	.7260	1.226	.8949	1.370
.52500000	1.421	.7536	1.234	.8914	1.384
.53000000	1.435	.7835	1.243	.8876	1.400

α	r/ρ_0	$C r^3$	x_0/r	y_0/r	x_0/y_0
.53500000	1.450	.8161	1.252	.8836	1.417
.54000000	1.467	.8518	1.263	.8792	1.436
.54500000	1.484	.8913	1.274	.8744	1.457
.55000000	1.504	.9354	1.287	.8690	1.481
.55500000	1.526	.9855	1.301	.8631	1.508
.56000000	1.550	1.0430	1.318	.8564	1.539
.56500000	1.578	1.1107	1.337	.8487	1.576
.57000000	1.611	1.1925	1.361	.8395	1.621
.57500000	1.652	1.2957	1.390	.8282	1.678
.57550000	1.656	1.3077	1.393	.8270	1.685
.57600000	1.661	1.3200	1.397	.8256	1.692
.57650000	1.666	1.3327	1.400	.8243	1.699
.57700000	1.671	1.3458	1.404	.8229	1.706
.57750000	1.676	1.3594	1.408	.8215	1.714
.57800000	1.681	1.3734	1.412	.8200	1.722
.57850000	1.687	1.3880	1.416	.8185	1.730
.57900000	1.692	1.4031	1.420	.8169	1.738
.57950000	1.698	1.4187	1.424	.8153	1.747
.58000000	1.704	1.4350	1.429	.8136	1.756
.58050000	1.710	1.4520	1.434	.8118	1.766
.58100000	1.717	1.4697	1.439	.8100	1.776
.58150000	1.723	1.4882	1.444	.8081	1.787
.58200000	1.730	1.5075	1.449	.8062	1.798
.58250000	1.738	1.5279	1.455	.8041	1.809

α	r/ρ_0	$C r^3$	x_0/r	y_0/r	x_0/y_0
.58300000	1.745	1.5492	1.461	.8020	1.821
.58350000	1.753	1.5718	1.467	.7997	1.834
.58400000	1.761	1.5956	1.474	.7974	1.848
.58450000	1.770	1.6210	1.481	.7949	1.863
.58500000	1.779	1.6479	1.488	.7923	1.878
.58550000	1.789	1.6768	1.496	.7895	1.895
.58600000	1.800	1.7077	1.505	.7865	1.913
.58650000	1.811	1.7412	1.514	.7834	1.932
.58700000	1.823	1.7776	1.524	.7799	1.954
.58750000	1.836	1.8174	1.535	.7762	1.977
.58800000	1.850	1.8614	1.547	.7722	2.003
.58850000	1.866	1.9106	1.560	.7678	2.032
.58900000	1.883	1.9662	1.575	.7628	2.065
.58950000	1.903	2.0303	1.593	.7572	2.103
.59000000	1.925	2.1059	1.613	.7507	2.149
.59010000	1.930	2.1227	1.618	.7493	2.159
.59020000	1.936	2.1403	1.622	.7478	2.169
.59030000	1.941	2.1586	1.627	.7463	2.180
.59040000	1.947	2.1778	1.632	.7447	2.192
.59050000	1.953	2.1978	1.638	.7430	2.204
.59060000	1.959	2.2188	1.643	.7413	2.217
.59070000	1.965	2.2409	1.649	.7395	2.230
.59080000	1.972	2.2643	1.656	.7376	2.245
.59090000	1.979	2.2889	1.662	.7356	2.260

α	r/ρ_0	$C r^3$	x_0/r	y_0/r	x_0/y_0
.59100000	1.986	2.3151	1.669	.7335	2.276
.59110000	1.994	2.3430	1.677	.7313	2.293
.59120000	2.002	2.3729	1.685	.7289	2.311
.59130000	2.011	2.4049	1.693	.7264	2.331
.59140000	2.021	2.4396	1.702	.7238	2.352
.59150000	2.031	2.4773	1.712	.7209	2.375
.59160000	2.042	2.5187	1.723	.7177	2.401
.59170000	2.054	2.5645	1.735	.7143	2.429
.59180000	2.068	2.6157	1.749	.7106	2.461
.59190000	2.083	2.6739	1.764	.7063	2.497
.59200000	2.100	2.7412	1.782	.7016	2.539
.59201000	2.102	2.7486	1.783	.7010	2.544
.59202000	2.104	2.7561	1.785	.7005	2.549
.59203000	2.106	2.7637	1.787	.7000	2.553
.59204000	2.108	2.7714	1.789	.6994	2.558
.59205000	2.110	2.7793	1.791	.6989	2.563
.59206000	2.112	2.7873	1.794	.6983	2.568
.59207000	2.114	2.7955	1.796	.6978	2.573
.59208000	2.116	2.8039	1.798	.6972	2.579
.59209000	2.118	2.8124	1.800	.6966	2.584
.59210000	2.120	2.8210	1.802	.6960	2.590
.59211000	2.122	2.8299	1.805	.6954	2.595
.59212000	2.125	2.8389	1.807	.6948	2.601
.59213000	2.127	2.8482	1.809	.6941	2.607

α	r/ρ_0	$C r^3$	x_0/r	y_0/r	x_0/y_0
.59214000	2.129	2.8576	1.812	.6935	2.613
.59215000	2.132	2.8673	1.814	.6928	2.619
.59216000	2.134	2.8771	1.817	.6922	2.625
.59217000	2.136	2.8873	1.820	.6915	2.631
.59218000	2.139	2.8976	1.822	.6908	2.638
.59219000	2.142	2.9082	1.825	.6901	2.644
.59220000	2.144	2.9191	1.828	.6894	2.651
.59221000	2.147	2.9302	1.831	.6886	2.658
.59222000	2.150	2.9417	1.834	.6879	2.666
.59223000	2.153	2.9534	1.837	.6871	2.673
.59224000	2.155	2.9655	1.840	.6863	2.681
.59225000	2.158	2.9779	1.843	.6855	2.689
.59226000	2.162	2.9907	1.846	.6846	2.697
.59227000	2.165	3.0039	1.850	.6838	2.705
.59228000	2.168	3.0176	1.853	.6829	2.714
.59229000	2.171	3.0316	1.857	.6820	2.723
.59230000	2.175	3.0461	1.860	.6810	2.732
.59231000	2.178	3.0612	1.864	.6801	2.741
.59232000	2.182	3.0767	1.868	.6791	2.751
.59233000	2.186	3.0929	1.872	.6780	2.762
.59234000	2.190	3.1097	1.877	.6770	2.772
.59235000	2.194	3.1272	1.881	.6759	2.783
.59236000	2.198	3.1454	1.886	.6747	2.795
.59237000	2.202	3.1644	1.891	.6735	2.807

α	r/ρ_0	ζr^3	x_0/r	y_0/r	x_0/y_0
.59238000	2.207	3.1842	1.896	.6723	2.820
.59239000	2.212	3.2051	1.901	.6710	2.833
.59240000	2.217	3.2270	1.907	.6697	2.847
.59241000	2.222	3.2500	1.913	.6683	2.862
.59242000	2.228	3.2744	1.919	.6668	2.878
.59243000	2.233	3.3002	1.925	.6653	2.894
.59244000	2.240	3.3277	1.932	.6636	2.912
.59245000	2.246	3.3570	1.940	.6619	2.931
.59246000	2.253	3.3885	1.948	.6600	2.951
.59247000	2.261	3.4224	1.956	.6581	2.973
.59248000	2.269	3.4592	1.966	.6560	2.996
.59249000	2.277	3.4994	1.976	.6537	3.022
.59250000	2.287	3.5438	1.987	.6512	3.051
.59250100	2.288	3.5485	1.988	.6509	3.054
.59250200	2.289	3.5533	1.989	.6507	3.057
.59250300	2.290	3.5581	1.990	.6504	3.060
.59250400	2.291	3.5629	1.992	.6501	3.063
.59250500	2.292	3.5679	1.993	.6498	3.067
.59250600	2.293	3.5728	1.994	.6496	3.070
.59250700	2.294	3.5778	1.995	.6493	3.073
.59250800	2.295	3.5829	1.997	.6490	3.076
.59250900	2.296	3.5881	1.998	.6487	3.080
.59251000	2.298	3.5933	1.999	.6484	3.083
.59251100	2.299	3.5986	2.000	.6482	3.086

α	r/ρ_0	$C r^3$	x_0/r	y_0/r	x_0/y_0
.59251200	2.300	3.6039	2.002	.6479	3.090
.59251300	2.301	3.6093	2.003	.6476	3.093
.59251400	2.302	3.6148	2.005	.6473	3.097
.59251500	2.303	3.6203	2.006	.6470	3.101
.59251600	2.305	3.6259	2.007	.6467	3.104
.59251700	2.306	3.6316	2.009	.6463	3.108
.59251800	2.307	3.6374	2.010	.6460	3.112
.59251900	2.308	3.6432	2.012	.6457	3.115
.59252000	2.309	3.6491	2.013	.6454	3.119
.59252100	2.311	3.6551	2.015	.6451	3.123
.59252200	2.312	3.6612	2.016	.6447	3.127
.59252300	2.313	3.6674	2.018	.6444	3.131
.59252400	2.315	3.6737	2.019	.6441	3.135
.59252500	2.316	3.6800	2.021	.6437	3.139
.59252600	2.317	3.6865	2.022	.6434	3.143
.59252700	2.319	3.6930	2.024	.6430	3.148
.59252800	2.320	3.6997	2.026	.6427	3.152
.59252900	2.321	3.7064	2.027	.6423	3.156
.59253000	2.323	3.7133	2.029	.6419	3.161
.59253100	2.324	3.7203	2.031	.6416	3.165
.59253200	2.326	3.7274	2.033	.6412	3.170
.59253300	2.327	3.7346	2.034	.6408	3.175
.59253400	2.329	3.7419	2.036	.6404	3.179
.59253500	2.330	3.7493	2.038	.6400	3.184

α	r/ρ_0	$C r^3$	x_0/r	y_0/r	x_0/y_0
.59253600	2.332	3.7569	2.040	.6396	3.189
.59253700	2.334	3.7646	2.042	.6392	3.194
.59253800	2.335	3.7725	2.044	.6388	3.199
.59253900	2.337	3.7805	2.046	.6384	3.204
.59254000	2.338	3.7886	2.048	.6380	3.210
.59254100	2.340	3.7970	2.050	.6375	3.215
.59254200	2.342	3.8054	2.052	.6371	3.221
.59254300	2.344	3.8141	2.054	.6367	3.226
.59254400	2.345	3.8229	2.056	.6362	3.232
.59254500	2.347	3.8319	2.058	.6357	3.238
.59254600	2.349	3.8411	2.061	.6353	3.244
.59254700	2.351	3.8505	2.063	.6348	3.250
.59254800	2.353	3.8601	2.065	.6343	3.256
.59254900	2.355	3.8699	2.068	.6338	3.263
.59255000	2.357	3.8799	2.070	.6333	3.269
.59255100	2.359	3.8902	2.073	.6328	3.276
.59255200	2.361	3.9007	2.075	.6322	3.283
.59255300	2.363	3.9115	2.078	.6317	3.290
.59255400	2.366	3.9226	2.081	.6311	3.297
.59255500	2.368	3.9340	2.084	.6306	3.304
.59255600	2.370	3.9457	2.086	.6300	3.312
.59255700	2.373	3.9577	2.089	.6294	3.320
.59255800	2.375	3.9700	2.092	.6288	3.328
.59255900	2.378	3.9827	2.096	.6281	3.336

α	r/ρ_0	$C r^3$	x_0/r	y_0/r	x_0/y_0
.59256000	2.380	3.9958	2.099	.6275	3.345
.59256100	2.383	4.0093	2.102	.6268	3.354
.59256200	2.386	4.0232	2.106	.6261	3.363
.59256300	2.389	4.0376	2.109	.6254	3.372
.59256400	2.392	4.0525	2.113	.6247	3.382
.59256500	2.395	4.0679	2.116	.6240	3.392
.59256600	2.398	4.0838	2.120	.6232	3.402
.59256700	2.401	4.1004	2.124	.6224	3.413
.59256800	2.404	4.1177	2.129	.6216	3.424
.59256900	2.408	4.1357	2.133	.6207	3.436
.59257000	2.411	4.1544	2.138	.6198	3.449
.59257100	2.415	4.1740	2.142	.6189	3.461
.59257200	2.419	4.1946	2.147	.6180	3.475
.59257300	2.423	4.2161	2.153	.6170	3.489
.59257400	2.428	4.2388	2.158	.6159	3.504
.59257500	2.432	4.2627	2.164	.6148	3.520
.59257600	2.437	4.2881	2.170	.6136	3.536
.59257700	2.442	4.3150	2.176	.6124	3.554
.59257800	2.447	4.3437	2.183	.6111	3.573
.59257900	2.453	4.3744	2.191	.6098	3.593
.59258000	2.459	4.4075	2.199	.6083	3.615
.59258100	2.466	4.4433	2.207	.6067	3.638
.59258200	2.473	4.4824	2.217	.6050	3.664
.59258080	2.465	4.4359	2.206	.6070	3.633

α	r/ρ_0	$C r^3$	x_0/r	y_0/r	x_0/y_0
.59258100	2.466	4.4433	2.207	.6067	3.638
.59258120	2.467	4.4508	2.209	.6064	3.643
.59258140	2.469	4.4585	2.211	.6061	3.648
.59258160	2.470	4.4663	2.213	.6057	3.653
.59258180	2.472	4.4743	2.215	.6054	3.659
.59258200	2.473	4.4824	2.217	.6050	3.664
.59258220	2.475	4.4906	2.219	.6047	3.669
.59258240	2.476	4.4990	2.221	.6043	3.675
.59258260	2.478	4.5076	2.223	.6039	3.680
.59258280	2.479	4.5164	2.225	.6036	3.686
.59258300	2.481	4.5253	2.227	.6032	3.692
.59258320	2.483	4.5344	2.229	.6028	3.698
.59258340	2.484	4.5438	2.231	.6024	3.704
.59258360	2.486	4.5533	2.234	.6020	3.711
.59258380	2.488	4.5630	2.236	.6016	3.717
.59258400	2.490	4.5730	2.238	.6011	3.723
.59258420	2.492	4.5832	2.241	.6007	3.730
.59258440	2.494	4.5936	2.243	.6003	3.737
.59258460	2.495	4.6043	2.246	.5998	3.744
.59258480	2.497	4.6153	2.248	.5994	3.751
.59258500	2.499	4.6265	2.251	.5989	3.759
.59258520	2.502	4.6381	2.254	.5984	3.766
.59258540	2.504	4.6500	2.257	.5979	3.774
.59258560	2.506	4.6622	2.260	.5974	3.782

α	r/ρ_0	$C r^3$	x_0/r	y_0/r	x_0/y_0
.59258580	2.508	4.6748	2.263	.5969	3.791
.59258600	2.510	4.6877	2.266	.5964	3.799
.59258620	2.513	4.7010	2.269	.5958	3.808
.59258640	2.515	4.7148	2.272	.5953	3.817
.59258660	2.518	4.7290	2.275	.5947	3.826
.59258680	2.520	4.7437	2.279	.5941	3.836
.59258700	2.523	4.7589	2.283	.5935	3.846
.59258720	2.526	4.7747	2.286	.5928	3.856
.59258740	2.529	4.7911	2.290	.5922	3.867
.59258760	2.532	4.8081	2.294	.5915	3.879
.59258780	2.535	4.8258	2.298	.5908	3.890
.59258800	2.538	4.8442	2.303	.5901	3.902
.59258820	2.541	4.8635	2.307	.5893	3.915
.59258840	2.545	4.8837	2.312	.5885	3.928
.59258860	2.549	4.9048	2.317	.5877	3.942
.59258880	2.552	4.9271	2.322	.5868	3.957
.59258900	2.556	4.9506	2.328	.5859	3.973
.59258905	2.558	4.9566	2.329	.5857	3.977
.59258910	2.559	4.9628	2.330	.5854	3.981
.59258915	2.560	4.9690	2.332	.5852	3.985
.59258920	2.561	4.9754	2.333	.5850	3.989
.59258925	2.562	4.9818	2.335	.5847	3.993
.59258930	2.563	4.9883	2.336	.5845	3.998
.59258933	2.564	4.9923	2.337	.5843	4.000

APPENDIX D

FORTRAN PROGRAM TO CALCULATE THE PROFILE OF THE PENDANT DROP.

```
      implicit real*8(a-h,m,o-z)
      dimension c(2,4),y(2),z(2),w(2)
      dimension xval(1500),yval(1500)
      character*5 ii
      character*15 filename,blank
      data con/57.29577951308232d0/,l/1/,nstep/6000/
      data blank/'              '/
110   xi= 0.0d0
      y(1)= 0.0d0
      y(2)= 0.0d0
      h=1.0d-3
      sw= 1.0d0
      ifreq= 20
      call bull(m,v,b,filename,blank)
      if(filename.eq.blank)stop
      x=xi
      ir=0
      kcount=0
      write(6,10)v,h,nstep
10    format(//,' beta=',d13.6,' interval=',d12.5,i7,6h steps)
      ii='dz/dx'
      if(l.eq.2)ii='dx/dz'
ck    write(6,14)x,y(1),ii,y(2)
14    format(/,' initial values x =',1pd15.8,' z =',d15.8,1x,a5,
     & ' =', d15.8)
ck    write(6,17)ii
17    format(/'  step',10x,'x',16x,'z',13x,a5,8x,'phi(deg) mode'/)
      hh=.5d0*h
      xx=x/2.54
      yy=y(1)/2.54
cf    write(20,300)xx,yy
      kcount= kcount + 1
      xval(kcount)=xx
      yval(kcount)=yy
cp    xx=-xx
cf    write(21,300)xx,yy
cp    xval(kcount + 500 )= xx
cp    yval(kcount + 500 )= yy
300   format(1x,1pe16.8,1x,e16.8)
      h6=h/6.d0
      do 70 i=1,nstep
      xh=x + h
      xhh=x+hh
      do 23 j=1,2
      c(j,1)=f(x,y(1),y(2),j,v,l)
```

```
23        z(j)=y(j)+hh*c(j,1)
          do 26 j=1,2
          c(j,2)=f(xhh,z(1),z(2),j,v,l)
26        w(j)=y(j)+hh*c(j,2)
          do 29 j=1,2
          c(j,3)=f(xhh,w(1),w(2),j,v,l)
29        z(j)=y(j)+h*c(j,3)
          do 32 j=1,2
          c(j,4)=f(xh,z(1),z(2),j,v,l)
32        y(j)=y(j)+h6*(c(j,1)+c(j,4)+2.d0*(c(j,2)+c(j,3)))
          x=xi+h*dfloat(i-ir)
          a=dabs(y(2))
          if(mod(i,ifreq).ne.0.and.a.lt.1.d1.and.a.gt.1.d-2)go to 49
          d=dsqrt(1.d0+y(2)**2)
          s=y(2)/d
          if(l.eq.2)goto43
          t=con*asin(sngl(s))
          xp=x*b*m
          yp=y(1)*b*m
          goto46
43        t=con*acos(sngl(s))
          yp=x*b*m
          xp=y(1)*b*m
46        continue
ck        write(6,47)i,xp,yp,y(2),t,l
47        format(i7,1p3d17.8,0pf11.5,i4)
          xx=xp/2.54
          yy=yp/2.54
cf        write(20,300)xx,yy
          kcount= kcount+1
          xval(kcount)= xx
          yval(kcount)= yy
cp        xx=-xx
cf        write(21,300)xx,yy
cp        xval(kcount + 500) = xx
cp        yval(kcount + 500) = yy
          xp=-xp
          if(a.gt.1.d10)go to 71
49        if(a.le.sw.or.sw.le.0.d0)go to 70
          l=3-l
          xi=y(1)
          y(1)=x
          x=xi
          ir=i
          if(y(2).lt.0.d0)h=-h
          hh=.5d0*h
          h6=h/6.d0
          y(2)=1.d0/y(2)
          if(l.eq.2)goto64
          ii='dz/dx'
          xp=x
          yp=y(1)
          goto67
64        ii='dx/dz'
```

```
      xp=y(1)
          yp=x
67        xp=xp*b*m
          yp=yp*b*m
ck        write(6,14)xp,yp,ii,y(2)
ck        write(6,17)ii
70        continue
71        continue
cf        close(20)
cf        close(21)
          call order(xval,yval,kcount,filename)
          goto 110
          end
c
          function f(y,u,w,k,v,l)
          implicit real*8(a-h,o-z)
          f=w
          if(k.lt.2)return
          t=w*w+1.d0
          s=dsqrt(t)
          if(l.gt.1)go to 90
          q=1.d0
          if(dabs(y).gt.1.d-30)q=w/(y*s)
          f=t*s*(v*u-q+2.d0)
          return
90        q=1.d30
          if(dabs(u).gt.1.d-30)q=1.d0/(u*s)
          g=v*y+2.d0
          if(u.lt.0.d0)g=-g
          f=t*s*(q-g)
          return
          end
c
          subroutine bull(m,beta,b,filename,blank)
          implicit real*8(a-h,m,o-z)
          character*15 filename,blank
          write(0,102)
102       format(/,/,' enter the name of output file ')
          read(5,103,end=109)filename
          if(filename.eq.blank)goto 109
          write(0,101)
101       format(' enter P, M, De, Ds, DELRHO, TEMP.')
          read(5,*)p,m,de,ds,delro,t
103       format(a15)
          s=ds/de
          h=((((((((((((-1.46968303d+02*s +4.51063013d+02)*s
         &  - 2.32103942d+02)*s - 4.42314089d+02)*s + 1.12175064d+02)*s
         &  + 8.23897542d+02)*s - 2.82708556d+02)*s - 1.10855392d+03)*s
         &  + 1.15840257d+03)*s - 1.21414986d+02)*s - 4.62509224d+02)*s
         &  + 3.50813741d+02)*s - 1.18301201d+02)*s + 2.02196936d+01)*s
         &  - 1.39155241d+00
          h=h/s**4
          g=980.4d0
          beta=-dexp(-6.70905 + 15.3002*s - 16.4479*(s**2)
```

```
     &  + 9.92425*s*(s**2) - 2.58503*(s**2)*(s**2))
        gamai=delro*g*((de/m)**2)*h
        e=((de/m)**2)
        c=(2*gamai)/(delro*g)
        b=dsqrt((dabs(beta)*c)/2)
        write(6,119)filename
119     format(/,/' NAME OF FILE = ',a15)
        write(6,120)p
120     format(/' PHOTO # =',f10.6)
        write(6,122)m
122     format(' MAGNITUDE =',f9.5)
        write(6,124)de
124     format(' De =',f8.4)
        write(6,126)ds
126     format(' Ds =',f8.4)
        write(6,128)s
128     format(' S =',f10.6)
        write(6,130)h
130     format(' 1/H =',f10.6)
        write(6,132)t
132     format(' TEMPERATURE =',f6.2)
        write(6,134)delro
134     format(' DENSITY DIFFERENCE =',f9.5)
        write(6,136)g
136     format(' G =',f6.2)
        write(6,138)e
138     format(' (De/M)**2 =',f10.6)
        write(6,140)gamai
140     format(' TENSION =',1pe12.5)
        write(6,142)c
142     format(' CAPILLARY CONSTANT =',f10.6)
        write(6,144)beta
144     format(' BETA =',f10.6)
        write(6,146)b
146     format(' RADIUS b =',f10.6)
        return
109     filename=blank
        return
        end
c
        subroutine order(x,y,kcount,filename)
        implicit real*8(a-h,m,o-z)
        dimension x(1500),y(1500)
        character*15 filename
        kct=kcount/2
        do 9  kk=1,kct
        attemptx=x(kk)
        attempty=y(kk)
        x(kk)=x(kcount+1-kk)
        y(kk)=y(kcount+1-kk)
        x(kcount+1-kk)=attemptx
        y(kcount+1-kk)=attempty
9       continue
        do 10      kk =1,kcount
```

```
      y(kcount + kk)= y(kcount-kk)
          x(kcount + kk)= -x(kcount-kk)
10        continue
          n2= 2*kcount - 1
          open(1,file=filename)
          write(1,3)(x(i),y(i),i=1,n2)
3         format(1x,1pe16.8,1x,e16.8)
          close(1)
          return
          end
```

APPENDIX E

OPTIMIZATION PROGRAM TO CALCULATE THE INTERFACIAL TENSION AND VISCOSITY FOR THE LIGHT SCATTERING METHOD

```
c        size of array x(400,3) was changed to x(400,1) to save space
c        on 6/22/84
c        channel 19,18,17,16 are being used at the present 6/15/84
cmain    main - calling program for nonlinear least squares fit.
c   main program for utilizing the nonlinear least squares fitting
c   procedure from bell labs.  this program will read in the data and
c   relevant program constants, determine the appropriate statistical
c   constants ff and t, call nllsq, and determine the nonlinear
c   condidence limits with phi minimized if final printout option
c   narray(6) =3, narray(3) contains the # of parameters and b(2)
c    contains the value of the parameters
      double precision a,sa
      character*15 filnam,blank,fitfil
      character*1 ians,clbt,chkopen16
      common/blk1/b(20),p(20),re,n,m,k
      common/blk2/a(40,20),sa(20),k2,ik
      common/blk4/al,delta,e,ff,gamcr,t,tau,zeta,phi,se,phicr
      common/sblk1/temp,nf21,kend,chkopen16,clbt
      common/sblk2/fitfil,filnam,blank
      dimension x(400,1),y(400),narray(8),array(8),res(400),ib(20)
      character*4 ichadum(16),ichary(2060)
      dimension idum(16),iy(2060),bres(20),sdb(20,4)
      equivalence (idum(1),ichadum(1)),(iy(1),ichary(1))
      data blank/'          '/,kend/'999'/
      data ichadum/'0','1','2','3','4','5','6','7','8','9','a','b',
     1   'c','d','e','f'/
      cntflg=0
      write(6,26)
26    format(' write the number of parameters (1/2): ',$)
      read(5,*)narri
      write(6,27)narri
27    format(i3)
      write(6,29)
29    format(/' printout of selected data points (y/n): ',$)
      read(5,*)ians
      write(6,30)ians
30    format(a2)
      if(ians.ne.'y')ians='n'
      narri=narri+2
      ikk=6
      if(narri.ne.3)narri=4
      call redat1(clbt,ichn5,ikk,cntflg)
```

```
32          continue
            goto 36
36          narray(3)=narri
            narray(2)=1
            narray(4)=0
            narray(5)=0
            narray(6)=0
c     the narray(7) stores the output channel 6
            narray(7)=ikk
            narray(8)=30
            do 44  j=1,8
44          array(j)=0.0
            m=narray(2)
            k=narray(3)
            ip=narray(4)
            ik=narray(7)
            iflag=0
            do 51 i=1,k
51          ib(i)=0
            if(narray(6).ne.3)goto 55
            narray(6)=2
            iflag=1
55          continue
            call redat2(filnam,blank)
            if(filnam.ne.blank)goto 57
58          write(6,56)
56          format()
            if(chkopen16.eq.'y')close(16)
            stop
57          open(19,file=filnam)
            rewind 19
            read(19,60)(ichary(j), j=1,2050)
60          format(70a1)
            close(19)
            do 71  j=1,2050
            do 67  k=1,16
            if(isign(iy(j),idum(k)).ne.iy(j))goto 66
            if(iy(j)-idum(k))66,70,66
66          continue
67          continue
            write(6,69)j
69          format('  error',i5)
70          iy(j)=k-1
71          continue
            do 90 j=50, 2045, 5
            ichar=iy(j+1)*4
            temp=0.1+float(iy(j+2))/4.0
            itemp1=int(temp)
            itemp2=iy(j+2)-4*itemp1
            ichar=ichar+itemp1
            if(ichar.gt.31)ichar=ichar-64
            char=2.0**ichar
            itemp2=itemp2*128
            itemp2=8*iy(j+3)+itemp2
```

```
      temp=float(iy(j+4))/2.0+0.1
           itemp3=int(temp)
           itemp2=itemp2+itemp3
           if(itemps2.gt.255)itemp2=itemp2-512
           amant=float(itemp2)/256.0
           k=int(float(j)/5.0-8.9)
           if(iy(j+5).eq.4)goto 90
           write(6,69)j
90         y(k)=amant*char
           j=0
           temp=0.1+float(iy(7))/4.0
           itemp1=int(temp)
           itemp2=iy(7)-4*itemp1
           itemp1=itemp1+4*mod(iy(6),2)
           if(itemp2.eq.0)freq=1.0
           if(itemp2.eq.1)freq=2.0
           if(itemp2.eq.2)freq=5.0
           if(itemp2.eq.3)write(6,69)j
           freq=freq*(10.0**itemp1)
           irange=int(freq)
           call redat3(irange,nstart,nstop,ichn5)
           narray(1)=nstop-nstart+1
           n=narray(1)
           nf21=n
           do 108 j=1,n
108        y(j)=y(nstart+j-1)
           yminpw=9.0e20
           ymaxpw=0
           do 117 j=1,n
           x(j,1)=float(nstart+j-1)*freq/400.0
           yminpw=amin1(yminpw,y(i))
           if(ymaxpw.ge.y(j))goto 117
           ymaxpw=y(j)
           xmaxpw=x(j,1)
           ind=j
           ichnn=nstart+j-1
117        continue
           write(ik,119)xmaxpw,ymaxpw,ichnn
119        format(/,' peak freq.= ',f8.2,3x,'max.power= ',1pe14.7,3x,
       1   'channel #= ',0pi4)
           b(1)=ymaxpw
           b(2)=99.9e30
           b(4)=99.9e30
           b(3)=ymaxpw-yminpw
           call scattr(xmaxpw,power,b(4),b(2),x,ind)
           if(filnam.eq.blank)goto 58
c     compute statistical constants ff and t
           df1=narray(3)-narray(4)
           df2=narray(1)-narray(3)+narray(4)
           if(array(4).ne.0.0)goto 135
           array(4)=qfdis(.6826,df1,df2)
135        if(array(6).ne.0.0)goto 138
           array(6)=qtdis(.8413,df2)
c     call nllsq fitting procedure
```

```
138       call nllsq(y,x,b,res,narray,array,ib)
c   final printout
          jp=4
          write(ik,142)
142       format(/' ----------final values----------')
          rphi=phi/(n-k+ip)
          dev=0.0
          filnam='exp.dat'
          call redat4(filnam,ichn5)
          fitfil='fit.dat'
          call redat4(fitfil,ichn5)
          open(18,file=filnam)
          open(17,file=fitfil)
152       do 164  i=1,n
          call model(f,y,x,res,i,jp)
          if(filnam.eq.blank)goto 58
          xx=100.0*(y(i)-f)/f
          dev=dev+xx*xx
          xx=float(i+nstart-1)
          write(18,163)x(i,1),y(i)
          write(17,163)x(i,1),f
163       format(2(1x,e13.5))
164       continue
          close(18)
          close(17)
168       dev=sqrt(dev/n)
          write(ik,170)rphi,dev
170       format(/' reduced chi squared='f12.7,5x,'rms % deviation='f11.6)
          kend=2
          call scattr(free,power,b(4),b(2),x,ind)
          if(filnam.eq.blank)goto 58
          kend=0
          xmin=x(1,1)
          xmax=x(n,1)
c         write(6,183)
c183          format(/' do you wish a printout for selected
     &  data points? (y/d)')
c         read(5,185)ians
185       format(a1)
          if(ians.ne.'y')goto 204
          write(6,188)
188       format(/,'  every',5h n'th,' data point will be printed.  n= ',$)
          read(5,*)hold
          itemp=ifix(hold)
          write(ikk,*)itemp
          write(ik,193)
193       format(/,10x,'residual=(data-fit)*sqrt(weight)',/)
          write(ik,195)
195       format(/,3x,'i',7x,'x(i,1)',10x,'x(i,2)',10x,'x(i,3)',
     &  10x,'data (i)',10x,'fit(i)',7x,'residual(i)',5x,
     &  '100(d-f)/f')
          nk=0
          do 202 i=1,n,itemp
          call model(f,y,x,res,i,jp)
```

```
      if(filnam.eq.blank)goto 58
          xx=100.0*(y(i)-f)/f
202       write(ik,203)i,x(i,1),x(i,2),x(i,3),y(i),f,re,xx
203       format(1x,i3,1p7e16.5)
204       continue
          if(iflag.ne.1)goto 260
c     determination of nonlinear confidence limits with phi minimized
          narray(4)=narray(4)+1
          ip=narray(4)
          if(ip.ne.k)goto 213
          write(ik,211)
211       format(//,2x,'no further confidence limits possible')
          goto 260
213       continue
          do 220 i=1,k
          do 217 j=1,ip
          if(ib(j).eq.i)goto 220
217       continue
          ib(ip)=i
          goto 221
220       continue
221       narray(5)=0
          narray(6)=-1
          do 224 j=1,k
224       bres(j)=b(j)
          ihold=ib(ip)
          ste=sa(ihold)*se
          fkw=k-ip+1
          hjtd=sqrt(ff*fkw)*ste
          eps2=hjtd/2.0
          write(ik,231)ib(ip)
231       format(//,2x,'nonlinear confidence limits, phi minimized',
         &  //,2x,'parameter to be incremented =',i4,//,2x,5h para,6x,
         &  8h lower b,8x,10h lower phi,10x,8h upper b,8x,10h upper phi)
          do 259 l=1,4
          b(ihold)=bres(ihold)+eps2
          do 245 la=1,3,2
          call nllsq(y,x,b,res,narray,array,ib)
          do 241 lb=1,k
          sdb(lb,la)=b(lb)
          sdb(lb,la+1)=phi
241       continue
          do 243 lc=1,k
243       b(lc)=bres(lc)
          b(ihold)=bres(ihold)-eps2
245       continue
          eps2=eps2+hjtd/2.0
          do 255 i=1,k
          if(sdb(i,1).le.sdb(i,3))goto 255
          save=sdb(i,1)
          sdb(i,1)=sdb(i,3)
          sdb(i,3)=save
          save=sdb(i,2)
          sdb(i,2)=sdb(i,4)
```

```
      sdb(i,4)=save
255   continue
      do 257 j=1,k
257   write(ik,258)j,(sdb(j,i), i=1,4)
258   format(4x,i3,1p4e18.5)
259   continue
260   continue
      write(6,262)
262   format(' --------- --------- -------- --------')
      goto 32
      end
c   computation of the statistical constants ff and t
      function qfdis(prob,df1,df2)
      external fdens
      common/blk6/vf,wf,bf
      bf=bfeta(df1/2.0,df2/2.0)
      qf=1.0
      pfold=0.99
      a=0.0
      vf=df1
      wf=df2
      del=0.001
      aold=0.0
      n=1000
      eps1=0.0005
      eps2=1.0
281   area=sfimps(a,qf,n,fdens)
      pf=aold+area
      if(pf-prob.gt.eps1)goto 287
      if(prob-pf.gt.eps1)goto 293
      qfdis=qf
      return
287   if(pfold.lt.prob)eps2=eps2/2.0
      qf=qf-eps2
      n=(qf-a)/del
      if(n.lt.10)n=10
      pfold=pf
      goto 281
293   if(pfold.gt.prob)eps2=eps2/2.0
      a=qf
      aold=pf
      qf=qf+eps2
      n=(qf-a)/del
      if(n.lt.10)n=10
      pfold=pf
      goto 281
      end
      function fdens(x)
      common/blk6/vf,wf,bf
      if(x.le.0.0)goto 314
      vh=vf/2.0
      wh=wf/2.0
      r=vf/wf
      fdens=(r**vh)/bf
```

```
      e=(vf-2.0)/2.0
          fdens=fdens*(x**e)
          e=(vf+wf)/2.0
          fdens=fdens/((1.0+r*x)**e)
          return
  314     fdens=0.0
          return
          end
          function sfimps(a,b,n,f)
          external f
          twoh=(b-a)/n
          h=twoh/2.0
          sumf1=0.0
          sumf2=0.0
          do 326 k=1,n
          x=a+float(k-1)*twoh
          sumf1=sumf1+f(x)
          sumf2=sumf2+f(x+h)
  326     continue
          sfimps=(2.0*sumf1+4.0*sumf2+f(b))*h/3.0
          return
          end
          function bfeta(v1,v2)
          numb=1000
          astart=0.0
          bend=1.0
          twohb=(bend-astart)/numb
          hinc=twohb/2.0
          sume=0.0
          summ=0.0
          u1=v1
          u2=v2-1.0
          do 350 ldo=1,numb
          var1=astart+float(ldo-1)*twohb
          var2=var1+hinc
          eta=(1.0-var1)**u2
          eta=eta*(var1**u1)
          sume=sume+eta
          eta=(1.0-var2)**u2
          eta=eta*(var2**u1)
c --- --- --- k --- 6/13/83 included.
          if(eta.lt.3.0e-37)goto 351
  350     summ=summ+eta
  351     bfeta=(2.0*sume+4.0*summ)*hinc/3.0
          bfeta=bfeta*(v1+v2)/v1
          return
          end
          function qtdis(oma,df2)
          common/blk7/vt,tb
          external tdens
          prob=1.0-2.0*(1.0-oma)
          qt=1.0
          ptold=0.99
          a=0.0
```

```
      vt=df2
         eps1=0.0005
         eps2=0.2
         n=100
         tb=bteta(df2/2.0)
         tb=tb*0.5641896/sqrt(df2)
368      pt=2.0*stimps(a,qt,n,tdens)
         if(pt-prob.gt.eps1)goto 373
         if(prob-pt.gt.eps1)goto 377
         qtdis=qt
         return
373      if(ptold.lt.prob)eps2=eps2/2.0
         qt=qt-eps2
         ptold=pt
         goto 368
377      if(ptold.gt.prob)eps2=eps2/2.0
         qt=qt+eps2
         ptold=pt
         goto 368
         end
         function tdens(z)
         common/blk7/vt,tb
         h2=vt/2.0+0.5
         tdens=tb/((1.0+z*z/vt)**h2)
         return
         end
         function stimps(a,b,n,f)
         external f
         twoh=(b-a)/n
         h=twoh/2.0
         sumt1=0.0
         sumt2=0.0
         do 397  k=1,n
         x=a+float(k-1)*twoh
         sumt1=sumt1+f(x)
         sumt2=sumt2+f(x+h)
397      continue
         stimps=(2.0*sumt1+4.0*sumt2-f(a)+f(b))*h/3.0
         return
         end
         function bteta(arg)
         bteta=0.6065307*sqrt(arg)
         bteta=bteta*(((arg+0.5)/arg)**arg)
         bteta=alog(bteta)-1.0/(24.0*arg*arg+12.0*arg)
         bteta=exp(bteta)
         return
         end
cmodel     model - computes value of the function and its partials
         subroutine model(f,y,x,res,i,jp)
         common/blk1/b(20),p(20),re,n,m,k
         common/modonly/pw(400,10),strb4(10),strb2(10),indclm,ncl
         dimension y(1),x(400,1),res(1)
         dimension pw(400,10),strb4(10),strb2(10)
c    determine appropriate weight of i'th data point
```

```
c   weight is equal to the inverse of the rms deviations in y(i)
          sigma=0.03*y(i)
          wt=1.0/sigma
c   compute the function
          omega=x(i,1)
          do 400 kp=1,ncl
          if(strb2(kp).eq.b(2).and.strb4(kp).eq.b(4))goto 420
400       continue
          call scattr(omega,power,b(4),b(2),x,i)
          kp=indclm
420       continue
          f=b(1)*pw(i,kp)+b(3)
ck        f=b(1)*power+b(3)
c   compute the weighted residual
422       re=(y(i)-f)*wt
c         if(b(4).lt.0.0)re=re*(1.0-b(4)+b(4)*b(4))
          goto(428,427,428,430),jp
c   return jp=3 and the weighted function
c   for computation of the partials by nllsq
427       jp=3
428       f=f*wt
          return
430       res(i)=re
          return
          end
```

PROGRAM SUBROUTINE TO INITIALIZE THE APPROPRIATE PARAMETERS AND TO CALL THE THEORETICAL POWER SPECTRUM OF THE SCATTERED LIGHT.

```
c              ----------
          subroutine scattr(omega,power,b4,b2,x,indrow)
          character*15 fitfil,filnam,blank,card,an
          character*1 clbt,chkopen16
          dimension wt(400),x(400,1),pw(400,10),strb4(10),strb2(10)
          common/pass/ichnl
          common/sblk1/temp,nint,kend,chkopen16,clbt
          common/sblk2/fitfil,filnam,blank
          common/instr/ahwins,ndeltq,istepq
          common/modonly/pw(400,10),strb4(10),strb2(10),indclm,ncl
          data ztwopi/6.2831853e0/,z/0.e0/,istepq/1/,wt/400*1.0/,ncl/10/
c
30        if(clbt.ne.'y'.and.kend.eq.2)goto 129
          if(clbt.eq.'y'.and.kend.eq.2)goto 112
          if(b4.lt.99.9e30.and.b2.lt.99.9e30)goto 61
c
c-----reading sequence is first line data filename ----------
c-----second line is temp,den1,visc1,den2,visc2,interf. tension,ID #-------
c---- third line refractive index, incident angle, d value, l value -----
c---- (see below in subroutine qvalue for better definition) ---
c
c ichnl refers to the output channel 6, the same channel as nnlsq
c and the main program output channel
c record.dat is a file which outputs in channel 1
```

```
c ------------      initialization procedure      ---------
          write(ichnl,15)
          call system ("date")
          write(ichnl,15)
15        format(/,/)
          ichn5=5
          write(ichnl,25)
25        format(/,' input values for:',/,' temp., den.1, visc.1,
         &   den.2, visc.2, interfacial tension and an ',/)
          read(ichn5,*)temp,den1,visc1,den2,visc2,tenson,an
          write(ichnl,27)an,temp,den1,visc1,den2,visc2,tenson
27        format(/' data #= ',a15,/,3x,'temperature= ',f7.2,3x,'density
         &    phase one= ',f7.4,/,' viscosity phase one= ',1pe11.4,3x,
         &   'density phase two= ',0pf7.4,3x,/,' viscosity phase two= '
         &   1pe11.4,3x,'tension= ',e11.4)
          zscale=1.0e20
          b4=visc2
          b2=tenson
          do 39 ii=1,10
          strb4(ii)=999999.0
39        strb2(ii)=999999.0
          nj=0
          nk=0
          icount=0
          an=filnam
          if(clbt.eq.'t')ndeltq=0
          irngeq=2*iabs(ndeltq)+1
c   In the initialization of the parameters:
c   If the second density is 0. The calculation assumes the conditions
c   at a critical point (where the kinematic viscosity of both
c   phases are equal).
c   If the first density is 0.  the calculation assumes an air-liquid
c   surface (assuming the kinematic viscosity of both phases are
c   equal and the upper phase viscosity is neglegible).  the zero
c   entries must be the first density and viscosity
c   the following conditions will result in an error in input data
c   for subroutine interf.
c       1    both densities have a 0.0
c       2    the second viscosity have 0.0
c       3    the first viscosity and the second density have 0.0
          card='ok'
          if(den2.eq.0.0)card='crit'
          if(den1.eq.0.0)card='air'
          if(den2.eq.z.and.den1.eq.z)card='error'
          if(visc2.eq.z)card='error'
          if(den2.eq.z.and.visc1.eq.z)card='error'
          if(card.eq.'error')write(6,52)den2,den1,visc2,visc1
52        format(/' the value of den2 is ',f6.4,' of den1 is ',f6.4,
         &   /' of visc2 is ',f6.5,' and of visc1 is ',f6.5)
          call qvalue(centeq,ichnl,ichn5)
          if((den2.le.z.and.den1.le.z).or.visc2.le.z.or.(visc1.le.z.and.
         &   den2.le.z).or.tenson.le.z.or.centeq.le.z)goto 141
c
c     ---------- the instrumentational width is b4 ----------
```

```
      if(ahwins.ne.0.0.and.clbt.eq.'y')b4=ahwins
         goto 67
c
c        ============    continuation process    ============
ck61          do 62 indclm=1,10
ck62          if(b4.eq.strb4(indclm).and.b2.eq.strb2(indclm))goto107
c
c        --------- spectral linewidth calibration process ---------
61       continue
         if(clbt.ne.'y')goto 70
         ahwins=b4
         tenson=b2
67       if(ahwins.ne.0.0)hwins=ahwins
         goto 72
c
c        --- interfacial tension and viscosity optimization process ---
70       tenson=b2
         visc2=b4
72       if(icount.eq.10)icount=0
         icount=icount+1
         strb4(icount)=b4
         strb2(icount)=b2
         indclm=icount
         if(b4.ge.0.0.or.b2.ge.0.0)goto 74
         power=1.0e12
         do 73 kk=1,nint
         pw(kk,icount)=0.0
73       continue
         return
74       if(clbt.eq.'t')goto 81
c
c        --- the instrument function of the spectrum is a  ----
c        --- lorentzian squared function              ----
c        -- ndeltq is the range of q values taken for calculation ------
c        -- centered at centeq.
         do 80 in=1,irngeq,istepq
         dq1=float(in-1-ndeltq)
         dq1=abs(dq1)
         wti=1.0/(dq1*dq1/(hwins*hwins)+1)
         wti=wti*wti
80       wt(in)=wti*zscale
81       continue
         nk=nk+1
         if(nk.ne.25)goto 86
         nk=0
         nj=nj+1
         write(6,85)nj
85       format(2x,i3)
86       continue
         call interf(wt,pw,x,icount,irngeq,istepq,ndeltq,centeq,
        &   temp1,tenson,den1,den2,visc1,visc2,ichn1,yk,tau,card)
107      power=pw(indrow,indclm)
         if(omega.ne.x(indrow,1))write(6,109)omega,x(indrow,1)
109      format(' frequency of ',1pe12.5,' does not match ',e12.5,' stop
```

```
     &  the program ')
        return
112     if(chkopen16.eq.'y')goto 250
        call ioinit(.false.,.false.,.true.,'',.false.)
        open(16,file='record.dat')
        chkopen16='y'
250     write(16,120)fitfil,temp1,den1,visc1,den2,visc2,tenson,centeq,
     &  b4,ndeltq,x(1,1),x(nint,1),an
        write(ichnl,120)fitfil,temp1,den1,visc1,den2,visc2,tenson,centeq,
     &  b4,ndeltq,x(1,1),x(nint,1),an
             zminwgt = wt(irngeq)/zscale * 100.0
        write(ichnl,119)yk,tau,clbt
        write(ichnl,130)zminwgt
        write(16,119)yk,tau,clbt
        write(16,130)zminwgt
119     format(3x'y value= ',e13.6,3x,'tau value= ',e13.6,3x'clbt= ',a1)
130     format(' percent of the lowest inst. weight contribut. = ',1pe13.6)
120     format(//1x,a15,3x,'temp= ',f7.2,3x,'den1= ',f7.4,3x,'visc1= ',
     &  1pe10.4,/,' den2= ',0pf6.4,' visc2= ',1pe11.4,3x,'tension= '
     &  1pe11.4,3x,/,' q= ',0pf8.3,' instrument function = ',1pe11.4,
     &  'q  spread= ',0pi3./,' intl freq.= ',1pe10.4,' final freq.= ',
     &  e10.4,2x,'file= ',a15)
        kend=0
        return
129     if(chkopen16.eq.'y')goto 260
        call ioinit(.false.,.false.,.true.,'',.false.)
        open(16,file='record.dat')
        chkopen16='y'
260     write(16,120)fitfil,temp1,den1,visc1,den2,b4,b2,centeq,hwins,
     &  ndeltq,x(1,1),x(nint,1),an
        write(ichnl,120)fitfil,temp1,den1,visc1,den2,b4,b2,centeq,hwins,
     &  ndeltq,x(1,1),x(nint,1),an
        write(ichnl,119) yk,tau,clbt
        write(16,119)yk,tau,clbt
        kend=0
        return
141     write(ichnl,142)
142     format(/' error in the scattering subroutine input')
        filnam=blank
        return
        end
c ccc ****** ****** ****** ****** ****** ****** ******
        subroutine interf(wt,pw,x,icount,irngeq,istepq,ndeltq,centeq,
     &  t,tenson,denup,denlr,viscup,visclr,ichnl,realy,tau,card)
        character*1 chkopen16,clbt
        character*5 card
        dimension wt(1),pw(400,1),x(400,1)
        common/sblk1/temp,nint,kend,chkopen16,clbt
        complex y,s,am,amu,coeff1,coeff2,s1term
        complex s2term,ds,one
        double precision ztwopi,boltz
        data ztwopi/6.28318530717959d0/,boltz/1.38066d-16/,z/0.e0/
        data zpi/3.141592/
        if(card.eq.'crit')denlr=denup/viscup*visclr
```

```
      if(card.eq.'air')viscup=visclr*1.0e-15
          if(card.eq.'air')denup=denlr*1.0e-15
          t=temp+273.16
          g=980.0
          sumden=(denup+denlr)
          sumvis=(viscup+visclr)
          one=cmplx(1.0,0.0)
          r=(visclr/denlr - viscup/denup)/(sumvis/sumden)
          an=2*sumden/(sumden+r*denup)
          anu=2.0*sumden/(sumden-r*denlr)
          an2=(denlr**2-denup**2+2*r*denlr*denup)/(sumden**2)
c  &&&&&&&&&  &&&&&&&&
          fmax=0.0
          pmax=0.0
          pmin=1e30
          aq=0
60          do 100 irow=1,nint
            w=ztwopi*x(irow,1)
            p2=0
c  aq must be zero if clbt= 't' or theoretical calculation only without
c  instrument function.
             do 99 in=1,irngeq,istepq
             aq=float(in-1-ndeltq)
             q=centeq+aq
c  Theoretical equation follows from here.
          alphaq=tenson+abs(denlr-denup)*g/(q*q)
          tau=sumden/(2*sumvis*q*q)
          realy=alphaq*sumden/(4*sumvis*sumvis*q)
          y=cmplx(realy,0.0)
          reals=-1*w*tau
          s=cmplx(0.0,reals)
          am=cmplx(1.0,an*reals)
          am=csqrt(am)
ck        write(6,70)am
ck70          format(' sqrt of am= ',1pe12.5,3x,1pe12.5)
          amu=cmplx(1.0,anu*reals)
          amu=csqrt(amu)
ck        write(6,76)amu
ck76          format(' sqrt amu= ',e12.5,2x,e12.5)
          coeff1=(visclr*(am-one)-viscup*(amu-one))
          coeff1=coeff1/(visclr*(am+one)+viscup*(amu+one))
          s1term=an2*coeff1*s
          coeff1=visclr*(am*am+one)+viscup*(am-one+amu*(am+one))
          coeff1=denlr*coeff1/(am-one)
          coeff2=viscup*(amu*amu+1)+visclr*(amu-one+am*(amu+one))
          coeff2=denup*coeff2/(amu-one)
          coeff2=(coeff2+coeff1)/sumden
          coeff2=coeff2/(visclr*(am+one)+viscup*(amu+one))
          s2term=coeff2*s*s
          ds=y+s1term+s2term
          tests=cabs(ds)
          if(tests.ge.1.d-30)goto 80
          write(ichnl,381)
381       format(' error imaginary absolute value too small, power=0')
```

```
      omega=w/ztwopi
          write(ichnl,384)omega
384       format(' frequency= ',1pe14.7,4x,'power(w)=0')
          pw(irow,icount)=0.0
          goto 60
80        ds=1/ds
          zim=aimag(ds)
c         coeff3=realy*boltz*t
c         coeff3=coeff3/(alphaq*q*q*zpi*w)
          coeff3=realy/(alphaq*q*q*zpi*w)
          pp=coeff3*zim
              p2=p2+wt(in)*pp
99            continue
             pw(irow,icount)=p2
             pmin=amin1(pmin,p2)
             pmax=amax1(pmax,p2)
ck           if(pmax.gt.p2)fmax=x(irow,1)
100          continue
          deltap=pmax-pmin
          do 106 nn=1,nint
          pw(nn,icount)=(pw(nn,icount)-pmin)/deltap
106       continue
          return
          end
c ccc ----- ----- ----- ---- ----- ----- ----- -----
c ccc ----- ----- ----- ---- ----- ----- ----- -----
c  the equation for q is q*q = k*k[sin(reflid angle)**2 + sin(scatt
c  angle)**2 - 2sin(reflid angle)*sin(scatt angle)*cos(phi)]
ck   To avoid numerical roundoff error the determination of
ck  q wavevector is done in double precision form 8/30/84
          subroutine qvalue(centeq,ichn1,ichn5)
          implicit real*8 (z)
          equivalence (centeq1,zcenteq)
          data zpi/3.14159265358979/
ck  ----- wavelength of an helium-neon laser in cm ------
          zwavel= 6.328d-5
          zphi=0.0d0
          write(ichn1,172)
172       format(/,' refr.  angle   dist   length   q ')
174       read(ichn5,*)zrefr,zangle,zd,zal
          zainang=(zangle)*zpi/180.0d0
          za=sin(zainang)/zrefr
          zreangl=asin(za)
          ztheta0=zpi/2.0 - zreangl
ck  For values of q the reading sequence is refr=refractive index.
ck  angle= angle of incident of the reflected beam
ck  normal to the cell wall in the air
ck  medium, d= distance from the pinhole to the
ck  center of the beam.  al=distance from the cell to the phototube.
ck  distance d measured from the reflected beam toward the normal
ck  of the reflected plane is taken as a positive distance.
ck  That from the reflected beam to the incident plane is
ck  taken as negative distance. 8-12/84
          zc=-zd/zal
```

```
      zdtheta= zc*cos(zainang)/(zrefr*cos(zreangl))
          zvectrl=2.0*zpi*zrefr/zwavel
          zsangle=ztheta0+zdtheta
          zascat=sin(zsangle)*sin(zsangle)
          zreflct=sin(ztheta0)*sin(ztheta0)
          zaph=2.0*sin(zsangle)*sin(ztheta0)*cos(zphi)
          zcenteq=zvectrl*zvectrl*(zascat+zreflct-zaph)
          zcenteq=sqrt(zcenteq)
          centeq = centeq1
          write(ichnl,192) zrefr,zangle,zd,zal,centeq
192       format(1x,f6.4,2x,f6.3,2x,f6.3,2x,f7.3,2x,f7.3)
          return
          end
c  $$$$$$ $$$$$$ $$$$$ $$$$$$ $$$$$$$
          subroutine redat1(clbt,ichn5,ikk,cntflg)
          common/pass/ichnl
          character*1 clbt
          if(cntflg.ne.0)goto 270
          cntflg=cntflg+1
          ichnl=ikk
          ichn5=5
264       write(6,265)
265       format(/'  calibrating spectrum (y/n/t):  ',$)
257       read(ichn5,267)clbt
267       format(a1)
          if(clbt.eq.' ')clbt='n'
          write(ichnl,271) clbt
271       format(a1)
          if(clbt.eq.'y'.or.clbt.eq.'n'.or.clbt.eq.'t')goto 270
258       write(6,259)clbt
259       format('  the calibration spectrum(y/n/t) was ',a2,
         &  ' type the correct symbol ',$)
          goto 257
270       continue
          call instpar(ichn5,clbt)
          return
          end
c  ######### $$$$$$$$ &&&&&&& ........ !!!!!!!!!!
c         if the calculation is theoretical ndeltq=0 and ahwins=1
          subroutine instpar(ichn5,clbt)
          common/pass/ichnl
          common /instr/ahwins,ndeltq,istepq
          character*1 clbt
          ns=0
          write(6,200)
200       format(/' type spread of q value and instrumental width:  ')
          read(ichn5,*)adq,ahwins
          if(clbt.ne.'t')goto 190
          ahwins=1.0
          ndeltq=0
          write(ichnl,210)ndeltq,ahwins
          return
190       ndeltq=ifix(adq)
          write(ichnl,210)ndeltq,ahwins
```

```
210       format(2x,i5,4x,f7.2)
209       if(mod(ndeltq,istepq).eq.0)goto 213
          ndeltq=ndeltq+1
          ns=1
          goto 209
213       if(ns.eq.1)write(ichnl,214)istepq,ndeltq
214       format(' q spread has to be multiple of ',i3,' selected spread
         &   is ',i4)
          return
          end
c   ######### $$$$$$$$$ &&&&&&& ........ !!!!!!!!!!
          subroutine redat2(filnam,blank)
          common/pass/ichnl
          character*15 filnam,blank
          ichn5=5
          write(6,245)
245       format(//,' write the file name for the data pts: ',$)
          read(ichn5,238,end=242)filnam
238       format(a15)
239       write(ichnl,240)filnam
240       format(3x,a15)
241       return
242       filnam=blank
          return
          end
c %%%% %%%%% %%%%%% %%%%%% %%%%%%%%%%
          subroutine redat3(irange,nstartc,nstopc,ichn5)
          common /pass/ichnl
          character*1 sletn
          write(ichnl,285)irange
285       format(/,' range of the spectrum is ',i6)
          write(ichnl,287)
287       format(' type starting and last frequency: ',$)
c
c ****  nstartc and sttop are the minima and maxima frequency or channels
c ****  sletn is given a value of c if it refers to channels default are
c ****  frequencies
297       read(ichn5,*)start,sttop
          write(ichnl,298)start,sttop
298       format(2x,f10.2,4x,f10.2)
          sletn='n'
299       if(sletn.ne.'c')nstartc=ifix(start*400/irange)
          if(sletn.ne.'c')nstopc=ifix(sttop*400/irange)
          if(sletn.ne.'c')write(ichnl,302)nstartc,nstopc
302       format(' starting channel = ',i5,'  last channel= ',i5)
31:       return
          end
c  ***** **** **** ****** *********
          subroutine redat4(outfil,ichn5)
          character*15 outfil
          common/pass/ichnl
          write(ichnl,317)outfil
317       format(/,' file name for ',a15,2x,$)
          read(ichn5,320)outfil
```

```
      write(ichnl,321)outfil
320       format(a15)
321       format(2x,a15)
          return
          end
c ccc ===== ===== ===== ===== ===== ===== ===== ====
c &&&&&&&& &&&&&&&&  &&&&&&& &&&&&&& &&&&&& &&&&&&
c  this is a line by line description of the sequence of data
c  that the program reads either from the terminal or from a file.
c line   comment
c  1     number of parameters, 1 or 2, to be optimized
c  2     selected output on the terminal? y or n
c  3     calculation for calibration or with instrument
c  3     function or only theoretical equation without any
c  3     instrument function involve (y, n, t)
c  4     spread of q value and the instrument halfwidth value
c  5     name of the data file
c  6     range in frequency which the program will try to optimize
c  6     minimum frequency, maximum frequency
c  7     data needed for calculating the theoretical model these are:
c  7      temp. ,den. 1, visc. 1, dens. 2, visc. 2, interf. tension,
c  7     and few characters (<15) for personal reference.
c  8     data needed for the calculation of the ripplon's wavevector these are
c  8     refractive indx., measured angle from the horizontal in the
c  8     air, distance from the main beam to the pinhole in cm.,
c  8     distance from the cell to the photomultiplier in cm.
c  9     file name for the output of the experimental data.
c 10     file name for the output of the theoretical data.
c 10.1    if line 2, selected output, is typed y then a value
c 10.1    must be inserted here to determine the output
c 10.1    at each ith interval.
c 10     go back to line 4 and so on
c       the program ends when there in no other data file
c       (line 4) to be read, or it reads a blank.
c
c
c
c
c  2  or 1      parameters
c  n  or y      selected output on terminal?
c  n  or y or tinstrument function, calibration, theoretical (only)
c  50 16.61    spread of q values and instrument function, (sigma)
c  3pa7e21     input data file name
c  180 1700    range of frequency to be optimized
c    23.0 .8573 .007618 .98044 .01660 2.5 pr3            data
c    1.4565 22.0 2.143 270.03       data
c  3pa7e21b.exp    exp output filename
c  3pa7e21b.fit     fit output filename
c  3pa7e22
c  195 1400
c    23.0 .8573 .007618 .98044 .01666 2.5 pr3
c    1.4565 22.0 2.143 270.03
c  3pa7e22b.exp
c  3pa7e22b.fit     end of execution
```

APPENDIX F

NONLINEAR LEAST SQUARE FITTING PROGRAM TO CALCULATE THE INTERFACIAL TENSION AND VISCOSITY FOR THE LIGHT SCATTERING METHOD

```
cnllsq    nllsq - non linear least squares fitting program
          subroutine nllsq(y,x,bb,res,narray,array,ibb)
c    nonlinear least squares fitting algorithm by d w marquard
c    original program rewritten by w a burnette  btl july  1967
c    narray contains program parameters  array contains statistical
c    constants   set array equal to 0.for standard set of constants
c    maximum number of parameters is 20 this may be changed by
c    altering dimension statements and matrix storing statements
          double precision a,sa,db,g,bs
          common/blk1/b(20),p(20),re,n,m,k
          common/blk2/a(40,20),sa(20),k2,ik
          common/blk3/bs(20),db(20),g(20),k3
          common/blk4/al,delta,e,ff,gamcr,t,tau,zeta,phi,se,phicr
          common/blk5/ib(20),ip
          dimension y(1),x(1,1),res(1)
          dimension bb(20),ibb(20)
          dimension narray(8),array(8)
          dimension const(8),sconst(8)
          equivalence(const(1),al)
          sconst(1)=0.1
          sconst(2)=1.e-5
          sconst(3)=5.e-5
          sconst(4)=4.
          sconst(5)=45.
          sconst(6)=2.0
          sconst(7)=0.001
          sconst(8)=1.e-31
          n=narray(1)
          m=narray(2)
          k=narray(3)
          k2=k
          k3=k
          ip=narray(4)
          intp=narray(5)
          ifp=narray(6)
          ik=narray(7)
          kiter=narray(8)
          if(kiter.eq.(-1))narray(8)=0
c    which of the constants have been determined by user
          do 477 j=1,8
          if(array(j).le.0.)goto 476
          const(j)=array(j)
          goto 477
```

```
476         const(j)=sconst(j)
477       continue
          if(kiter.le.0)kiter=30
          if(ik.le.0)ik=6
480       if(ifp.eq.(-1))goto 483
          write(ik,706)
          write(ik,679)n,k,m,delta,e,ff,gamcr,t,tau,zeta,al
483       do 486 j=1,k
          bs(j)=bb(j)
          b(j)=bb(j)
486       ib(j)=ibb(j)
          call sumsq(phi,y,x,res)
          lj=0
489       if(lj.ge.kiter)goto 593
          lj=lj+1
c   begin ljth iteration
          call newa(y,x,res)
493       if(al.lt..1d-07)goto 495
          al=al/1.d+01
495       call scale
          phiold=phi
c   store matrix
          do 501 i=1,k
          ii=i+20
          do 501 j=1,k
501       a(ii,j)=a(i,j)
          call solve
503       do 504j=1,k
504       b(j)=bs(j)+db(j)
c   compute gamma
506       dd=0.
          dg=0.
          gg=0.
          do 513j=1,k
          if(sa(j).eq.0.d+00)goto 513
          gg=gg+g(j)*g(j)/(sa(j)*sa(j))
          dd=dd+db(j)*db(j)*sa(j)*sa(j)
513       dg=dg+db(j)*g(j)
          xl=sqrt(dd)
          if(dd*gg.gt.0.)goto 518
516       gamma=0.
          goto 521
518       cgam=dg/sqrt(dd*gg)
          ws=sqrt(1.-cgam*cgam)
          gamma=57.2957795*atan2(ws,cgam)
521       call sumsq(phi,y,x,res)
522       if(phi.le.phiold)goto 524
          if(gamma-gamcr)563,563,529
524       do 525j=1,k
525       bs(j)=b(j)
          if(gamma.lt.90.)goto 533
c   gamma lambda test
528       if(al-1.d+00)533,589,589
529       al=al*1.d+01
```

```
      call solve
          goto 503
c   epsilon test
533       call etest(1)
          goto (575,536),1
c   begin intermediate output routine
536       if(intp.eq.0)goto 489
          write(ik,678)
          write(ik,683)lj,phi,al,(b(j),j=1,k)
          write(ik,685)gamma,xl,(db(j),j=1,k)
          if(intp.eq.1)goto 489
          call newa(y,x,res)
c   store matrix
          do 546 i=1,k
          ii=i+20
          do 546j=1,k
546       a(ii,j)=a(i,j)
          call gjr(ms)
          goto (549,489),ms
549       if(intp.eq.2)goto 552
          write(ik,687)
          call print1
552       call scale
          write(ik,688)
          call print2
c   get matrix from storage
          do 559 i=1,k
          ii=i+20
          do 559j=1,k
559       a(i,j)=a(ii,j)
          if(lj.ge.kiter)goto 593
          lj=lj+1
          goto 493
563       do 565j=1,k
          db(j)=db(j)/2.d+00
565       b(j)=bs(j)+db(j)
c   gamma epsilon test
          call etest(1)
          goto (579,569),1
569       call sumsq(phi,y,x,res)
          if(phiold.lt.phi)goto 563
          do 572j=1,k
572       bs(j)=b(j)
          goto 536
c   begin final  printout routine
575       if(ifp.eq.(-1))goto 668
          write(ik,678)
          write(ik,689)
          goto 597
579       if(ifp.eq.(-1))goto 582
          write(ik,678)
          write(ik,690)
582       if(ifp.ne.(-1).and.phiold.lt.phi)write(ik,707)
          if(phiold.ge.phi)goto 587
```

```
      phi=phiold
            do 586j=1,k
586         b(j)=bs(j)
587         if(ifp.eq.(-1))goto 668
            goto 597
589         if(ifp.eq.(-1))goto 668
            write(ik,678)
            write(ik,691)
            goto 597
593         write(ik,678)
            write(ik,692)
            narray(8)=-1
            if(ifp.eq.(-1))goto 668
597         do 599j=1,k
            bs(j)=b(j)
599         bb(j)=b(j)
            write(ik,683)lj,phi,al,(b(j),j=1,k)
            write(ik,685)gamma,xl,(db(j),j=1,k)
            call newa(y,x,res)
            if(ifp.le.1)goto 618
            do 607 i=1,k
            ii=i+20
            do 607j=1,k
607         a(ii,j)=a(i,j)
            write(ik,693)
            call print1
            call scale
            write(ik,694)
            call print2
c     get matrix from storage
            do 617 i=1,k
            ii=i+20
            do 617j=1,k
617         a(i,j)=a(ii,j)
618         call gjr(ms)
            goto (622,620),ms
620         write(ik,705)
            goto 628
622         if(ifp.eq.0)goto 625
            write(ik,695)
            call print1
625         call scale
            write(ik,696)
            call print2
628         if(ifp.eq.0)goto 664
            do 632 i=1,n
c     residual array option satisfied here
            call model(f,y,x,res,i,4)
632         continue
c     one parameter support plane computations
            fnkw=n-k+ip
            if(fnkw.le.0.)goto 663
            fkw=k-ip
            se=sqrt(phi/fnkw)
```

```
      write(ik,697)
          do 654 i=1,k
c     check for omitted parameters
          if(ip.eq.0)goto 645
          do 644j=1,ip
          if(i.eq.ib(j))goto 653
644       continue
645       ste=sa(i)*se
          hjtd=sqrt(ff*fkw)*ste
          opl=bs(i)-ste*t
          opu=bs(i)+ste*t
          spl=bs(i)-hjtd
          spu=bs(i)+hjtd
          write(ik,700)i,ste,opl,opu,spl,spu
          goto 654
653       write(ik,701)i
654       continue
          if(ifp.eq.1)goto 671
c     nonlinear confidence region calculations
          ws=fkw/fnkw
          phicr=phi*(1.+ws*ff)
          write(ik,702)phicr
          call confrg(y,x,res)
          if(ifp.ge.0)write(ik,706)
          return
663       write(ik,705)
664       if(ifp.eq.0)goto 671
665       if(ifp.ge.0)write(ik,706)
          return
c     returning parameters with no output
668       do 669j=1,k
669       bb(j)=b(j)
c     residual array option with no output
671       j=4
          call model(f,y,x,res,1,j)
          goto (665,665,665,674),j
674       do 675i=2,n
675       call model(f,y,x,res,i,j)
          if(ifp.ge.0)write(ik,706)
          return
678       format(/51h xxxxxxxxxxxxxxxxxxxxxxxxxxxxxxxxxxxxxxxxxxxxxxxxxxxxxxxx/)
679       format(/,1x,20hno of data points is,i4,21h  no of parameters is,
         & i3,3x,30hno of independent variables is,i3//,1x,6hdelta=,1pe12.5,
         & 5h  e=,e15.8,6h  ff=,1pe12.5,9h  gamcr=,1pe12.5,/,1x,5h  t=,
         & 1pe12.5,7h  tau=,1pe12.5,8h  zeta=,1pe12.5,6h  al=,1pe12.5 )
683       format(1x,//,19h no of iterations =,i3,//,1x,5hphi =,1pe12.5,4x,
         & 8hlambda =,1pe12.5,//,1x,10hparameters,/(1x,1p7e17.5/))
685       format(/,1x,7hgamma =,1pe12.5,4x,14hlength of db =,1pe12.5//,1x,
         & 20hdb correction vector/(1x,1p7e17.5/))
687       format(1x//,1x,11hptp inverse)
688       format(1x//,1x,24hcorrelation coefficients)
689       format(/,1x,27hconvergence by epsilon test)
690       format(/,1x,33hconvergence by gamma epsilon test)
691       format(/,1x,32hconvergence by gamma lambda test)
```

```
692       format(//,1x,10h force off)
693       format(1x//,1x,10hptp matrix)
694       format(1x//,1x,28hptp correlation coefficients)
695       format(1x//,1x,11hptp inverse)
696       format(1x//,1x,34hparameter correlation coefficients)
697       format(1x//,12x,4h std,18x,15hone - parameter,22x,
     &  13hsupport plane/2x,4hpara,7x,5herror,13x,
     &  5hlower,13x,5hupper,13x,5hlower,13x,
     &  5hupper)
700       format(2x,i3,1p5e18.5)
701       format(2x,i3,5x,23hparameter held constant)
702       format(1x//28h nonlinear confidence limits//15h phi critical =,
     &  1pe12.5.//,5h para,6x,8h lower b,8x,10h lower phi,
     &  10x,8h upper b,8x,10h upper phi)
705       format(/54h abbreviated output due to mathematical
     &  considerations)
706       format(//)
707       format(/,1x,49hcorrection vector for last iteration was not used)
          end
csumsq       computes sum of squares
          subroutine sumsq(phi,y,x,res)
c     computes sum of squares
          dimension y(1),x(1,1),res(1)
          common/blk1/b(20),p(20),re,n,m,k
          double precision dphi,dre
          dphi=0.d+00
          do 719 i=1,n
          call model(f,y,x,res,i,1)
          dre=re
719       dphi=dphi+dre*dre
          phi=dphi
          return
          end
cnewa        newa - calculates ptp matrix, a, and gradient vector, g.
          subroutine newa(y,x,res)
          dimension y(1),x(1,1),res(1)
          double precision a,sa,db,g,bs
          common/blk1/b(20),p(20),re,n,m,k
          common/blk2/a(40,20),sa(20),k2,ik
          common/blk3/bs(20),db(20),g(20),k3
          common/blk4/al,delta,e,ff,gamcr,t,tau,zeta,phi,se,phicr
          common/blk5/ib(20),ip
          do 736j=1,k
          g(j)=0.d+00
          p(j)=0.
          do 736 i=1,k
736       a(j,i)=0.d+00
          do 765 ii=1,n
c     look for partials
          j=2
          call model(f,y,x,res,ii,j)
          rd=re
          do 761jj=1,k
c     check for omitted parameters
```

```
      if(ip.gt.0)goto 755
745       goto (747,761,747),j
c   compute partials if necessary
747       ab=b(jj)
          b(jj)=ab+delta*ab
          j=1
          call model(fdel,y,x,res,ii,j)
          re=rd
          p(jj)=(fdel-f)/(delta*ab)
          b(jj)=ab
          goto 761
755       do 757 i=1,ip
          if(jj.eq.ib(i))goto 759
757       continue
          goto 745
759       p(jj)=0.
c   using partials at ith data point
761       g(jj)=g(jj)+re*p(jj)
          do 764 i=1,k
          do 764j=i,k
764       a(i,j)=a(i,j)+p(i)*p(j)
765       continue
          do 768 i=1,k
          do 768j=i,k
768       a(j,i)=a(i,j)
c       a(i,i)=1.0 for omitted parameter i
          if(ip.eq.0)return
          do 773 i=1,ip
          do 773j=1,k
773       if(j.eq.ib(i))a(j,j)=1.d+00
          return
          end
cscale    subroutine scale
          subroutine scale
c   scales according to diagonal elements
          double precision ws,a,sa
          common/blk2/a(40,20),sa(20),k2,ik
          k=k2
          do 787 i=1,k
          if(a(i,i).gt.0.d-00)goto 786
          sa(i)=0.d+00
          goto 787
786       sa(i)=dsqrt(a(i,i))
787       continue
          do 796 i=1,k
          do 795j=1,i
          ws=sa(i)*sa(j)
          if(ws.gt.0.d+00)goto 794
          a(i,j)=0.d+00
          goto 795
794       a(i,j)=a(i,j)/ws
795       a(j,i)=a(i,j)
796       a(i,i)=1.d+00
          return
```

```
      end
csolve    solves (ptp)(db)=(g)  where ptp is stored in a(i+20,j)
          subroutine solve
c   solves  a set of linear equations in db determined by matrix
c   a and vector g. uses subroutine gjr to invert matrix
          double precision a,sa,db,g,bs
          common/blk2/a(40,20),sa(20),k2,ik
          common/blk3/bs(20),db(20),g(20),k3
          common/blk4/al,delta,e,ff,gamcr,t,tau,zeta,phi,se,phicr
          k=k2
          l=1
c   get matrix from storage
810       do 814 i=1,k
          ii=i+20
          do 813j=1,k
813       a(i,j)=a(ii,j)
814       a(i,i)=1.d+00+al
815       call gjr(ms)
          goto (817,827),ms
817       do 825 i=1,k
          db(i)=0.d+00
          if(sa(i).le.0.d+00)goto 825
          do 823j=1,k
          if(sa(j).le.0.d+00)goto 823
          db(i)=a(i,j)*g(j)/sa(j)+db(i)
823       continue
          db(i)=db(i)/sa(i)
825       continue
          return
827       al=al*1.d+01
          l=l+1
          if(l.ge.6)stop
          goto 810
          end
cetest    subroutine etest
          subroutine etest(ml)
          double precision db,g,bs
          common/blk1/b(20),p(20),re,n,m,k
          common/blk3/bs(20),db(20),g(20),k3
          common/blk4/al,delta,e,ff,gamcr,t,tau,zeta,phi,se,phicr
          eps=e
          ml=1
          do 843 i=1,k
          w=dabs(db(i))/(tau+abs(b(i)))
          if(w.ge.eps)goto 845
843       continue
          goto 846
845       ml=2
846       return
          end
cgjr      gjr - inverts a matrix in a(i,j), i=1,20,j=1,20
          subroutine gjr(msing)
c   gauss-jordan-rutishauser matrix inversion with double pivoting
          double precision a,sa,eps,pivot,z,b,c
```

```
      common/blk2/a(40,20),sa(20),k2,ik
          common/blk4/al,delta,e,ff,gamcr,t,tau,zeta,phi,se,phicr
          dimension p(20),q(20),b(20),c(20)
          integerp,q
          eps=zeta
          n=k2
          msing=1
          do 897k=1,n
c   determination of pivot element
          pivot=0.d+00
          do 868i=k,n
          do 868j=k,n
          if(dabs(a(i,j))-dabs(pivot))868,868,865
865       pivot=a(i,j)
          p(k)=i
          q(k)=j
868       continue
          if(dabs(pivot)-eps)915,915,871
c   exchange of pivotal row with kth row
871       if(p(k).eq.k)goto 878
          do 876j=1,n
          l=p(k)
          z=a(l,j)
          a(l,j)=a(k,j)
876       a(k,j)=z
c   exchange of column
878       if(q(k).eq.k)goto 884
          do 883 i=1,n
          l=q(k)
          z=a(i,l)
          a(i,l)=a(i,k)
883       a(i,k)=z
884       continue
c   jordan step
          do 894j=1,n
          if(j.eq.k)goto 891
          b(j)=-a(k,j)/pivot
          c(j)=a(j,k)
          goto 893
891       b(j)=1.d+00/pivot
          c(j)=1.d+00
893       a(k,j)=0.d+00
894       a(j,k)=0.d+00
          do 897 i=1,n
          do 897j=1,n
897       a(i,j)=a(i,j)+c(i)*b(j)
c   reordering the matrix
          do 913m=1,n
          k=n-m+1
          if(p(k).eq.k)goto 907
          do 906 i=1,n
          l=p(k)
          z=a(i,l)
          a(i,l)=a(i,k)
```

```
906         a(i,k)=z
907         if(q(k).eq.k)goto 913
            do 912j=1,n
            l=q(k)
            z=a(l,j)
            a(l,j)=a(k,j)
912         a(k,j)=z
913         continue
            return
915         write(ik,916)p(k),q(k),pivot
916         format(/,20h singular matrix  i=,i3,4h  j=,i3,8h  pivot=,e16.8/)
            msing=2
            return
            end
cprint1     subroutine print1
            subroutine print1
c     prints a k by k single precision matrix
            double precision a,sa
            common/blk2/a(40,20),sa(20),k2,ik
            k=k2
            l=1
927         jj=7*l
            ll=jj-6
            if(k.lt.ll)goto 939
            if(k.lt.jj)goto 936
            write(ik,940)ll,jj
            do 933 i=1,k
933         write(ik,941)(a(i,j),j=ll,jj)
            l=l+1
            goto 927
936         write(ik,940)ll,k
            do 938 i=1,k
938         write(ik,941)(a(i,j),j=ll,k)
939         return
940         format(1x,/,1x,7hcolumns,i4,9h  through,i4)
941         format(1x,1p7e17.5)
            end
cprint2     subroutine print2
            subroutine print2
c     prints a k by k correlation coefficient matrix
            double precision a,sa
            common/blk2/a(40,20),sa(20),k2,ik
            l=1
            k=k2
950         jj=13*l
            ll=jj-12
            if(k.lt.ll)goto 962
            if(k.lt.jj)goto 959
            write(ik,963)ll,jj
            do 956 i=1,k
956         write(ik,964)(a(i,j),j=ll,jj)
            l=l+1
            goto 950
959         write(ik,963)ll,k
```

```
      do 961 i=1,k
961   write(ik,964)(a(i,j),j=ll,k)
962   return
963   format(1x,/,1x,7hcolumns,i4,9h  through,i4)
964   format(1x,13f9.4)
      end
cconfrg          confrg - non linear confidence region calculations
      subroutine confrg(y,x,res)
      dimension y(1),x(1,1),res(1)
      double precision a,sa,bs,db,g
      common/blk1/b(20),p(20),re,n,m,k
      common/blk2/a(40,20),sa(20),k2,ik
      common/blk3/bs(20),db(20),g(20),k3
      common/blk4/al,delta,e,ff,gamcr,t,tau,zeta,phi,se,phicr
      common/blk5/ib(20),ip
      logicalnolo
      do 1032 j=1,k
      nolo=.false.
c     check for omitted parameters
      if(ip.eq.0)goto 986
      do 982 i=1,ip
      if(j.eq.ib(i))goto 984
982   continue
      goto 986
984   write(ik,1033)j
      goto 1032
986   dds=-1.
987   d=dds
      dj=se*sa(j)
      b(j)=bs(j)+d*dj
      call sumsq(ph,y,x,res)
      if(ph.lt.phicr)goto 997
992   d=d/2.
      if(abs(d).le..001)goto 1017
      b(j)=bs(j)+d*dj
      call sumsq(pph,y,x,res)
      if(pph-phicr)1002,1002,992
997   d=d+dds
      if(abs(d).ge.5.0)goto 1017
      b(j)=bs(j)+d*dj
      call sumsq(pph,y,x,res)
      if(pph.lt.phicr)goto 997
1002        q=1.-d
      xk1=phi/d+ph/q-pph/(d*q)
      xk2=-phi*(1.+d)/d-ph*d/q+pph/(d*q)
      xk3=phi-phicr
      bc=(-xk2+sqrt(xk2**2-4.*xk1*xk3))/(2.*xk1)
      if(dds.gt.0.)goto 1013
      b(j)=bs(j)-bc*dj
      bl=b(j)
      call sumsq(pl,y,x,res)
1011  dds=1.
      goto 987
1013  b(j)=bs(j)+bc*dj
```

```
      bu=b(j)
          call sumsq(pu,y,x,res)
          goto 1027
1017      if(dds.gt.0.)goto 1020
          nolo=.true.
          goto 1011
1020      if(nolo)goto 1025
c     omitting upper limits
          write(ik,1035)j,bl,pl
          goto 1032
c     omitting both
1025      write(ik,1037)j
          goto 1032
1027      if(nolo)goto 1031
          write(ik,1034)j,bl,pl,bu,pu
          goto 1032
c     omitting lower limits
1031      write(ik,1036)j,bu,pu
1032      b(j)=bs(j)
1033      format(2x,i3,5x,23hparameter held constant)
1034      format(2x,i3,1p4e18.5)
1035      format(2x,i3,1p2e18.5,11h  not found)
1036      format(2x,i3,11h  not found,25x,1p2e18.5)
1037      format(2x,i3,18x,11h  not found)
          return
          end
```

REFERENCES

1. Smoluchowski, M. V., Ann. Phys. Leipzig 25, 225 (1908).

2. Langevin, D. and Meunier, J., "Light Scattering by Liquid Interfaces" in: *Photon Correlation and Velocimetry*, edited by H.Z. Cummins and E. R. Pike, Plenum Press, N.Y., (1977).

3. Langevin, D., J. Colloid Interface Sci. 80, 412 (1981)

4. Stone, J.A. and Rice, W.J., J. Coll. Interface Sci., 61, 160, (1977).

5. Byrne, D. and Earnshaw, J.C., J. Coll. interface Sci., 74, 467, (1980).

6. Edwards, R.V., Sirohi, R.S.,Mann, J.A., Shih, L.B., and Lading, L., Appl. Optics, 21, 3555, (1982).

7. Voeght, De F. and Joos, P., J. of Colloid and interface Science, 98, 20, (1984).

8. Bouchiat, M.A., and Meunier, J., J. Physique, 33, C1-141, (1972).

9. Hård, S and Johansson, K., J. of Colloid and Interface Science, 60, 467, (1977).

10. Hård, S. and Löfgren, H., J. of Colloid and interface science, 60, 529, (1977).

11. Kim, M.W., Huang, J.S., Bock, J., Society of Petroleum Engineers/U.S. Department of Energy (SPE/DOE) 10788, 911, (1982).

12. Lachaise, J., Graciaa, A., Martinez, A., Rousset, A., Le Journal Physique - LETTRES, 40, L-599, (1979).

13. Löfgren, H., Newman, R.D., Scriven, L.E., and Davis H.T., J of Colloid and Interface Science, 98, (1984).

14. Fisk, S. and Widom, B., J. Chem. Phys., 50, 3219, (1969).

15. Faraday Society, General discussions, 59, papers 2,3,4, (1975).

16. Vonnegut, B. Rev. Sci. Instr., 13 6 (1942)

17. Silberg, A., PhD. Thesis, Basel University, Switzerland, (1952).

18. Margenau, H., Murphy, G.M., The Mathematics of Physics and Chemistry, 2nd Ed., Van Nostrand, pp 490-491, (1956).

19. Andreas, J.H., Hauser, E.A., and Tucker, W.B., J.Phys. Chem., **42**, 1001, (1938).

20. Bashforth, F., Adams, J.C., *An Attempt to Test the Theories of Capillary Action*. University Press, Cambridge, England, (1883).

21. Huh, C. and Reed, R. L., J. Phys. Chem. 91, 472, (1983).

22. Mandelstam, L., Ann. Physik, **41**, 609, (1913).

23. Andronov, A.A. and Leontovich, M.A., Z. Phys. **38**, 485, (1926).
Andronov A.A., Collected works, Izd Akad Nauk SSSR, (1956).
Gans R, Ann Physik 79, 204, (1926).

24. Komarov L.I. and Fisher I.Z., Sov. Phys., **A16**, 290, (1942).
Pecora R., J. Chem. Phys., **40**, 1604, (1963).

25. Cummins H.Z. and Swinney H.L., in *Progress in Optics*, Vol. 8, E. Wolf, Ed., Academic, New York, pp.133-200, (1970).

26. Byrne D. and Earnshaw J. C., J. Phys. D **12**, 1133, (1979).

27. Byrne D. and Earnshaw J. C., J. Phys. D **10**, L207, (1977).

28. Hård S., Hamnerius Y., and Nilsson O., J. Appl. Phys. **47**, 2433, (1976).

29. Meunier, J., Thesis, Université De Paris VI, chap. I, (1971).

30. Levich, V.G. Physicochemical Hydrodynamics (Englewood Cliffs, N.J.; Prentice-Hall), (1962).

31. Bouchiat, M.A. and Meunier, J., J. Physique, **32**, 561, (1971).

32. Born, M. and Wolf, E. *Principle of Optics*, Pergamon Press, New York, 2nd edition, pp. 498, (1964).

33. Raleigh, J.W., Scientific Papers, A. **322**, pp. 388, (1907).

34 Pouchelon, A., Meunier, J., Langevin, D., Chatenay, D., and Cazabat, A.M., Chem. Phys. Letters, **76**, 277, (1980).

35. Cazabat, A.M., Langevin, D., Meunier, J., Pouchelon, A., private comunications.

36. Langevin, D., J. Chem. Soc., Faraday Trans. 1, 70, 95, (1974).

37. Rosano H.L., Tan, L., Weiss, A., Gerbacia, W., Whittam, J., Colloid Interface Sci., **72**, 233, (1981).

38. Gerbacia, W. and Rosano, H.L., J. Colloid Interface Sci., **44**, 242, (1973).

39. Gerbecia W., Rosano, H.L., and Whittam, J.H., in Colloids and Interface Science, Vol II, edited by Kerker, Academic Press, New York, N.Y., pp. 245, (1976).

40 Rosano, H.L., Jon, D., and Whittam, J.H., JACS, 59, 360, (1982).

41 Bird, M., Hills, G. Physicochemical Hydrodynamics, Vol 2, 609, Advance Publications, (1977), (Oxford Conference).

42 Byrne, D. and Earnshaw, J.C., Lasers in Chemistry, pg. 29 by West, Michael A., Elselvier Scientific Publishing Co. N.Y. (1977).

43 Zollweg, J., Hawkins, G., and Benedek, G.B., private comunications.

44 Bouchiat, M.A., and Meunier, J., Phys. Rev. Let., 23, 752, (1969).

45 Princen, H.M., Zia, I.Y.Z. and Mason, S.G., J. Coll. Interface Sci., 23, 99, (1967).

46 *Handbook of Chemistry and Physics*, 40th ed. pg. 259. Chemical Rubber Publishing Co., Cleverland (1958).

47 Grobner, W., and Hofreiter,N., *Integraltafel*, 3rd ed., Vol 1, pg.78. Springer Verlag, Vienna, (1961).

48 Emde, F., *A. M. Legendres Tafeln der Elliptichen Normalintegrale*. Konrad Witter, Stuttgart, (1931).

49 Cayias, J. L., Schechter, R.S., and Wade, W.H., ACS Symposium series number 8, (1975).

50 Margenau, H.; Murphy, G.M.; The Mathematics of Physics and Chemistry, 2nd Ed., Van Nostrand, pp. 490-491, (1956).

51 Neiderhauser, D.O.; Bartell, P.E., Report of Progress Fundamental Research on Occurrence and Recovery of Petroleum - API, p.144, (1948).

52 Fordham, S., Proc. of the Roy. Soc. of London, A., Vol 194, p. 1, (1948).

53 Staufer, C.E.; J. Phys. Chem. 69, p. 1933, (1965).

54 Mitsotakis, L.S., Master's Thesis, The City College of N.Y., C.U.N.Y., (1983).